INL/EXT-11-23295
Rev. 1

Critical Configuration and Physics Measurements for Assemblies of $U(93.15)O_2$ Fuel Rods

Margaret A. Marshall
John D. Bess
J. Blair Briggs
Michael F. Murphy
John T. Mihalczo

September 2012

Idaho National Laboratory

The INL is a U.S. Department of Energy National Laboratory
operated by Battelle Energy Alliance

INL/EXT-11-23295
Rev. 1
NEA/NSC/DOC(2006)1
SCCA-FUND-EXP-001

Critical Configuration and Physics Measurements for Assemblies of U(93.15)O_2 Fuel Rods

Margaret A. Marshall[3]
John D. Bess
J. Blair Briggs
Michael F. Murphy[1]
John T. Mihalczo[2]

[1]Under Subcontract to the OECD NEA
[2]Oak Ridge National Laboratory
[3]Idaho National Laboratory/University of Idaho

September 2012

Idaho National Laboratory
Idaho Falls, Idaho 83415

http://www.inl.gov

Prepared for the
U.S. Department of Energy
Office of Nuclear Energy
Under DOE Idaho Operations Office
Contract DE-AC07-05ID14517

NEA/NSC/DOC(2006)1

Fundamental-FUND

SCCA-FUND-EXP-001
CRIT-*SPEC*-REAC-RRATE

CRITICAL CONFIGURATION AND PHYSICS MEASUREMENTS FOR ASSEMBLIES OF U(93.15)O_2 FUEL RODS

Evaluator

Margaret A. Marshall
Idaho National Laboratory/University of Idaho

Internal Reviewers

John D. Bess
J. Blair Briggs
Idaho National Laboratory

Independent Reviewers

Michael F. Murphy
Under Subcontract to the OECD NEA

John T. Mihalczo
Oak Ridge National Laboratory

Status of Compilation/Evaluation/Peer Review

Section 1	Compiled	Independent Review	Working Group Review	Approved
1.0 DETAILED DESCRIPTION				
1.1 Description of the Critical and/or Subcritical Configuration	YES	YES	YES	YES
1.2 Description of Buckling and Extrapolation Length Measurements	NA	NA	NA	NA
1.3 Description of Spectral Characteristics Measurements	YES	YES	YES	YES
1.4 Description of Reactivity Effects Measurements	YES	YES	YES	YES
1.5 Description of Reactivity Coefficient Measurements	NA	NA	NA	NA
1.6 Description of Kinetics Measurements	NA	NA	NA	NA
1.7 Description of Reaction-Rate Distribution Measurements	YES	YES	YES	YES
1.8 Description of Power Distribution Measurements	NA	NA	NA	NA
1.9 Description of Isotopic Measurements	NA	NA	NA	NA
1.10 Description of Other Miscellaneous Types of Measurements	NA	NA	NA	NA
Section 2	**Evaluated**	**Independent Review**	**Working Group Review**	**Approved**
2.0 EVALUATION OF EXPERIMENTAL DATA				
2.1 Evaluation of Critical and/or Subcritical Configuration Data	YES	YES	YES	YES
2.2 Evaluation of Buckling and Extrapolation-Length Data	NA	NA	NA	NA
2.3 Evaluation of Spectral Characteristics Data	NO	NO	NO	NO
2.4 Evaluation of Reactivity Effects Data	YES	YES	YES	YES
2.5 Evaluation of Reactivity Coefficient Data	NA	NA	NA	NA
2.6 Evaluation of Kinetics Measurements Data	NA	NA	NA	NA
2.7 Evaluation of Reaction-Rate Distributions	YES	YES	YES	YES
2.8 Evaluation of Power Distribution Data	NA	NA	NA	NA
2.9 Evaluation of Isotopic Measurements	NA	NA	NA	NA
2.10 Evaluation of Other Miscellaneous Types of Measurements	NA	NA	NA	NA

Section 3	Compiled	Independent Review	Working Group Review	Approved
3.0 BENCHMARK SPECIFICATIONS				
3.1 Benchmark-Model Specifications for Critical and / or Subcritical Measurements	YES	YES	YES	YES
3.2 Benchmark-Model Specifications for Buckling and Extrapolation Length Measurements	NA	NA	NA	NA
3.3 Benchmark-Model Specifications for Spectral Characteristics Measurements	NO	NO	NO	NO
3.4 Benchmark-Model Specifications for Reactivity Effects Measurements	YES	YES	YES	YES
3.5 Benchmark-Model Specifications for Reactivity Coefficient Measurements	NA	NA	NA	NA
3.6 Benchmark-Model Specifications for Kinetics Measurements	NA	NA	NA	NA
3.7 Benchmark-Model Specifications for Reaction-Rate Distribution Measurements	YES	YES	YES	YES
3.8 Benchmark-Model Specifications for Power Distribution Measurements	NA	NA	NA	NA
3.9 Benchmark-Model Specifications for Isotopic Measurements	NA	NA	NA	NA
3.10 Benchmark-Model Specifications of Other Miscellaneous Types of Measurements	NA	NA	NA	NA
Section 4	**Compiled**	**Independent Review**	**Working Group Review**	**Approved**
4.0 RESULTS OF SAMPLE CALCULATIONS				
4.1 Results of Calculations of the Critical or Subcritical Configurations	YES	YES	YES	YES
4.2 Results of Buckling and Extrapolation Length Calculations	NA	NA	NA	NA
4.3 Results of Spectral Characteristics Calculations	NO	NO	NO	NO
4.4 Results of Reactivity Effect Calculations	YES	YES	YES	YES
4.5 Results of Reactivity Coefficient Calculations	NA	NA	NA	NA
4.6 Results of Kinetics Parameter Calculations	NA	NA	NA	NA
4.7 Results of Reaction-Rate Distribution Calculations	YES	YES	YES	YES
4.8 Results of Power Distribution Calculations	NA	NA	NA	NA
4.9 Results of Isotopic Calculations	NA	NA	NA	NA
4.10 Results of Calculations of Other Miscellaneous Types of Measurements	NA	NA	NA	NA
Section 5	**Compiled**	**Independent Review**	**Working Group Review**	**Approved**
5.0 REFERENCES	YES	YES	YES	YES
Appendix A: Computer Codes, Cross Sections, and Typical Input Listings	YES	YES	YES	YES

CRITICAL CONFIGURATION AND PHYSICS MEASUREMENTS FOR ASSEMBLIES OF U(93.15)O_2 FUEL RODS

IDENTIFICATION NUMBER: SCCA-FUND-EXP-001
CRIT-*SPEC*-REAC-RRATE

KEY WORDS: acceptable, assembly, cadmium ratios, close packed, critical experiments, dioxide, fuel rods, graphite-reflected, highly enriched, reactivity worth measurements, unmoderated, uranium, medium power reactor experiments, space reactor, small modular reactor

SUMMARY INFORMATION

1.0 DETAILED DESCRIPTION

A series of critical experiments were completed from 1962–1965 at Oak Ridge National Laboratory's (ORNL's) Critical Experiments Facility (CEF) in support of the Medium-Power Reactor Experiments (MPRE) program. In the late 1950s, efforts were made to study "power plants for the production of electrical power in space vehicles."[(a)] The MPRE program was a part of those efforts and studied the feasibility of a stainless-steel system, boiling potassium 1 MW(t), or about 140 kW(e), reactor. The program was carried out in [fiscal years] 1964, 1965, and 1966. A summary of the program's effort was compiled in 1967.[a] The delayed critical experiments were a mockup of a small, potassium-cooled space power reactor for validation of reactor calculations and reactor physics methods.

Initial experiments, performed in November and December of 1962, consisted of a core of unmoderated stainless-steel tubes, each containing 26 UO_2 fuel pellets, surrounded by a graphite reflector. Measurements were made to determine critical reflector arrangements, fission-rate distributions, and cadmium ratio distributions. Subsequent experiments used beryllium reflectors and also measured the reactivity for various materials placed in the core. "The [assemblies were built] on [a] vertical assembly machine so that the movable part was the core and bottom reflector" (see Reference 1). The experiment studied in this evaluation was the first of the series and had the fuel tubes packed tightly into a 22.87-cm outside diameter (OD) core tank. Two critical configurations were found by varying the amount of graphite reflector (see References 1 and 2). Once the critical configurations had been achieved, various measurements of reactivity, relative axial and radial activation rates of ^{235}U,[b,c] and cadmium ratios were performed. The cadmium ratio, reactivity, and activation rate measurements performed on the critical configurations are described in Sections 1.3, 1.4, and 1.7, respectively.

Information for this evaluation was compiled from References 1 and 2, reports on subsequent experiments in the series[d,e] and the experimental logbook,[a] and from communication with the experimenter, John T. Mihalczo.

---

a. A. P. Fraas, "Summary of the MPRE Design and Development Program," ORNL-4048, Oak Ridge National Laboratory (1967).

b. What was referred to as the fission rates in References 1 and 2 are induced fissions in a uranium fission counter for the axial measurements and relative activation of 235U fission foils for the radial measurements (see Section 1.7.1). (Personal communication with J.T. Mihalczo, September 19, 2011).

c. Axial measurements in the core were made to determine the axial power density distribution.

d. J. T. Mihalczo, "A Small Graphite-Reflected UO2 Critical Assembly, Part II," ORNL-TM-561, Oak Ridge National Laboratory (1963).

e. J. T. Mihalczo, "A Small Beryllium-Reflected UO2 Assembly," ORNL-TM-655, Oak Ridge National Laboratory (1963).

1.1 Description of the Critical and/or Subcritical Configuration

1.1.1 Overview of Experiment

The experimenter began by adding fuel rods to an unreflected tank of 9.5-inch (24.13 cm) diameter laid horizontally. A Po-Be neutron source (~10^7 neutrons-s^{-1}) was mounted in a tube among the fuel tubes and count rates were measured until 279 fuel rods had been added. These initial tests were performed to verify that the tank could be safely loaded.[b]

Next, 253 fuel rods were arranged in the vertical core tank, 22.87-cm OD, used for the critical configurations. The amount of reflector surrounding the core tank was varied to obtain the critical configurations. For the initial trials, a Pu-Be source (#M226) was placed at the side of the reflector. During the final approaches to critical, the source was mounted in one of the 1.27-cm radial holes in the reflector. When all radial holes in the graphite radial reflector were filled, the source was adjacent to the outside of the radial reflector. The source was withdrawn into a shield for the final critical measurements and had negligible contribution to k_{eff}.[c] The core tank was raised stepwise into the reflector as each configuration was tested. Two critical configurations were obtained by varying the side and top reflector sizes; additional physics measurements were also performed. The center fuel rod was removed for the critical assembly; thus, only 252 fuel rods were present in the core. The first and second critical configurations/assemblies had 19.25-cm-thick and 24.34-cm-thick side reflectors and 12.70-cm-thick and 5.08-cm-thick top reflectors, respectively (see Figure 1.1-6). The excess reactivity of the first assembly was +7.2 ¢ and +3.4 ¢ for the second assembly.

The uncertainty in both mass and size measurements was “one in the last significant digit given.”[d]

Both assemblies have been evaluated as acceptable benchmark experiments. These experiments are highly correlated with the second part of the experimental series, which is evaluated in HEU-COMP-FAST-002.[e]

1.1.2 Geometry of the Experiment Configuration and Measurement Procedure

1.1.2.1 Assembly Placement on the Criticality Testing Unit

The assemblies were built on a vertical assembly machine in the east experimental cell of the Oak Ridge Critical Experiments Facility (ORCEF). Safety mechanisms of the device and facility are discussed in the facility safety review.[f] The machine was located such that the center of the core was 3.67 m from the 1.5-m-thick west wall, 3.9 m from the 0.6-m-thick north wall, and 2.8 m above the concrete floor in the 10.7 × 10.7-m-square, 9.1-m-tall room (see Reference 2). Figure 1.1-1 is a photograph of the vertical assembly machine.

---

a. Radiation Safety Information Computation Center (RSICC), The ORNL Critical Experiments Logbooks, Book 75r, http://rsicc.ornl.gov/RelatedLinks.aspx?t=criticallist, logbook page 10-60 (PDF page 3-43).

b. RSICC Logbook 75r, p. 21–27 and personal email communication with J. T. Mihalczo, September 26, 2011, and November 14, 2011.

c. Personal email communication with J.T. Mihalczo, September 29, 2011.

d. Personal email communication with J. T. Mihalczo, May 23, 2011.

e. International Handbook of Evaluated Criticality Safety Benchmark Experiments, NEA/NSC/DOC(95)03, OECD-NEA, Paris, 2012

f. *Safety Review of the Oak Ridge Critical Experiments Facility*, Union Carbide Nuclear Corporation, Oak Ridge National Laboratory (1962).

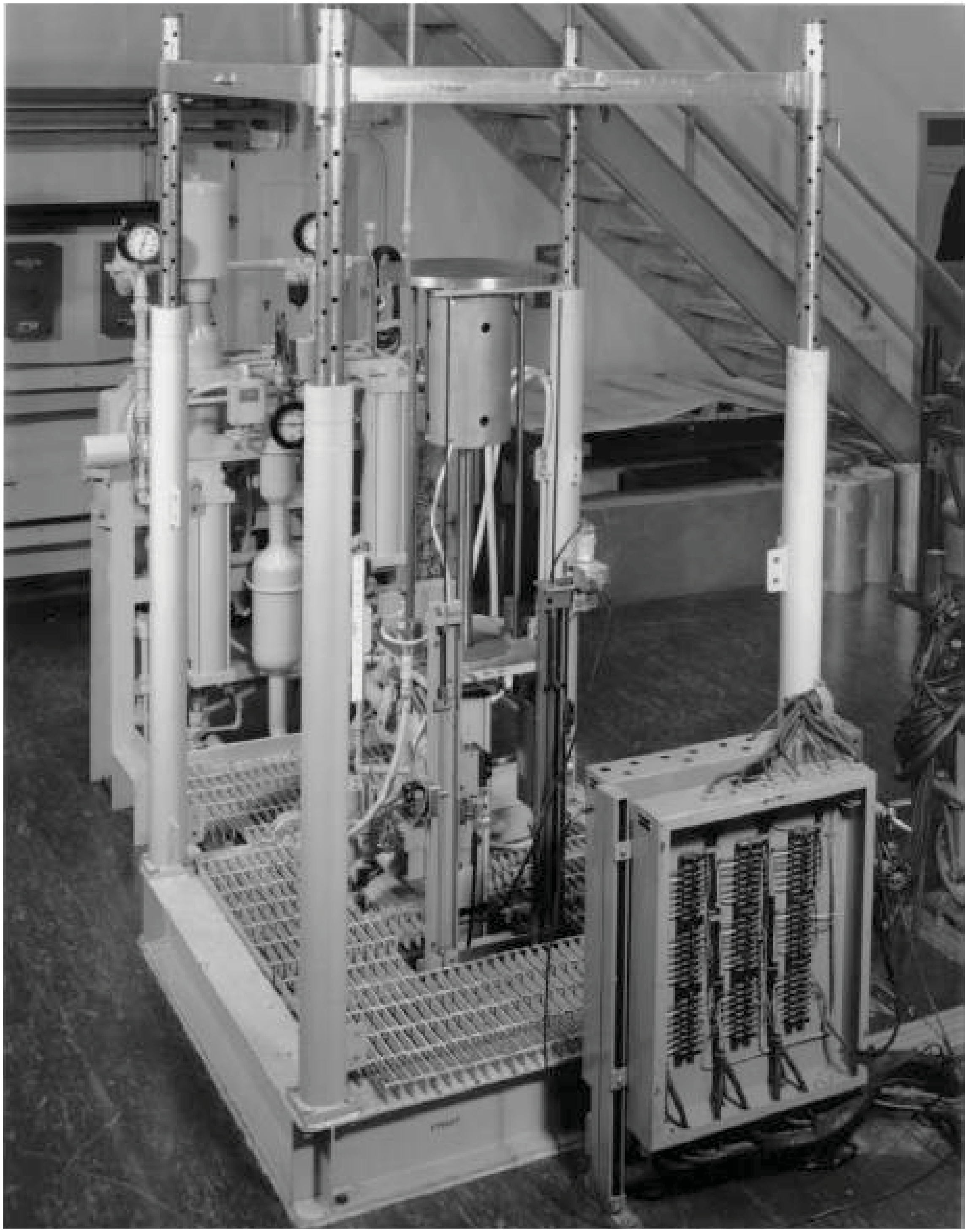

Figure 1.1-1. Photograph of the Vertical Assembly Machine.[a]

a. *Safety Review of the Oak Ridge Critical Experiments Facility*, Union Carbide Nuclear Corporation, Oak Ridge National Laboratory (1962).

The top and side reflectors were mounted from the four poles of the vertical assembly machine (see top of Figure 1.1-2). The bottom reflector and the core were placed on the moveable portion of the table and raised into the side reflector such that the core came into contact with the top reflector or within 0.001 inches of it and usually lifted it ~0.001 inches.[a] A gauge was placed on top of the graphite to determine when the core was in the up position and in contact with the top reflector.[b] In addition, the core and graphite bottom reflector were supported on a Type 1100 aluminum cylinder and disc, which was attached to the Type 304 stainless-steel moveable platform of the vertical assembly machine.
Figures 1.1-2, 1.1-3, and 1.1-4 are photographs of the reflectors and core on the vertical assembly machine.

a. Personal email communication with J. T. Mihalczo, May 23 and September 19, 2011. This gauge was also used to ensure that the core did not lift the top and side reflector as it was being inserted.

b. RSICC Logbook 75r, p. 41.

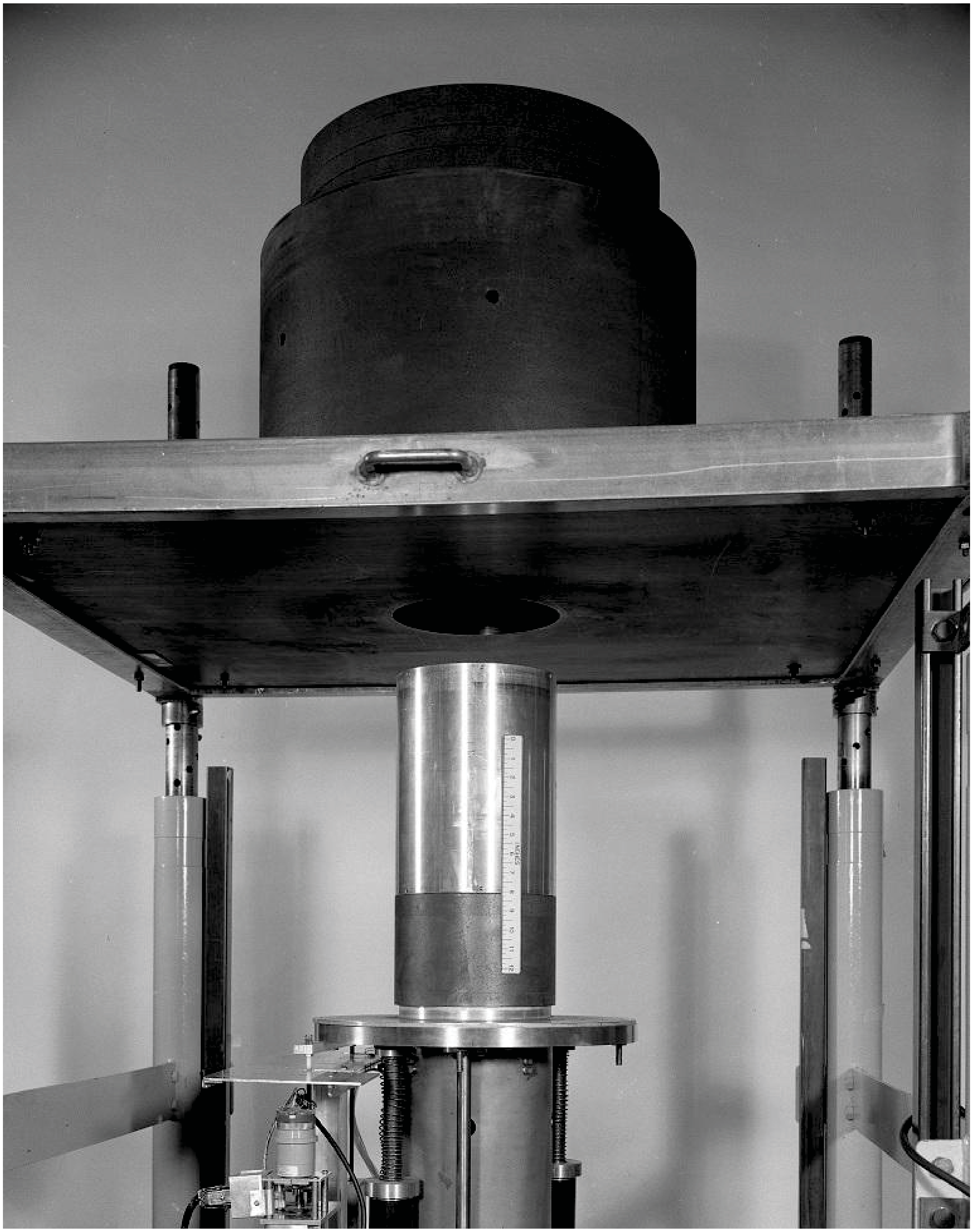

Figure 1.1-2. Lower (Movable Core and Bottom Graphite Reflector) and Upper (Fixed Top and Side Reflectors) Portions of Assembly.[a]

a. ORNL Photograph 39302.

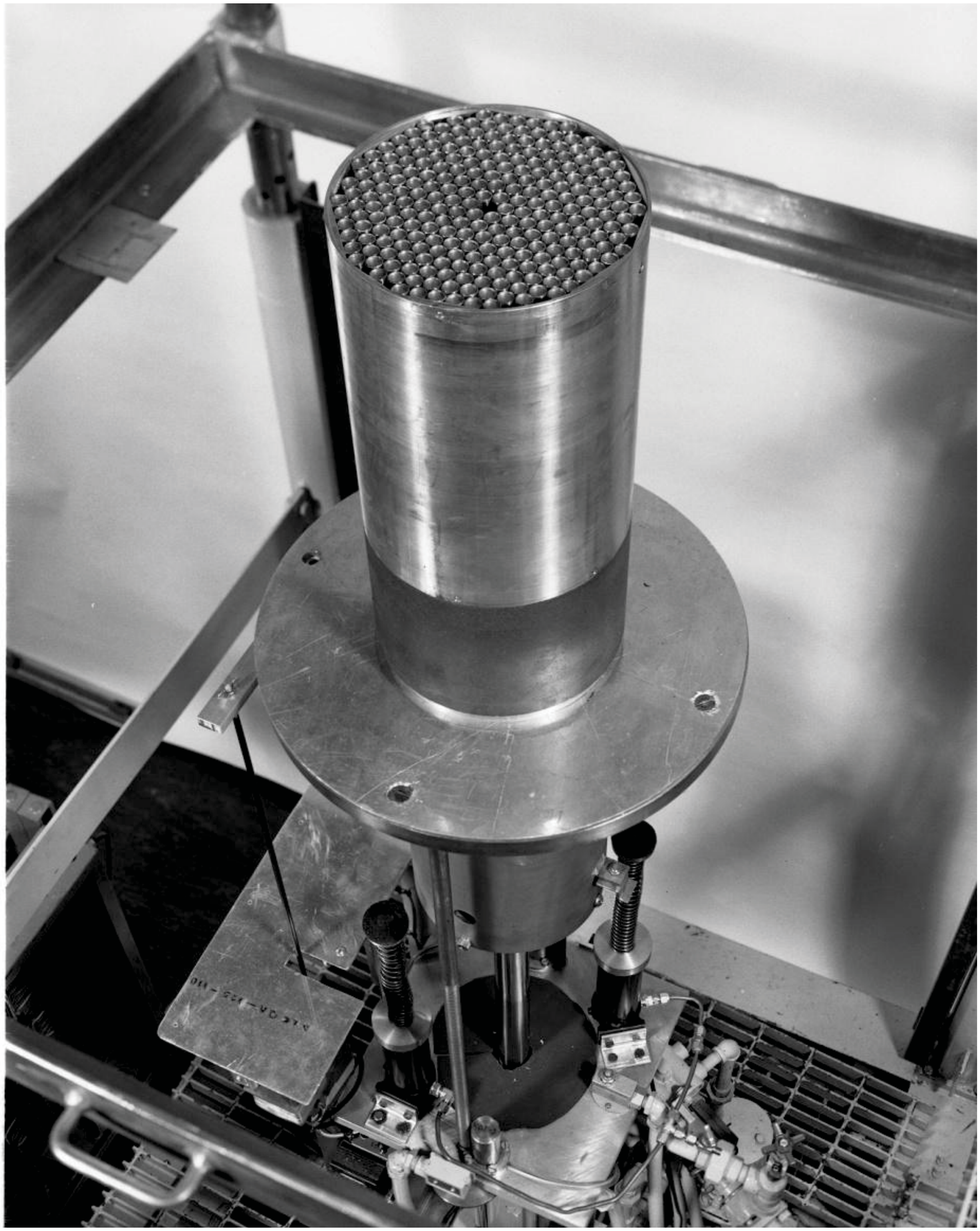

Figure 1.1-3. Lower Portion of the Vertical Assembly Machine with the Core (Center Fuel Pin Removed) and Bottom Reflector.[a]

a. ORNL Photograph 39305.

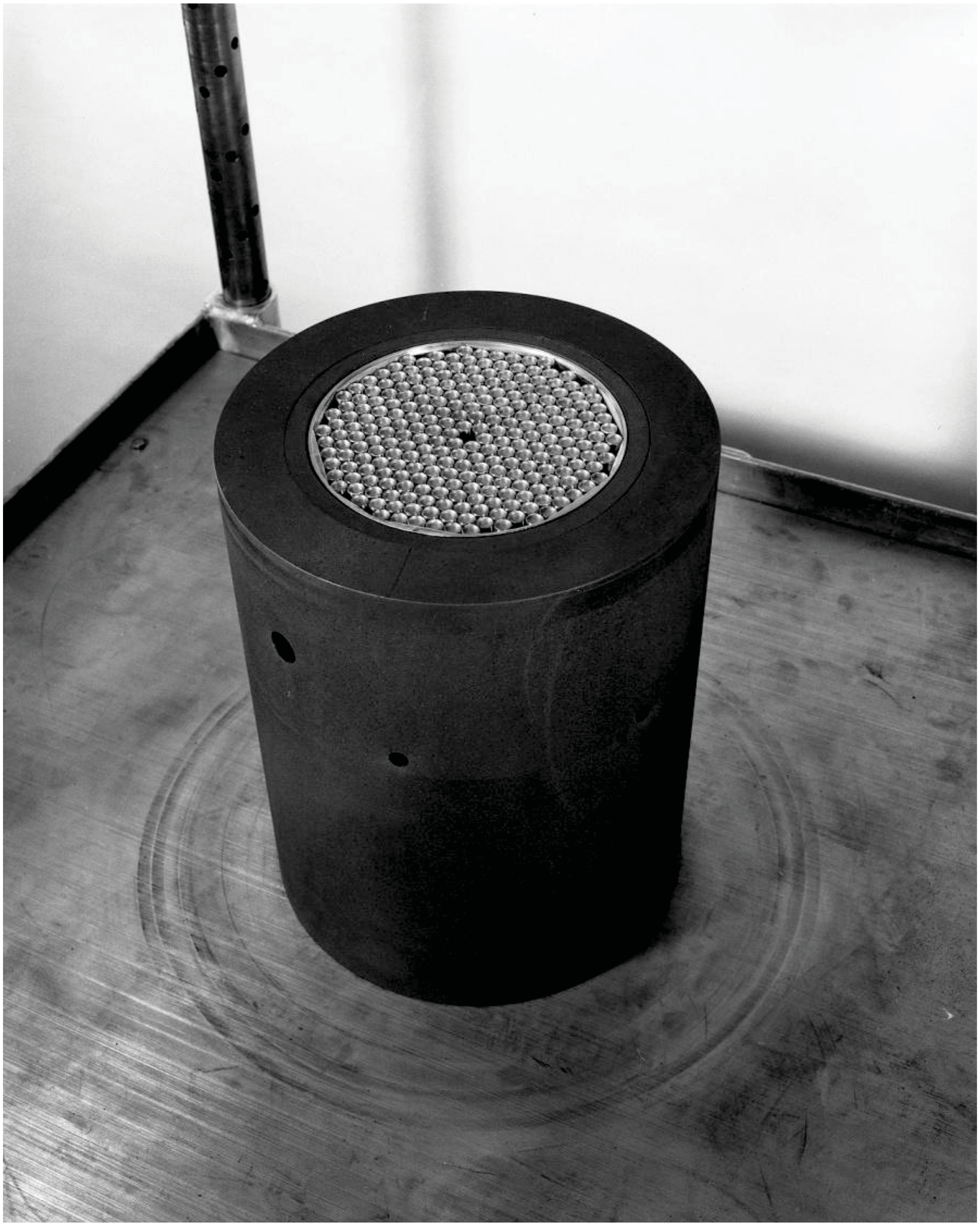

Figure 1.1-4. Upper Portion of the Vertical Assembly Machine with the Core and Bottom Reflector and the 6.35-cm-thick Portion of the Radial Reflector.[a] (Note the large lifting hole and the smaller hole for reactivity adjustment and foil activation measurements.)

a. ORNL Photograph 39304.

1.1.2.2 The Core

The critical core assembly consisted of 252, 1.27-cm OD[a] fuel tubes tightly packed into a Type 1100 aluminum cylindrical core tank with the center fuel tube removed (see Figure 1.1-3). The center-to-center spacing between fuel pins was 1.27 cm. Each fuel tube contained 26 UO_2 fuel pellets. Pellets were packed into Type 347 stainless-steel tubes and held in using end caps. The tubes were made of standard commercially available tubing.[b] The end caps created small wells at the top and bottom of the fuel tubes, as can be seen in Figures 1.1-3 and 1.1-4.[c] Dimensions and a photograph of the fuel pellets and tubes as taken from Reference 1 can be found in Tables 1.1-1 and 1.1-2 and Figure 1.1-5.

Table 1.1-1. Uranium Oxide Dimensions (see References 1 and 2).

Number of Pellets per Tube	26	
UO_2 Density	9.71	g/cm^3
UO_2 Mass per Tube	295.8	g
Pellet Diameter	1.141	cm
Length of One Pellet	1.145	cm
Length of 26 Pellets	29.88	cm[(a)]

(a) This length "includes 0.110 cm of void or ~0.0044 cm of void between each pellet." (Reference 2)

Table 1.1-2. Fuel-Tube Dimensions (see References 1 and 2).

Length	30.48	cm
Outside Diameter	1.27[(a)]	cm
Wall Thickness	0.051	cm
Weight with End Caps	45.37	g[(b)]
Weight of One End Cap	0.64	g

(a) References 1 and 2 report only two significant digits beyond the decimal for the pin OD, but according to the experiment, it was actually measured to three significant digits. The value reported in References 1 and 2, 1.27 cm, has been used for this evaluation.

(b) Compared to values in the logbook, this weight is too low by the weight of one end cap (see following paragraph and Section 2.1.4).

---

a. References 1and 2 only give two significant digits but according to the experimenter the diameter was measured to three significant digits (September 19, 2011). A value of 1.27 cm, as reported in Reference 1 and 2, has been used in this evaluation.

b Personal email communication with J.T. Mihalczo, June 28, 2012.

c. Personal email communication with J. T. Mihalczo, May 23, 2011.

Figure 1.1-5. Stainless-Steel Tube (With One End Cap Removed) and Fuel Pellets.[a,b]

The logbook[c] contains the experimenter's notes of the mass measurements for the fuel tubes, end caps, and fuel mass per tube. The mass of 314 stainless-steel tubes plus the 397-g box they were in was 14,442 g; this yields a mass of 14,045 g for 314 fuel tubes. An average mass per tube of 44.729 g was calculated. The mass of 324 end caps was measured to be 207.706 g, which averages to 0.64107 g per end cap. The mass of fuel per tube was found by weighing all 26 pellets from each of the 279 fuel tubes, one tube at a time, and then finding the average mass of fuel per tube. The total fuel weight was 82,533.26 g, which averaged to 295.818 g per tube. The uncertainty in these mass measurements was one in the last significant digit: ±1 g for the mass of 314 fuel tubes, ±0.001 g for the mass of 324 end caps, and ±0.01 g for the mass of each fuel tube. However, the mass of a fuel tube and end cap, as calculated using these numbers, does not agree with the weight of the tube with end caps provided in Table 1.1-2 (see Section 2.1.4)[d].

a. "The edges of the pellets were chipped during their removal from the tube preparatory to this photograph" (see Reference 1).

b. ORNL Photograph 39309.

c. RSICC Logbook 75r, pp. 10–19.

d. The experimenter confirmed that the fuel tube mass reported in References 1 and 2 is with one end cap removed (September 19, 2011).

Fuel tubes were arranged in a close-packed array inside a Type 1100 aluminum core tank. Dimensions of the core tank are provided in Table 1.1-3.

Table 1.1-3. Core Tank Dimensions (see References 1 and 2).

Side Wall Thickness	0.29	cm
Bottom Thickness	0.35	cm
Outside Diameter	22.87	cm
Outside Length	31.11	cm
Weight (kg)	2.134	kg

Aluminum shims were used at the periphery of the array, top and bottom of the core tank, to keep the fuel tubes tightly packed. The shims were 1.91 cm tall, were 24° and 34° circular segments of a circle of 22.29-cm diameter, and weighed a total of 185 g for all 24 shims (see References 1 and 2). The logbook has the aluminum shim masses recorded as 63.72 g for 12 shims and 206.5 g for the other 12 shims, which yields a total mass of 270.22 g for 24 shims. This discrepancy is discussed in Section 2.1.3.

1.1.2.3 Reflectors

The core was reflected on all sides by Type ATL graphite. Two critical configurations were obtained by varying the amount of side and top reflection (see Figure 1.1-6). The dimensions of both configurations are given in Table 1.1-4. Each section of reflector was a single solid mass, except the top and side reflector, which has holes filled with graphite plugs. Five of six 1.27-cm-diameter radial holes in the side reflector were plugged. The five radial holes and an axial hole in the top reflector were plugged with 0.95-cm-diameter graphite plugs (see References 1 and 2). The diameter of the radial holes as reported in the logbook agrees with the published value; however, the diameter of the plug was reported as 0.437 inches (1.11 cm) in the logbook.[a] The graphite plugs were inserted into the small holes in the radial reflector (see Figure 1.1-4) for fine adjustment of the reactivity. Two larger radial holes (2.54-cm-diameter) were present for lifting and were always plugged during the experiments (see Reference 2). The plugs were in place when the masses of the reflectors were measured.[b]

Additional reflection was provided by aluminum and stainless-steel plates below the bottom reflector and the iron table of the vertical assembly machine below the side reflector. (These parts are referred to as additional bottom reflectors in References 1 and 2.) The dimensions and masses of these support plates are also given in Table 1.1-4, and the plates are shown in Figure 1.1-6. The mass for the Type 304 stainless-steel plate is given as 3.91 kg in Reference 1 and 7.76 kg in Reference 2; however, both of these masses are quite a bit lower than would be expected for a solid steel plate and are clearly wrong. The published report for the third part of the experimental series reports the same stainless-steel plate as having a mass of 31.2 kg, which gives a calculated density close to the nominal density for stainless steel.[c]

a. RSICC Logbook 75r, p. 40.

b. Personal email communication with J. T. Mihalczo, May 23, 2011.

c. J. T. Mihalczo, “A Small Beryllium-Reflected UO2 Assembly,” ORNL-TM-655, Oak Ridge National Laboratory (1963).

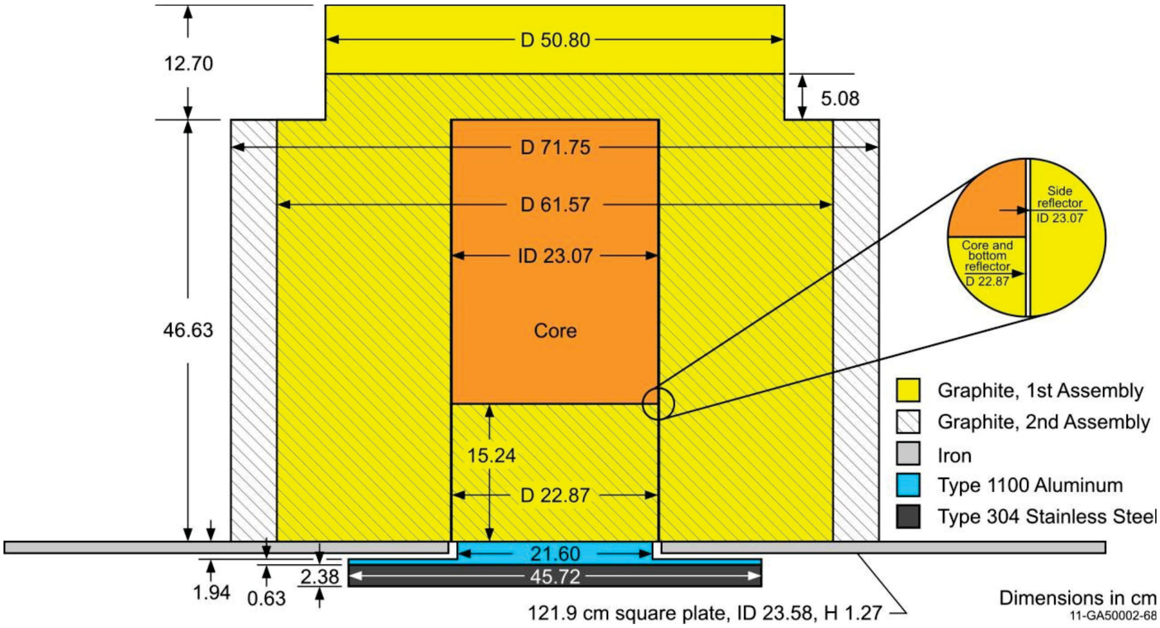

Figure 1.1-6. Reflector Arrangement in the Two Assemblies (Redrawn from References 1 and 2). See Figure 1.1-4 for additional dimension details.[a]

a. ORNL Drawing Identification: ORNL-LR-DWG 76383.

Table 1.1-4. Reflector Dimensions (see References 1 and 2).

	First Assembly		Second Assembly	
Side Reflector-Graphite (Type ATL)				
Thickness	19.25	cm	24.34	cm
Inside Diameter	23.07	cm	23.07	cm
Length	46.63	cm	46.63	cm
Mass	210.5	kg	298.0	kg
Top Reflector-Graphite (Type ATL)				
Thickness	12.70	cm	5.08	cm
Diameter	50.80	cm	50.80	cm
Mass	42.36	kg	16.94	kg
Bottom Reflector-Graphite (Type ATL)				
Thickness	15.24		cm	
Diameter	22.87		cm	
Mass	11.05		kg	
Additional Bottom Reflectors				
Aluminum (Type 1100)				
Thickness	1.94		cm	
Diameter	21.60		cm	
Mass	1.920		kg	
Aluminum (Type 1100)				
Thickness	0.63		cm	
Diameter	45.72		cm	
Mass	2.787		kg	
Stainless Steel (Type 304)				
Thickness	2.38		cm	
Diameter	45.72		cm	
Mass	3.91		kg[(a)]	
Iron				
Thickness	1.27		cm	
Inside Diameter	23.58		cm	
Outside Dimensions	121.9 × 121.9		cm	
Mass	137.9		kg	

(a) This mass is given as 7.76 kg in Reference 2; however, both of these masses are much lower than expected for nominal stainless steel.

1.1.2.4 Reactivity of Final Configurations

The two assemblies had a reactivity of +7.2 ¢ for the first assembly and +3.4 ¢ for the second. These reactivities were obtained from positive reactor period measurements using the delayed neutron parameters of Keepin, Wimett, and Zeigler (see Reference 2).[a] It is believed that these values were obtained by combining multiple experimental measurements performed between November 16 and December 5, 1962, but it is not known exactly which measurements were combined. An appropriate effective delayed neutron fraction, β_{eff}, for the system was 0.0068. (This β_{eff} value is an approximation made by the experimenter.)[b]

1.1.3 Material Data

Impurity analyses for the uranium oxide and the graphite and an isotopic analysis for the uranium were performed (see Reference 1). The fuel tubes were made of Type 347 stainless steel; the core tank and the aluminum shims were made of Type 1100 aluminum; and the vertical assembly machine support structures were made of Type 1100 aluminum, Type 304 stainless steel, and iron, as discussed in References 1 and 2. According to the experimenter, the iron table that supported the top and radial reflector was typical normal low-carbon steel.[c] The composition for these materials was not given. The material composition for the aluminum shims in the core tank was not given in the references or the logbooks. The core was reported to contain a ^{235}U mass of 61.39 kg, UO_2 mass of 74.84 kg, and a stainless-steel mass of 11.48 kg[d] (see References 1 and 2).

1.1.3.1 Fuel Composition

The basic fuel units were pellets of UO_2 with a density of 9.71 g/cm^3. The pellets were pressed and sintered at the Oak Ridge Y-12 Plant (see Reference 2). Table 1.1-5 shows an impurity analysis, and Table 1.1-6 shows the uranium isotopic distribution. The uncertainty in the isotopic distribution was ±0.005 wt.% for ^{234}U, ^{235}U, and ^{236}U.[e]

---

a. G. R. Keepin, T. F. Wimett, and R. K. Zeigler, "Delayed Neutrons from Fissionable Isotopes of Uranium, Plutonium and Thorium," *J. Nucl. Energy*, **6**, (1957).

b. Personal email communication with J. T. Mihalczo, August 19, 2011 and November 14, 2011.

c. Personal email communication with J. T. Mihalczo, May 23, 2011.

d. The UO_2 is based off of a fuel mass of 295.8 g per tube; 253 fuel rods in the core even though only 252 were actually present in the final configuration; and disregards impurities. The total stainless-steel mass is incorrect due to the incorrect fuel-tube mass given in Table 1.1-2.

e. According to J. T. Mihalczo (personal email communication, August 19, 2011), the uncertainty in the isotopic was the same as those given in HEU-MET-FAST-051 (*International Handbook of Evaluated Criticality Safety Benchmark Experiments*, NEA/NSC/DOC(95)03, OECD-NEA, Paris, 2012). This report gives the isotopic uncertainties stated above.

Table 1.1-5. Mass Spectrographic Analysis of Uranium Oxide (see Reference 1).[(a)]

Silver, Ag	<	40	ppm[(b)]
Beryllium, Be	<	0.3	ppm
Chromium, Cr		6 to 40	ppm
Lithium, Li	<	1.5	ppm
Nickel, Ni	<	25	ppm
Tin, Sn		5 to 25	ppm
Aluminum, Al		3 to 30	ppm
Calcium, Ca		50	ppm
Copper, Cu		3 to 35	ppm
Magnesium, Mg	<	12	ppm
Phosphorous, P	<	100	ppm
Boron, B	<	1	ppm
Iron, Fe		10 to 250	ppm
Manganese, Mn	<	8	ppm
Barium, Ba	<	10	ppm
Potassium, K	<	50	ppm
Sodium, Na	<	10	ppm
Silicon, Si		10 to 50	ppm

(a) Reference 1 reports these as results of spectrochemical analysis, but according to the experimenter, they were found using mass spectrographic analysis.
(b) These were measured by weight (Personal email communication with J. T. Mihalczo, September 13, 2011).

Table 1.1-6. Uranium Isotopic Composition (wt.%) (see References 1 and 2).

^{234}U	1.01
^{235}U	93.15
^{236}U	0.47
^{238}U	5.37

1.1.3.2 Graphite

The reflectors were all Type ATL graphite. A spectrochemical analysis of the graphite was performed for which results are given in Table 1.1-7.

Table 1.1-7. Spectrochemical Analyses of Type ATL Graphite (see Reference 1).

Element	ppm[(a)]	Element	ppm[(a)]
Aluminum, Al	270	Magnesium, Mg	1
Barium, Ba	22	Manganese, Mn	1
Boron, B	< 1	Molybdenum, Mo	5
Calcium, Ca	820	Sodium, Na	3
Cobalt, Co	3	Nickel, Ni	27
Chromium, Cr	16	Silicon, Si	54
Copper, Cu	1	Strontium, Sr	5
Iron, Fe	3940	Titanium, Ti	54
Potassium, K	5	Vanadium, V	220
Lithium, Li	2	Yttrium, Y	11
Lutetium, Lu	1	Ytterbium, Yb	3

(a) According to the experimenter (September 13, 2011), these were measured by weight.

1.1.4 Temperature Information

The temperature of the experiment was 72°F[a] (22°C).

1.1.5 Additional Information Relevant to Critical and Subcritical Measurements

Additional information was not identified.

1.2 Description of Buckling and Extrapolation Length Measurements

Buckling and extrapolation-length measurements were not made.

1.3 Description of Spectral Characteristics Measurements

1.3.1 Overview of the Measurements

Cadmium ratios were measured with enriched uranium metal foils through the radial reflector for the first assembly and are described in the following subsections.

1.3.2 Geometry of the Experiment Configuration and Measurement Procedure

The experiment configuration was the same as the critical configuration described in Section 1.0. The 1.27-cm-diameter radial holes, in the radial reflector located at the midplane of the core, were used for the cadmium ratio measurements. The experimenter inserted 0.75-cm-diameter × 0.010-cm-thick 93.15%-^{235}U-enriched uranium metal foils[b], some with 0.051-cm-thick cadmium covers and some without, into the radial holes in the side reflector by placing them between sections of graphite plugs. The activation of the uranium metal foils was measured after removal from the assembly using two lead-shielded NaI scintillation detectors as follows. These NaI scintillators were carefully matched and had detection efficiencies for counting delayed-fission-product gamma rays with energies above

a. Personal email communication with J. T. Mihalczo, May 23, 2011.

b. References 1 and 2 report the foil enrichment as 93.2 wt.%, but according to the experimenter, it was 93.15 wt.% (September 19, 2011).

250 KeV within 5%. In all foil activation measurements, one foil at a specific location was used as a normalizing foil to remove the effects of the decay of fission products during the counting measurements with the NaI detectors. The normalization foil was placed on one NaI scintillator and the other foil on the other NaI detector and the activities measured simultaneously. The activation of a particular foil was compared to that of the normalization foil by dividing the count rate for each foil by that of the normalization foil. To correct for the differing efficiencies of the two NaI detectors, the normalization foil was counted in Detector 1 simultaneously with the foil at position *x* in Detector 2, and then the normalization foil was counted simultaneously in Detector 2 with the foil from position *x* in Counter 1. The activity of the foil from position *x* was divided by the activity of the normalization foil counted simultaneously. This resulted in obtaining two values of the ratio that were then averaged. This procedure essentially removed the effect of the differing efficiencies of the two NaI detectors. Differing efficiencies of 10% resulted in errors in the ratios measured to less than 1%. The background counting rates with no foils on the NaI detectors were subtracted from all count rates. [a] The results of the cadmium ratio measurements are given in Table 1.3-1 and Figure 1.3-1. The experimenter pointed out that at a radial distance of 0.5 cm from the core, a cadmium ratio of 1.77 indicates that ~60% of the fission in the uranium foils were induced by neutrons with energies above the cadmium cutoff of 0.5 eV.

Table 1.3-1. Radial Cadmium Ratio (see Reference 1).[(a)]

Distance from Core[(b)]	Cadmium Ratio[(c)]
0.0	--[(d)]
0.5	1.77
1.0	1.81
2.0	1.92
3.5	2.03
5.5	2.18
6.5	--[(d)]
8.0	2.34
10.5	2.43
13.0	2.35
16.0	2.41

(a) These ratios coincide with the position of the relative activation of ^{235}U fission foils in the radial reflector measurements in Table 1.7-2.
(b) Reported as measured from the core-reflector interface; no additional information was given.
(c) The cadmium ratio is defined as the ratio of the bare-to-cadmium-covered foil activity.
(d) Cadmium ratios were not measured at this position.

a. Personal email communication with J. T. Mihalczo, September 27, 2011, and November 23, 2011. The experimenter believes a 250-KeV threshold was used “so as to not count the natural activity of the uranium foils” (November 14, 2011).

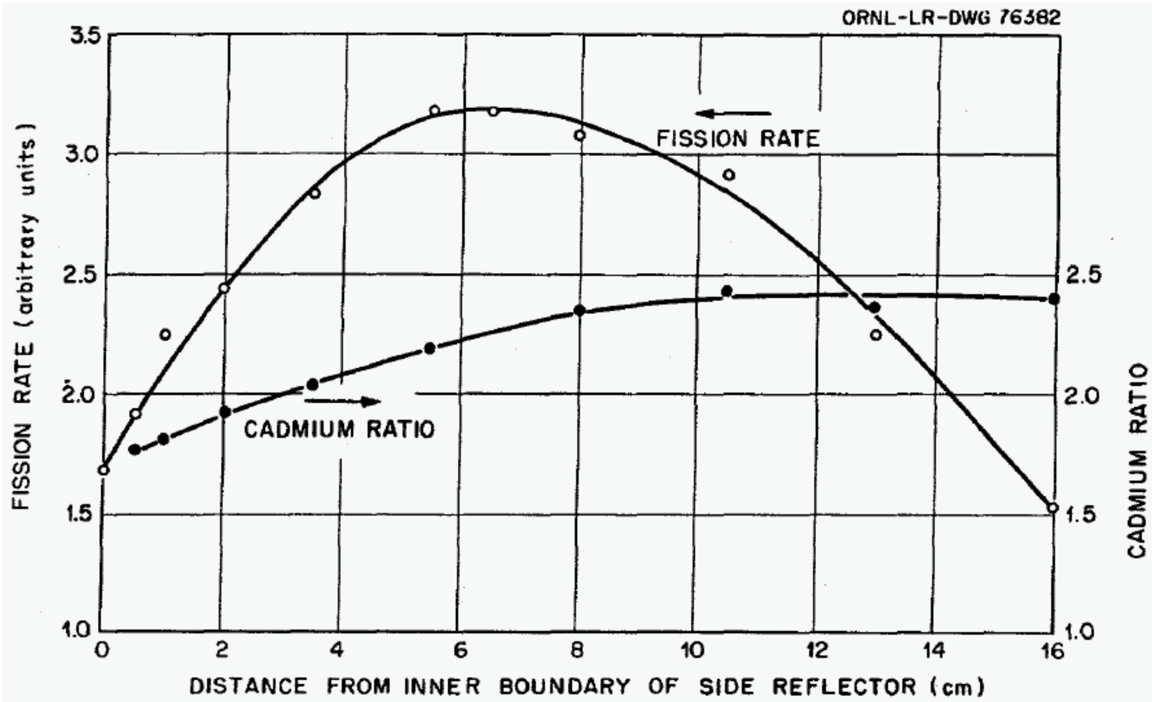

Figure 1.3-1. Plot of Relative Activation of ^{235}U Fission Foils (see Section 1.7) and Cadmium Ratios in the Radial Reflector of the First Assembly (see Reference 2).

1.3.3 Material Data

The uranium foils were 93.15 wt.% enriched. No impurity data were given for the uranium or cadmium foils. The impurity content of the uranium foil was similar to that for the uranium metal described in HEU-MET-FAST-051.[a] Material data for the core and reflector parts are the same as those given in Section 1.1.3.

1.3.4 Temperature Information

The temperature is the same as for the critical configuration (see Section 1.1.4).

1.3.5 Additional Information Relevant to Spectral Characteristics Measurements

Additional information was not identified.

a. International Handbook of Evaluated Criticality Safety Benchmark Experiments, NEA/NSC/DOC(95)03, OECD-NEA, Paris (2012).

1.4 Description of Reactivity Effects Measurements

1.4.1 Overview of the Measurements

The critical configurations included five of six graphite plugs inserted into 1.27-cm-diameter radial holes in the graphite side reflector. The worth of these graphite plugs was measured and reported in References 1 and 2 for Configuration 1. The graphite plugs were inserted into the holes in the radial reflector for fine adjustment of the reactivity (see Reference 2). The worth of the center fuel tube for Configuration 1[a] was also measured and reported.

1.4.2 Geometry of the Experiment Configuration and Measurement Procedure

The reactivities were measured using the reactor period method.

The worth of the center fuel element for Configuration 1 was about 32 ¢.

The plugs in the graphite were 0.95-cm-diameter graphite plugs (see Reference 1 and 2). The worth of one of these plugs was about +1.5 ¢ for Configuration 1. It is shown in the logbook (Page 44) that two radial plugs were removed and a 2.95 ¢ reactivity change was measured. This corresponds to a worth per plug of approximately 1.5 ¢.

1.4.3 Material Data

The material data are the same as those given for the critical configuration (see Section 1.1.3).

1.4.4 Temperature Information

The temperature is the same as for the critical configuration (see Section 1.1.4).

1.4.5 Additional Information Relevant to Reactivity Effects Measurements

Additional information was not identified.

1.5 Description of Reactivity Coefficient Measurements

Reactivity coefficient measurements were not performed.

1.6 Description of Kinetics Measurements

Kinetics measurements were not performed.

---

a. Personal communication with J. T. Mihalczo, September 19, 2011.

1.7 Description of Reaction-Rate Distribution Measurements

1.7.1 Overview of the Measurements

The relative axial distribution of induced fission in a uranium fission counter was measured for both assemblies. Within the core region of the assembly, this distribution is directly proportional to the fission-rate distribution.

Radial distribution of the relative activation of ^{235}U fission foils in the reflector was measured for the first assembly only. This measurement was also labeled as fission rate in References 1 and 2; however, according to the experimenter, it should be called the relative activation of ^{235}U fission foils in the radial reflector or the radial distribution of the relative activation of ^{235}U fission foils.[a]

Henceforth, the measurements labeled *fission rate* in References 1 and 2 will be called *axial distribution of the induced fission in a uranium fission counter* for the axial measurements and *activation of* ^{235}*U fission foils* for the radial measurements. *Relative activation* and *activation measurements* are used as a general term to refer to both of these measurements.

1.7.2 Geometry of the Experiment Configuration and Measurement Procedure

The activation measurements were performed for the critical assembly (as described in Section 1.1).

1.7.2.1 Axial Measurements

A 2.5-cm-long × 0.64-cm-diameter ^{235}U fission counter was used for the axial scans. The counter was inserted through a hole in the top reflector and into the space from which the center fuel rod had been removed. Counts were recorded on a digital readout scaler.[b] During the axial fission-rate scans, the reactor power was monitored with an external BF_3 counter sitting on the floor meters away from the assembly.[c] Normalized results, related to the BF_3 counter, are in Table 1.7-1, and the results are plotted in Figures 1.7-1 and 1.7-2. The normalization for results for the two assemblies was done independently. About 100,000 counts were collected on the BF_3 monitor at each point and an average of about 10,000 counts on the fission counter.

a. Personal communication with J. T. Mihalczo, September 19, 2011. and November 14, 2011.

b. Personal email communication with J. T. Mihalczo, November, 14, 2011.

c. Personal email communication with J. T. Mihalczo, September 29, 2011.

Table 1.7-1. Relative Axial Induced Fission in a Uranium Fission Counter (see Reference 1).

Distance from Bottom of Core[(a)] (cm)	Relative Activation[(b)] (Arbitrary Units)	
	First Assembly	Second Assembly
3.81	0.81	1.03
6.35	0.82	1.03
8.89	0.84	1.07
11.43	0.88	1.07
12.70	0.86	1.07
13.97	0.88	1.02
14.60	-	1.03
15.24	0.85	1.04
15.87	-	1.02
16.51	0.84	1.00
17.14	-	0.99
17.78	0.82	-
19.05	0.82	0.95
21.59	0.77	0.89
24.13	0.68	0.75
26.67	0.62	0.63
27.94	0.60	-
29.21	0.64	0.54
31.75	0.91	0.50
33.02	1.00	-
34.29	1.06	0.37
36.83	1.04	0.24
38.10	0.93	-
39.37	0.80	-
41.91	0.55	-

(a) Measured from the bottom of the stainless-steel fuel tubes.
(b) The detector was a ^{235}U fission counter 2.5 cm long × 0.64 cm diameter. All ratios were normalized to the values at 33.02 and 16.51 cm for the first and second assemblies, respectively.

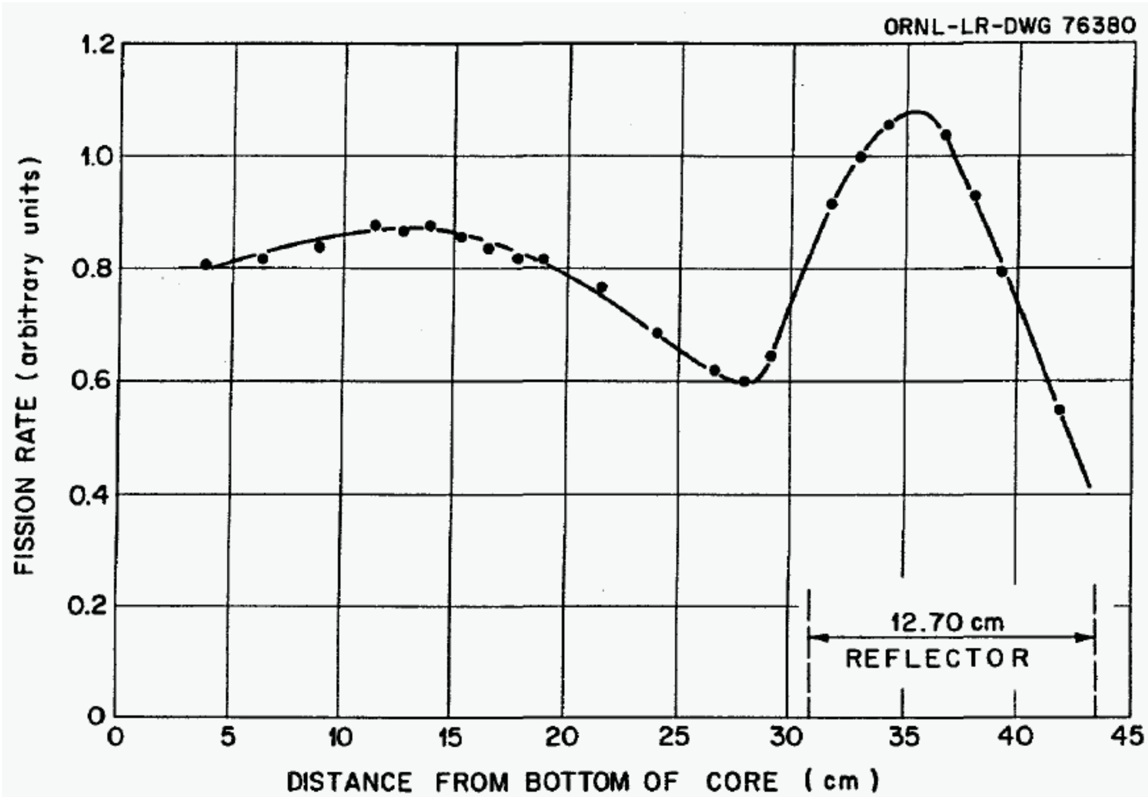

Figure 1.7-1. Normalized Axial Fission Distribution in a Uranium Fission Counter for Assembly 1 (Normalized to 33.02 cm, see Reference 2).

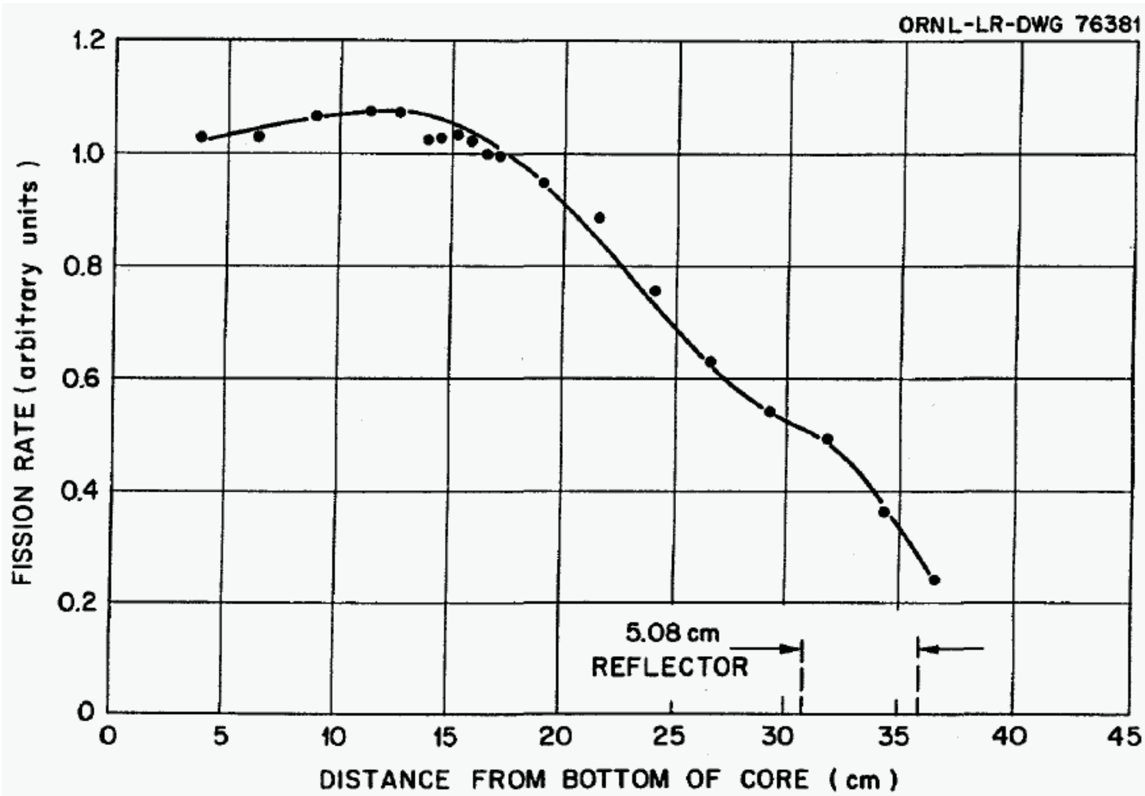

Figure 1.7-2. Relative Axial Fission Distribution in a Uranium Fission Counter for Assembly 2 (Normalized to 16.51 cm, see Reference 2).

1.7.2.2 Radial Measurements

The relative activation of ^{235}U fission foils was measured in the radial reflector of the first assembly (as described in Section 1.3.2), from the core tank out through the side reflector at the midplane of the core, using the radial holes in the reflectors. Foils were placed between sections of radial graphite plugs and placed at predetermined locations in the side reflector.[a] In addition, it is seen from the log book that a normalization foil was placed horizontally in the top reflector near the vertical center point of the reflector to relate the axial and radial scans. After activation, foils were placed in NaI detectors and the activity of the foils was measured, as described in Section 1.3.[b] The relative radial distribution activation of ^{235}U fission foils is given in Table 1.7-2 and Figure 1.7-3. A test irradiation, noted in the log book, showed counts of up to 40,000 per minute, depending on the discriminator setting. The data from the axial and radial measurements of the first assembly were expressed in the same arbitrary units, via the foil in the top reflector.

a. Personal email communication with J. T. Mihalczo, September 13, 2011.

b. Personal email communication with J. T. Mihalczo, September 27, 2011, and November 23, 2011. The experimenter believes a 250-KeV threshold was used "so as to not count the natural activity of the uranium foils" (November 14, 2011).

Table 1.7-2. Relative Activation of ^{235}U Fission Foils in Radial Reflector (see Reference 1).[a]

Distance from Core (cm)[b]	Relative Radial Distribution[c]
0.0	1.68
0.5	1.92
1.0	2.25
2.0	2.43
3.5	2.84
5.5	3.19
6.5	3.19
8.0	3.08
10.5	2.92
13.0	2.25
16.0	1.54

(a) These ratios were measured at locations that coincide with the position of the cadmium ratio measurements in Table 1.3-1.
(b) Measured from the core-reflector interface.
(c) Measured only through 19.25-cm-thick- side reflector of the first assembly.

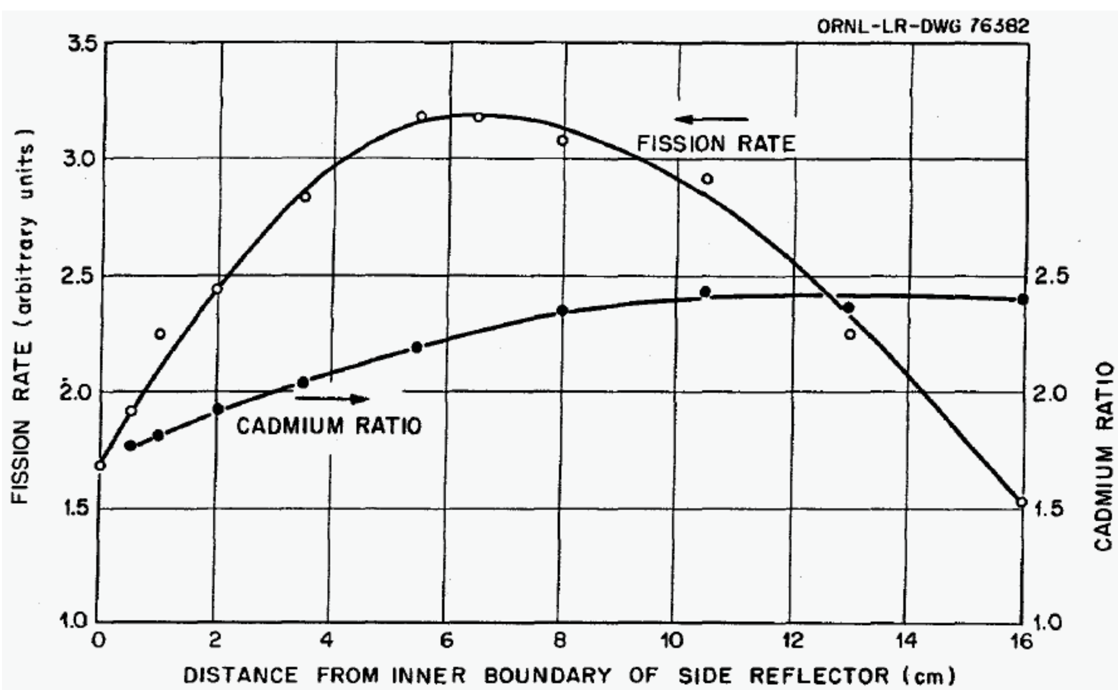

Figure 1.7-3. Relative Activation of ^{235}U Fission Foils in the Radial Reflector for Assembly 1 (see Reference 2).

1.7.3 Material Data

Material data for the core and reflector parts are the same as those given for the critical configuration (see Section 1.1.3).

1.7.3.1 Axial Measurements

The counter was ^{235}U, but the material of the counter housing was brass.[a] According to the experimenter, the enrichment and isotopics of the uranium metal in the counter was the same as the uranium metal described in HEU-METAL-FAST-052.[b,c]

1.7.3.2 Radial Measurements

The irradiated foils were 93.15 wt.% ^{235}U. The purity of the foils was not given. According to the experimenter, the enrichment and isotopics of the uranium metal foils was the same as the uranium metal described in HEU-METAL-FAST-052.[b,c]

1.7.4 Temperature Information

The temperature is the same as for the critical configuration (see Section 1.1.4).

1.7.5 Additional Information Relevant to Reaction-Rate Distribution Measurements

Additional information is not available.

1.8 Description of Power Distribution Measurements

The axial relative power distribution is the same as the relative fission rate that was measured in the core region of Assembly 1 (see Section 1.7).

1.9 Description of Isotopic Measurements

Isotopic measurements were not performed.

1.10 Description of Other Miscellaneous Types of Measurements

Other miscellaneous types of measurements were not performed.

---

a. Personal communication with J. T. Mihalczo, September 19, 2011.

b. Persona communication with J. T. Mihalczo, November 23, 2011.

c. International Handbook of Evaluated Criticality Safety Benchmark Experiments, NEA/NSC/DOC(95)03, OECD-NEA, Paris (2012).

2.0 EVALUATION OF EXPERIMENTAL DATA

2.1 Evaluation of Critical and/or Subcritical Configuration Data

Two critical configurations were evaluated using Monte Carlo N-Particle (MCNP) Versions 5-1.51 and 5-1.60[a] and ENDF/B-VII.0[b] neutron cross section libraries. Unless stated otherwise, the benchmark model, as described in Section 3, was used for the uncertainty analyses. The effect of the uncertainty in all measured parameters was found individually by increasing and decreasing the specified value by a given amount; the Δk_{eff} for that uncertainty was found by taking one-half of the difference between the k_{eff} values for the perturbed models. The magnitude of most perturbations was increased from the 1σ uncertainties in order to obtain statistically significant results. The ratio of the perturbation to the 1σ uncertainty for the parameter was used as a "scaling factor" to convert the calculated Δk_{eff} to a 1σ uncertainty in k_{eff}. All models were calculated such that the statistical uncertainty, σ_{MC}, is less than or equal to ±0.00006. An uncertainty was considered to have a negligible effect (NEG) when the magnitude of the 1σ Δk_{eff} was ≤0.00010.

Henceforth, Configurations/Assemblies 1 and 2 will be referred to as Cases 1 and 2, respectively.

2.1.1 Uncertainty in Reactivity of Critical Configurations

The two critical configurations had positive reactivities of 7.2 and 3.4 ¢. The experimenter estimated the β_{eff} for the system to be 0.0068. The β_{eff} also was calculated for both cases using two methods; the four β_{eff}'s were averaged. The first method used k_{prompt}, calculated by MCNP5, and compared it to k_{eff} to calculate β_{eff} ($\beta_{eff} = 1 - k_{prompt}/k_{eff}$) (see HEU-MET-FAST-059).[c] The second method used MCNP5 to calculate β_{eff} directly. The four values were averaged to obtain a β_{eff} of 0.0072. This value was used for this evaluation.[d] An uncertainty in the reactivity measurements of 10% and 5% in the β_{eff} value were assumed as 1σ uncertainties, typical for this facility, as shown in HEU-MET-FAST-059 and HEU-MET-FAST-069.[c] However, since the reactivity values were obtained from an unknown combination of experiment runs, the 1σ uncertainty was arbitrarily increased to 20%. The measured reactivity in cents, β_{eff}, and the calculated measured reactivity in terms of Δk_{eff} are given in Table 2.1-1.

Table 2.1-1. Uncertainty in Reactivity Measurement of Critical Configurations.

Case	Measured Reactivity (¢)	±	20% (1σ)	β_{eff} ± 5% (1σ)	Reactivity (Δk_{eff})	±	σ
1	+7.2	±	1.44	0.0072 ± 0.00036	0.00052	±	0.00011
2	+3.4	±	0.68		0.00025	±	0.00005

a. F. B. Brown, R. F. Barrett, T. E. Booth, J. S. Bull, L. J. Cox, R. A. Forster, T. J. Goorley, R. D. Mosteller, S. E. Post, R. E. Prael, E. C. Selcow, A. Sood, and J. Sweezy, "MCNP Version 5," LA-UR-02-3935, Los Alamos National Laboratory (2002).

b. M. B. Chadwick, et al., "ENDF/B-VII.0: Next Generation Evaluated Nuclear Data Library for Nuclear Science and Technology," *Nucl. Data Sheets*, **107**: 2931-3060 (2006).

c. International Handbook of Evaluated Criticality Safety Benchmark Experiments, NEA/NSC/DOC(95)03, OECD-NEA, Paris (2012).

d. B.C. Kiedrowski, et. al., "MCNP5-1.60 Feature Enhancements and Manual Clarifications," LA-UR-10-06217, Los Alamos National Laboratory (2010).

2.1.2 Graphite Reflector Dimensions Uncertainties

The dimensions of the reflectors were varied to obtain the two different critical configurations. The uncertainty in the dimensions of the top, side, and bottom reflector was ±1 in the last significant digit for the mass and dimension measurements. This value was taken to be the 1σ total uncertainty. Each reflector size measurement for each configuration was perturbed individually by 5 times the given uncertainty. The mass of the reflector was conserved when the dimensions were varied. The reflector thickness was perturbed by varying the outer diameter of the side reflector and keeping the inside diameter constant. The inner diameter was perturbed by varying the inside diameter of the side reflector while keeping the thickness of the reflector constant—thus the outer diameter was also varied. Total mass was conserved when performing these perturbations. The results are given in Table 2.1-2.

Table 2.1-2. Uncertainty in Reflector Dimensions.

Case	Deviation	Δk_{eff}	±	σ_{MC}	Scaling Factor	Δk_{eff} (1σ)	±	σ
Side Reflector Thickness								
1	±0.05 cm	0.00082	±	0.00004	5	0.00016	±	0.00001
2		0.00082	±	0.00004	5	0.00016	±	0.00001
Side Reflector Inner Diameter								
1	±0.05 cm	0.00105	±	0.00004	5	0.00021	±	0.00001
2		0.00112	±	0.00004	5	0.00022	±	0.00001
Side Reflector Height								
1	±0.05 cm	0.00046	±	0.00004	5	0.00009	±	0.00001
2		0.00029	±	0.00004	5	0.00006	±	0.00001
Top Reflector Height								
1	±0.05 cm	0.00018	±	0.00004	5	0.00004	±	0.00001
2		0.00005	±	0.00004	5	0.00001	±	0.00001
Top Reflector Diameter								
1	±0.05 cm	0.00014	±	0.00004	5	0.00003	±	0.00001
2		0.00002	±	0.00004	5	<0.00001	±	0.00001
Bottom Reflector Height								
1	±0.05 cm	0.00012	±	0.00004	5	0.00002	±	0.00001
2		0.00007	±	0.00004	5	0.00001	±	0.00001
Bottom Reflector Diameter								
1	±0.05 cm	0.00004	±	0.00004	5	0.00001	±	0.00001
2		0.00006	±	0.00004	5	0.00001	±	0.00001

The total mass of the reflectors (263.91 and 325.99 kg) was averaged over the volume of all the reflectors (151342.8 and 185603.1 cm^3) for the benchmark models, giving an average density of 1.74379 and 1.76538 g/cm^3 for Cases 1 and 2, respectively. It was assumed that the mass of the side reflector included the mass of five plugs, and the mass of the top reflector included the mass of one plug. The mass of the top and bottom reflectors had an uncertainty of 0.01 kg and the side reflector had a mass uncertainty of 0.1 kg. These mass uncertainties were combined to obtain a total reflector mass uncertainty of 0.101 kg. The total mass of the reflectors was perturbed by 25 times this value to obtain the results in Table 2.1-3.

Table 2.1-3. Uncertainty in Total Reflector Mass.

Case	Deviation		Δk_{eff}	±	σ_{MC}	Scaling Factor	Δk_{eff} (1σ)	±	σ
1	±2.525 kg	±0.01668 g/cm^3	0.00237	±	0.00004	25	0.00009	±	<0.00001
2		±0.01360 g/ cm^3	0.00196	±	0.00004	25	0.00008	±	<0.00001

The uncertainty in the diameter of the holes was ±0.01 cm. The diameter of the holes was varied by ±0.15 cm. Total reflector mass was conserved during this perturbation. The Δk_{eff} for the uncertainty in the hole diameter is given in Table 2.1-4.

Table 2.1-4. Uncertainty in Hole Diameter.

Case	Deviation	Δk_{eff}	±	σ_{MC}	Scaling Factor	Δk_{eff} (1σ)	±	σ
1	±0.15 cm	0.00012	±	0.00001	15	0.00001	±	<0.00001
2		0.00012	±	0.00001	15	0.00001	±	<0.00001

The side reflectors had six radial holes, five of which were plugged, and a plugged hole in the top reflector. The diameter of these seven holes was 1.27 cm. The logbook lists the diameters of the plugs as 0.437 inches or 1.11 cm, which is larger than the value given in References 1 and 2 by 0.16 cm. According to the experimenter, the value from the logbook, 1.11 cm, is the correct plug diameter. The uncertainty in this value would have been ±0.01 cm; however, due to the disagreement between the published value and the logbook value, the uncertainty was arbitrarily increased to ±0.1 cm (1σ). A more detailed model than the benchmark model was used to determine the effect in the uncertainty of the diameter of the plug. The total mass of graphite was conserved when the plug diameter was varied by ±0.16 cm. The results can be found in Table 2.1-5.

Table 2.1-5. Uncertainty in Plug Diameter.

Case	Deviation	Δk_{eff}	±	σ_{MC}	Scaling Factor	Δk_{eff} (1σ)	±	σ
1	±0.16 cm	0.00006	±	0.00001	1.6	0.00004	±	0.00001
2		0.00010	±	0.00001	1.6	0.00006	±	0.00001

2.1.3 Core Tank Dimensions Uncertainty

The fuel tubes were tightly packed into an aluminum core tank and held tight using shims. All of the tank dimensions were perturbed by ±0.05 cm (5σ). The thickness of the side wall was varied by holding the OD of the tank constant while varying the inside diameter. The OD was varied while holding the wall thickness constant—thus the inside diameter was also varied. The varying of the bottom thickness and the height of the core tank affected the position of the bottom reflector in relation to the side reflector. Mass was conserved during all of these perturbations. Results are summarized in Table 2.1-6. The uncertainty in the core tank mass is summarized in Table 2.1-7.

Table 2.1-6. Uncertainty in Core Tank Dimensions.

Case	Deviation	Δk_{eff}	±	σ_{MC}	Scaling Factor	Δk_{eff} (1σ)	±	σ
Side Wall Thickness								
1	±0.05 cm	0.00006	±	0.00004	5	0.00001	±	0.00001
2		0.00012	±	0.00004	5	0.00002	±	0.00001
Bottom Thickness								
1	±0.05 cm	0.00004	±	0.00004	5	0.00001	±	0.00001
2		0.00028	±	0.00004	5	0.00006	±	0.00001
Outside Diameter								
1	±0.05 cm	0.00007	±	0.00004	5	0.00001	±	0.00001
2		0.00008	±	0.00004	5	0.00002	±	0.00001
Outside Length (Height)								
1	±0.05 cm	0.00002	±	0.00004	5	<0.00001	±	0.00001
2		0.00006	±	0.00004	5	0.00001	±	0.00001

Table 2.1-7. Uncertainty in Core Tank Mass.

Case	Deviation	Δk_{eff}	±	σ_{MC}	Scaling Factor	Δk_{eff} (1σ)	±	σ
1	±0.005 kg	0.00004	±	0.00004	5	0.00001	±	0.00001
2		<0.00001	±	0.00004	5	<0.00001	±	0.00001

Twenty-four shims at the periphery of the array were used to keep the fuel tubes tightly packed; twelve shims were used at the top of the core and twelve at the bottom. Shims were approximately 24° and 34° segments of a circle of 22.29-cm diameter and were 1.91 cm tall. All 24 shims weighed 185 g according to References 1 and 2. In the logbook, aluminum shim masses were given as being 63.72 g for 12 shims and 206.5 g for the other twelve shims, for a total mass of 270.22 g for 24 shims. If the density of the shims is calculated using the given dimensions and the two different masses, the 185 g mass yields a density of 2.80 g/ cm^3, which is very close to the nominal aluminum density. A shim mass of 270.22 g, however, yields a density much larger than the nominal aluminum density; therefore, it is assumed that the 185 g is the correct mass for the shims used in these experiments.[a] The 1σ uncertainty in the height of the shims was ±0.01 cm. The height of the shims was perturbed by moving the shim surface toward the midline of the core. The total mass of the shims was varied by ±5 g (5σ). The effect of these uncertainties on k_{eff} is summarized in Table 2.1-8.

a. The experimenter verified the 185-g shim mass as the correct mass (September 19, 2011).

Table 2.1-8. Uncertainty in Shim Size and Mass.

Case	Deviation	Δk_{eff}	±	σ_{MC}	Scaling Factor	Δk_{eff} (1σ)	±	σ
Uncertainty in Shim Size								
1	±0.05 cm	0.00005	±	0.00004	5	0.00001	±	0.00001
2		0.00004	±	0.00004		0.00001	±	0.00001
Uncertainty in Shim Mass								
1	±5 g	0.00001	±	0.00004	5	<0.00001	±	0.00001
2		0.00001	±	0.00004		<0.00001	±	0.00001

The core was lifted into the side reflector until it came into contact with the top reflector. According to the experimenter, the core placement would have been within 0.00254 cm of the top reflector (lower perturbation) and may actually have lifted the top reflector ~0.00254 cm (upper perturbation) (see Section 1.1.2.1). These are bounding uncertainties with a uniform distribution. Because the upper and lower uncertainties were not equal, this uncertainty was evaluated by comparing the upper and lower perturbed case to the benchmark model rather than to each other. As can be seen in Table 2.1-9, the uncertainty in core placement had a negligible effect.

Table 2.1-9. Uncertainty in Core Placement.

Case	Deviation	Δk_{eff}	±	σ_{MC}	Scaling Factor	Δk_{eff} (1σ)	±	σ
1	+0.00254 cm	-0.00016	±	0.00005	$\sqrt{3}$	-0.00009	±	0.00001
	-0.0254 cm	-0.00009	±	0.00005	$10\sqrt{3}$	<0.00001	±	0.00001
2	+0.00254 cm	-0.00001	±	0.00005	$\sqrt{3}$	-0.00001	±	0.00001
	-0.0254 cm	0.00001	±	0.00005	$10\sqrt{3}$	<0.00001	±	0.00001

2.1.4 Fuel and Fuel-Tube Dimensions Uncertainty

A total of 252 fuel tubes were used in the experiments. It is not known whether or not the dimensions of the fuel tubes were measured for multiple fuel tubes. The total uncertainty in the dimensions was given by the experimenter as plus or minus the last reported significant digit. This would have been ±0.01 cm for the fuel and fuel tube length.

Measurements in the logbook are often reported in inches to three significant digits. This would correspond to an uncertainty of ±0.001 in (or 0.00254 cm). This value is taken to the systematic component of the total uncertainty and is about 25% of the total. Thus the 0.01 cm uncertainty in the fuel and fuel tube lengths was split 25%/75% systematic/random uncertainties using Equation 2.1. When fuel-tube dimensions were perturbed, all 252 fuel tubes were perturbed simultaneously.

$$\Delta k_{eff,1\sigma} = \frac{1}{Scaling\ Factor} \cdot \sqrt{\left(\Delta k_{eff} \cdot 25\%\right)^2 + \frac{\left(\Delta k_{eff} \cdot 75\%\right)^2}{N}}. \qquad \text{Equation 2.1}$$

where $\Delta k_{eff,1\sigma}$ is the combined 1σ effect on k_{eff} and Δk_{eff} is the change in k_{eff} when all 252 fuel rods were perturbed simultaneously. N is 252.

The tolerance on the outside diameter of half-inch, stainless-steel tubing sold today (2011) is ±0.005 in. (0.0127 cm).[a] This is taken to be a bounding uncertainty with an equal probable distribution; thus, the1σ uncertainty is 0.00733 cm (0.0127/√3 cm). The thickness of the fuel tube was held constant when the outer diameter was varied; thus, the inside diameter was also varied. The thickness of the fuel tube could have varied by a maximum of 0.012 cm based on the pellet diameters; this value was taken to be a 3σ uncertainty; thus, the 1σ uncertainty would be 0.004 cm (0.012/3 cm). This uncertainty, 0.004 cm, was also used for the fuel pellet diameter uncertainty. Although the derivation of the uncertainty for the fuel tube diameter, fuel tube thickness, and fuel tube pellet diameter differed from the fuel and fuel tube length, it is judged that Equation 2.1 can still be used to account for systematic and random components of the uncertainty. The outer diameter of the fuel tube was held constant while varying the thickness of the fuel tube. The effects of these uncertainties are summarized in Table 2.1-10.

Table 2.1-10. Uncertainty in Fuel and Fuel-Tube Dimensions.

Case	Deviation	Δk_{eff}	±	σ_{MC}	Scaling Factor	Δk_{eff} (1σ)[(a)]	±	σ
Fuel-Tube Length								
1	±0.05 cm	<0.00001	±	0.00004	5	<0.00001	±	0.00001
2		0.00009	±	0.00004		<0.00001	±	0.00001
Fuel-Tube Outside Diameter								
1	±0.01 cm	0.00278	±	0.00004	1.36	0.00030	±	<0.00001
2		0.00276	±	0.00004		0.00030	±	<0.00001
Fuel-Tube Thickness								
1	±0.008 cm	0.00005	±	0.00004	2	0.00001	±	0.00002
2		0.00007	±	0.00004		0.00001	±	0.00002
Fuel Length								
1	±0.05 cm	0.00040	±	0.00004	5	0.00002	±	0.00001
2		0.00046	±	0.00004		0.00002	±	0.00001
Fuel-Pellet Diameter								
1	±0.005 cm	0.00006	±	0.00004	1.25	0.00001	±	0.00001
2		0.00001	±	0.00004		<0.00001	±	0.00001

(a) Equation 1.1 was used in addition to the scaling factor to find the overall Δk_{eff}. A more detailed model than the benchmark model was used to evaluate this uncertainty.

As discussed in Section 1.1.2.2, masses of the fuel and fuel tube were recorded and calculated in the logbook. These logbook masses were used in the benchmark model and are summarized in Table 2.1-11. Aside from rounding differences, these values agree with those in Table 1.1-2, except for the mass calculated for a fuel tube with two end caps. The calculated mass, which is the correct value, is greater than the reported mass by the mass of one end cap. The uncertainties in the measured masses were one in the last significant digit. The uncertainty for the measured masses and the propagated uncertainties from the calculated masses are given in Table 2.1-11. See Appendix B for the derivation of these values.

a. http://www.speedymetals.com/information/Material82.html#Tolerances (accessed November 12, 2011).

Table 2.1-11. Fuel and Fuel-Tube Mass.[(a)]

314 Fuel Tubes + Box	14,442	±	1	g
Box	397	±	1	g
314 Fuel Tubes	14,045	±	$1 \cdot \sqrt{2}$	g
1 Fuel Tube	44.729	±	$1 \cdot \sqrt{2}/314$ (0.0045)	g
324 End Cap	207.706	±	0.001	g
1 End Cap	0.64107	±	$0.001/324$ (3.1E-06)	g
1 Fuel Tube + 2 End Caps[(b)]	46.01114	±	0.0045[(c)]	g
Total Fuel Mass (279 tubes)	82,533.26	±	$0.01 \cdot \sqrt{279}$ (0.1670)	g
Average Fuel Mass per Tube	295.818	±	0.0006	g

(a) Number of digits was preserved to match the logbook.
(b) This value was calculated and used by the evaluator for the benchmark model and differs from the mass given in Reference 1 by the weight of one end cap.
(c) The uncertainty in the end cap mass is negligible in comparison to the uncertainty in the fuel-tube mass.

This method of averaging masses and uncertainty propagation washes out the uncertainty in the masses of individual fuel rods. Thus, the uncertainties derived in Table 2.1-11 were taken to be systematic uncertainties, and random uncertainties of ±0.5 g for the fuel-tube mass and ±1 g for the fuel mass per tube were arbitrarily chosen.[a] The systematic and random uncertainties were combined to obtain a total uncertainty using Equation 2.2. Total uncertainties of ±0.032 g and ±0.063 g for the fuel-tube mass and mass of fuel per tube, respectively, were obtained.

$$\sigma_{tot.} = \sqrt{\left(\sigma_{sys.}\right)^2 + \frac{(\sigma_{rand.})^2}{252}}. \qquad \text{Equation 2.2}$$

The mass of the 26 fuel pellets was averaged over the volume inside the fuel tube to obtain a smeared density for the benchmark model. Thus, the voids between and around the pellets were not present when evaluating the uncertainty in the mass of the fuel. As can be seen in Section 3.1.1, the effect of doing this is negligible. Results are given in Table 2.1-12.

It should be noted that the mass of fuel per tube that is calculated using the reported density of 9.71 g/cm^3 and the pellet dimensions is 295.57 g, which does not agree with the reported mass per tube of 295.818 g. Since a density is a derived value, the reported density of 9.71 g/cm^3 is not used in the benchmark model and the measured mass and dimensions were used in the calculation of atom densities instead.

a. The uncertainty in fuel mass was chosen based on the uncertainty in fuel mass of HEU-COMP-MIXED-001 (*International Handbook of Evaluated Criticality Safety Benchmark Experiments*, NEA/NSC/DOC(95)03, OECD-NEA, Paris, 2012).

Table 2.1-12. Uncertainty in Fuel and Fuel-Tube Masses.

Case	Deviation	Δk_{eff}	±	σ_{MC}	Scaling Factor	Δk_{eff} (1σ)	±	σ
Mass of Fuel (26 pellets)								
1	±0.50 g	0.00100	±	0.00004	7.9	0.00013	±	<0.00001
2		0.00095	±	0.00004		0.00012	±	<0.00001
Mass of Fuel Tube								
1	±0.05 g	0.00001	±	0.00004	1.6	0.00001	±	0.00002
2		0.00004	±	0.00004		0.00002	±	0.00002

2.1.5 Material Property Uncertainties

Material impurities were given for the uranium oxide and graphite as well as a uranium isotopic composition. ASTM standards were used for all other material compositions. When calculating atom densities, measured masses and calculated volumes were always used to find the material density even if a density was reported in Reference 1. When calculating atom densities from material impurity data and composition data, typically three types of values were given: (1) a single value (i.e., 15 ppm or 20 wt.%), which gives the actual content of the element in the material; (2) a maximum value (i.e., <15 ppm or <20 wt.%), which gives the maximum amount of an element present in the material; and (3) a range of values (i.e., 15–17 ppm or 20–22 wt.%), which gives the minimum and maximum amount of an element present in the material. When calculating atom densities for models, the actual content of the element, one-half of the maximum element content, and/or the middle of the range of element content were used for the material composition, respectively. When perturbing compositions, single values were perturbed by plus or minus the square root of the value[a], maximum values were varied between zero and the maximum, and range values were varied between the top and bottom of the range. These uncertainties are assumed to be bounding with uniform distribution probability.

2.1.5.1 Uranium Oxide Composition

The fuel was pellets of uranium oxide, UO_2. A spectrochemical analysis of the fuel is given in Table 1.1-5. These impurities are not included in the benchmark model; however, an uncertainty analysis was still completed on the fuel composition using a more detailed model than the benchmark model. The impurity content was calculated and perturbed using methods described in Section 2.1.5. All impurities were varied simultaneously, and results are summarized in Table 2.1-13.

Table 2.1-13. Uncertainty in Fuel Impurity Composition.

Case	Δk_{eff}	±	σ_{MC}	Scaling Factor	Δk_{eff} (1σ)	±	σ
1	0.00017	±	0.00004	$\sqrt{3}$	0.00010	±	0.00002
2	0.00015	±	0.00004	$\sqrt{3}$	0.00009	±	0.00002

a. Using the square root of the content as the uncertainty was used because compositions come from spectrographic results, which report contents in "counts." The uncertainty in the composition can then be defined as the square root of the value, as is commonly assumed for spectrographic measurements with a Poisson distribution. It is believed that this method provides an overestimate of the actual uncertainty.

The effect of variations on the ratio of oxygen to uranium, which has an assumed nominal value of 2.00 ± 0.02 (1σ), in the fuel was also evaluated by varying the ratio between 1.95 and 2.05. Results are summarized in Table 2.1-14.

Table 2.1-14. Uncertainty in Oxygen-to-Uranium Ratio.

Case	Deviation	Δk_{eff}	±	σ_{MC}	Scaling Factor	Δk_{eff} (1σ)	±	σ
1	±0.05	0.00044	±	0.00004	2.5	0.00018	±	0.00002
2		0.00031	±	0.00004	2.5	0.00012	±	0.00002

The uncertainty in the isotopic distribution of uranium was also evaluated. According to the experimenter, the uncertainty in the ^{234}U, ^{235}U, and ^{236}U content was ±0.005 wt.%; however, typical uncertainties for this time period at Oak Ridge National Laboratory would have been 0.0017 wt.%, 0.0177 wt.%, 0.0130 wt.% for the ^{234}U, ^{235}U, and ^{236}U, respectively. These typical values were used for the uranium isotopic uncertainties rather than the values given by the experimenter. It was assumed that the ^{238}U content was found by subtracting the ^{234}U, ^{235}U, and ^{236}U contents from unity; thus, when the content of a single isotope was perturbed, the ^{238}U content was varied to maintain unity. ^{234}U and ^{235}U were varied individually by ±0.5 wt.%, and ^{236}U was varied by ±0.45 wt.%. Results are summarized in Table 2.1-15.

Table 2.1-15. Uncertainty in Uranium Isotopic Distribution.

Case	Deviation	Δk_{eff}	±	σ_{MC}	Scaling Factor	Δk_{eff} (1σ)	±	σ
^{234}U Isotopic Content								
1	±0.5 wt.%	0.00108	±	0.00004	294.12	<0.00001	±	<0.00001
2		0.00106	±	0.00004		<0.00001	±	<0.00001
^{235}U Isotopic Content								
1	±0.5 wt.%	0.00228	±	0.00004	28.25	0.00008	±	<0.00001
2		0.00225	±	0.00004		0.00008	±	<0.00001
^{236}U Isotopic Content								
1	±0.45 wt.%	0.00009	±	0.00004	34.62	<0.00001	±	<0.00001
2		0.00006	±	0.00004		<0.00001	±	<0.00001

2.1.5.2 Graphite Composition

The reflectors were Type ATL graphite. A spectrochemical analysis of the graphite is given in Table 1.1-7. These impurities are not included in the benchmark model; however, an uncertainty analysis was still completed on the reflector composition using a more detailed model than the benchmark model. The impurity content was calculated and perturbed using methods described in Section 2.1.5. All impurities were varied simultaneously, and results are summarized in Table 2.1-16.

Table 2.1-16. Uncertainty in Graphite Composition.

Case	Δk_{eff}	±	σ_{MC}	Scaling Factor	Δk_{eff} (1σ)	±	σ
1	0.00012	±	0.00004	$\sqrt{3}$	0.00007	±	0.00002
2	0.00010	±	0.00004	$\sqrt{3}$	0.00006	±	0.00002

2.1.5.3 Fuel-Tube Composition

The fuel was clad in Type 347 stainless steel. The composition of the Type 347 stainless steel was not given, so a standard composition was used. The standard composition and the model composition, as determined using the methods described in Section 2.1.5, are given in Table 2.1-17. The perturbation of the composition was performed on all elements simultaneously using the method described in Section 2.1.5. When the composition was varied, iron content was varied to maintain a balance. The results of the perturbation of the composition are given in Table 2.1-18.

Table 2.1-17. Type 347 Stainless Steel Composition.

Element	Standard Composition[(a)(b)]	Model Composition
Iron, Fe	Balance	68.7225 wt.%
Carbon, C	0.08 wt.%	0.04 wt.%
Manganese, Mn	2.00 wt.%	1.00 wt.%
Silicon, Si	1.00 wt.%	0.50 wt.%
Chromium, Cr	17.0-19.0 wt.%	18.0 wt.%
Nickel, Ni	9.0-13.0 wt.%	11.0 wt.%
Phosphorus, P	0.045 wt.%	0.0225 wt.%
Sulfur, S	0.030 wt.%	0.0150 wt.%
Tantalum+Niobium, Ta + Nb	10×C min., 1.0 wt.% max	0.7 wt.% total 0.644 wt.% Nb, 0.056 wt.% Ta[(c)]

(a) ASTM Standard A 312/A 312M-09.
(b) Single values are maximum values.
(c) The split between Nb and Ta was determined based on the natural abundances of Nb and Ta in the earth's crust, 8 and 0.7 ppm, respectively. Shaw, R., Goodenough, K., et. al., "Niobium-tantalum," British Geological Survey, April 2011, www.MineralsUK.com, (accessed June 8, 2012).

Table 2.1-18. Uncertainty in Fuel-Tube Composition.

Case	Δk_{eff}	±	σ_{MC}	Scaling Factor	Δk_{eff} (1σ)	±	σ
1	0.00016	±	0.00004	$\sqrt{3}$	0.00009	±	0.00002
2	0.00024	±	0.00004	$\sqrt{3}$	0.00014	±	0.00002

2.1.5.4 Core Tank Composition

The core tank was made of Type 1100 aluminum. The composition of the aluminum was not given, so a standard composition was used. Silicon and iron content was given as a maximum of the sum of the two elements. For the model, one-half the maximum was assumed as the total for both elements; thus, one-quarter of the maximum content was used for silicon and iron. All other element contents were found using methods described in Section 2.1.5. Aluminum was varied to maintain unity. For all elements except silicon and iron, perturbation methods described in Section 2.1.5 were used. For the uncertainty perturbation of iron and silicon, the iron content was set to the maximum (0.95 wt.%) for the upper uncertainty, and silicon was set to zero and vice versa for the lower uncertainty. The standard composition and the model composition are given in Table 2.1-19. Composition perturbation results are given in Table 2.1-20.

Table 2.1-19. Type 1100 Aluminum Composition.

Element	Standard Composition[(a)(b)]	Model Composition
Aluminum, Al	99.00 wt.% minimum	99.37 wt.%
Copper, Cu	0.05–0.20 wt.%	0.125 wt.%
Silicon, Si	0.95 wt.% Si + Fe	0.2375 wt.%
Iron, Fe		0.2375 wt.%
Manganese, Mn	0.05 wt.%	0.025 wt.%
Zinc, Zn	0.01 wt.%	0.005 wt.%
Other[(c)]	0.03 wt.% each 0.015 wt.% total	0.00 wt.%

(a) ASTM Standard B 209 - 07.
(b) Single values are maximum values.
(c) "Other" impurities were assumed have a negligible effect on k_{eff} and thus were not included in the benchmark model.

Table 2.1-20. Uncertainty in Core Tank Composition.

Case	Δk_{eff}	±	σ_{MC}	Scaling Factor	Δk_{eff} (1σ)	±	σ
1	0.00009	±	0.00004	$\sqrt{3}$	0.00005	±	0.00002
2	0.00009	±	0.00004	$\sqrt{3}$	0.00005	±	0.00002

The shims were assumed to be made of the same material as the core tank. The shim composition was evaluated with the same method as the evaluation of the core tank composition. The effect of the uncertainty in the shim composition is given in Table 2.1-21.

Table 2.1-21. Uncertainty in Shim Composition.

Case	Δk_{eff}	±	σ_{MC}	Scaling Factor	Δk_{eff} (1σ)	±	σ
1	0.00001	±	0.00004	$\sqrt{3}$	<0.00001	±	0.00002
2	0.00009	±	0.00004	$\sqrt{3}$	0.00005	±	0.00002

2.1.6 Uncertainty in Vertical Assembly Machine Support Plates

The support plates of the vertical assembly machine were removed in the benchmark model. A more detailed model than the benchmark model was used to determine the effect of the uncertainty in the dimensions, mass, and composition of those plates.

2.1.6.1 Uncertainty in Dimensions and Composition of Aluminum Plates

Two Type 1100 aluminum plates were positioned below the bottom reflector of the assembly. The dimensions and masses of these plates are given in Table 1.1-4. Dimensions and masses of these plates were perturbed by plus and minus twenty times the last significant digit (20σ). When perturbing the plate dimensions, mass was conserved. The results of this analysis are given in Tables 2.1-22 and 2.1-23.

Table 2.1-22. Uncertainty in Aluminum Support Plate Dimensions.

Case	Deviation	Δk_{eff}	±	σ_{MC}	Scaling Factor	Δk_{eff} (1σ)[(a)]	±	σ
Uncertainty in 1.94-cm-Thick-Plate Thickness								
1	± 0.25 cm	0.00009	±	0.00004	25	<0.00001	±	<0.00001
2		0.00013	±	0.00004		0.00001	±	<0.00001
Uncertainty in 1.94 cm-Thick- Plate Diameter								
1	± 0.5 cm	0.00003	±	0.00004	50	<0.00001	±	<0.00001
2		<0.00001	±	0.00004		<0.00001	±	<0.00001
Uncertainty in 0.63-cm-Thick-Plate Thickness								
1	± 0.5 cm	0.00021	±	0.00004	50	<0.00001	±	<0.00001
2		0.00023	±	0.00004		<0.00001	±	<0.00001
Uncertainty in 0.63-cm-Thick-Plate Diameter								
1	± 0.5 cm	0.00006	±	0.00004	50	<0.00001	±	<0.00001
2		0.00007	±	0.00004		<0.00001	±	<0.00001

Table 2.1-23. Uncertainty in Aluminum Support Plate Masses.

Case	Deviation	Δk_{eff}	±	σ_{MC}	Scaling Factor	Δk_{eff} (1σ)[(a)]	±	σ
Uncertainty in 1.94-cm-Thick-Plate Mass								
1	0.1 kg	0.00005	±	0.00004	100	<0.00001	±	<0.00001
2		0.00001	±	0.00004		<0.00001	±	<0.00001
Uncertainty in 0.63-cm-Thick-Plate Mass								
1	0.1 kg	0.00002	±	0.00004	100	<0.00001	±	<0.00001
2		0.00004	±	0.00004		<0.00001	±	<0.00001

The composition of the plates was calculated using the same method described in Section 2.1.2 and the composition given in Table 2.1-19. The composition was perturbed in the same manner as was done for the core tank. The results of this analysis are given in Table 2.1-24.

Table 2.1-24. Uncertainty in Aluminum Support Plate Composition.

Case	Δk_{eff}	±	σ_{MC}	Scaling Factor	Δk_{eff} (1σ)	±	σ
Uncertainty in Composition of 1.94-cm-Thick Plate							
1	0.00005	±	0.00004	$\sqrt{3}$	0.00003	±	0.00002
2	0.00001	±	0.00004		<0.00001	±	0.00002
Uncertainty in Composition of 0.63-cm-Thick Plate							
1	0.00005	±	0.00004	$\sqrt{3}$	0.00003	±	0.00002
2	<0.00001	±	0.00004		<0.00001	±	0.00002

2.1.6.2 Uncertainty in Dimensions and Composition of Stainless-Steel Plate

The vertical table assembly had a stainless-steel plate for the movable platform to which the core and bottom reflector were attached. The dimensions and mass of this plate were given in Reference 1. When the density of the plate is calculated using the 3.91 kg given in Reference 1 and the 7.76 kg given in Reference 2, the results are much lower than the typical density of Type 304 stainless steel—about 1.00 and 2.00 g/cm^3 compared to 7.9 g/cm^3.[a] This is believed to be a mistake in the reporting of the mass of the plate. The mass given in the published report for part three of the experimental series, 31.2 kg, was used for the models. This mass yields a density of 7.985 g/cm^3. The effects of the uncertainty in the dimensions of the stainless-steel plate, which are plus or minus the last significant digit, are given in Table 2.1-25. The density is held constant when perturbing the plate dimensions. The density of the stainless steel is varied between 7.5 and 8.03 g/cm^3 to obtain the uncertainty in density results in Table 2.1-25.

a. "Engineering Data for Metals and Alloys," *Metals Handbook Desk Edition*, Second Edition, ASM International, 1998, in ASM Handbooks Online, http://www.asmmaterials.info ASM International, 2002. (Accessed Aug. 18, 2011.)

Table 2.1-25. Uncertainty in Stainless-Steel Support Plate Dimensions and Density.

Case	Deviation	Δk_{eff}	±	σ_{MC}	Scaling Factor	Δk_{eff} (1σ)[a]	±	σ
Uncertainty in Plate Thickness								
1	± 0.5 cm	0.00040	±	0.00004	50	0.00001	±	<0.00001
2		0.00055	±	0.00004		0.00001	±	<0.00001
Uncertainty in Plate Diameter								
1	± 0.5 cm	0.00006	±	0.00004	50	<0.00001	±	<0.00001
2		0.00001	±	0.00004		<0.00001	±	<0.00001
Uncertainty in Plate Density								
1	±0.26 g/cm^3	0.00007	±	0.00004	2	0.00004	±	0.00002
2		<0.00001	±	0.00004		<0.00001	±	0.00002

The composition of Type 304 stainless steel was not given; thus, a standard had to be used. The same method described in Section 2.1.5 was used to determine the Type 304 stainless steel material composition for the models. The standard and model compositions used are given in Table 2.1-26.

Table 2.1-26. Type 304 Stainless Steel Composition.

Element	Standard Composition[a][b]	Model Composition
Iron, Fe	Balance	69.9225 wt.%
Carbon, C	0.08 wt.%	0.04 wt.%
Manganese, Mn	2.00 wt.%	1.00 wt.%
Silicon, Si	1.00 wt.%	0.50 wt.%
Chromium, Cr	18.0-20.0 wt.%	19.00 wt.%
Nickel, Ni	8.0-11.0 wt.%	9.50 wt.%
Phosphorus, P	0.045 wt.%	0.0225 wt.%
Sulfur, S	0.03 wt.%	0.015 wt.%

(a) ASTM Standard A 312/A 312M-09.
(b) Single values are maximum values.

The composition of the stainless steel was perturbed using the methods described in Section 2.1.5. The results of the perturbation are given in Table 2.1-27.

Table 2.1-27. Uncertainty in Stainless-Steel Support Plate Composition.

Case	Δk_{eff}	±	σ_{MC}	Scaling Factor	Δk_{eff} (1σ)	±	σ
1	0.00008	±	0.00004	$\sqrt{3}$	0.00004	±	0.00002
2	0.00004	±	0.00004		0.00003	±	0.00002

2.1.6.3 Uncertainty in Dimensions and Composition of Iron Support Table

The vertical table assembly had an iron (low-carbon steel) table to support the upper portion of the assembly. The dimensions and mass of this table are given in Reference 1. When perturbing the table dimensions, mass was conserved. The uncertainty in dimensions and mass of the iron table are plus or minus the last significant digit and are evaluated in Table 2.1-28.

Table 2.1-28. Uncertainty in Iron Support Table Dimensions and Masses.

Case	Deviation	Δk_{eff}	±	σ_{MC}	Scaling Factor	Δk_{eff} (1σ)[a]	±	σ
Uncertainty in Table Thickness								
1	±0.25 cm	0.00019	±	0.00004	25	0.00001	±	<0.00001
2		0.00028	±	0.00004		0.00001	±	<0.00001
Uncertainty in Table Inside Diameter								
1	±0.5 cm	<0.00001	±	0.00004	50	<0.00001	±	<0.00001
2		0.00002	±	0.00004		<0.00001	±	<0.00001
Uncertainty in Table Outer Dimensions								
1	± 0.5 cm	0.00003	±	0.00004	5	0.00001	±	0.00001
2		0.00006	±	0.00004		0.00001	±	0.00001
Uncertainty in Table Mass								
1	±5 kg	0.00006	±	0.00004	50	<0.00001	±	<0.00001
2		0.00001	±	0.00004		<0.00001	±	<0.00001

The table was reported as being iron. According to the experimenter it was, more specifically, typical low-carbon steel. The carbon steel composition given in Table 2.1-29 was used.

Table 2.1-29. Carbon Steel Composition.

Element	Standard Composition[a]	Model Composition
Fe	Balance	98.305 wt.%
Carbon	0.25 wt.%	0.25 wt.%
Mg	0.80–1.20 wt.%	1.00 wt.%
P	0.04 wt.% max	0.02 wt.%
S	0.05 wt.% max	0.025 wt.%
Si	0.40 wt.% max	0.20 wt.%
Cu	0.20 wt.%	0.20 wt.%

(a) ASTM Standard A 36/A36M 08.

The composition of the iron table was perturbed using the methods described in Section 2.1.5. The results of the perturbation are given in Table 2.1-30.

Table 2.1-30. Uncertainty in Iron Support Table Composition.

Case	Δk_{eff}	±	σ_{MC}	Scaling Factor	Δk_{eff} (1σ)	±	σ
1	0.00001	±	0.00004	$\sqrt{3}$	<0.00001	±	0.00002
2	0.00008	±	0.00004		0.00004	±	0.00002

2.1.7 Temperature Uncertainty

The experiments were carried out at 22°C or 295.15 K. The temperature in the facility could have varied a few degrees (1°C is 1σ). The temperature coefficient for bare, highly enriched uranium metal experiments at this facility was 0.3 ¢/ΔT(°C). The temperature coefficient for this experiment would have been less than this because of the reflector, and thus the effect of the uncertainty in the temperature on k_{eff} would have been negligible.[a]

2.1.8 Total Uncertainty in Critical Experiments

All 1σ uncertainties were compiled and are summarized in Table 2.1-31. An uncertainty is considered to have a negligible effect (NEG) when the magnitude of the 1σ Δk_{eff} is ≤0.00010. The negligible uncertainties are within the statistical noise of the Monte Carlo calculations. It is not feasible to further reduce the already small statistical uncertainty; therefore, it is judged that the total contribution of all negilibile uncertainties to the total experimental uncertainty would also be neligible.

The main contributors to the total uncertainty were the side reflector thickness and inside diameter and the diameter of the fuel tube. The magnitudes of the effect of non-negligible uncertainties are shown in Figure 2.1-1. The statistical uncertainties in the Monte Carlo calculation were not preserved in Table 2-1.31, but can be found in the preceding sections if necessary.

The two described experiments are judged to be acceptable criticality safety benchmark experiments.

Table 2.1-31. Summary of Uncertainties.

	Case 1				Case 2			
	Parameter Value[(a)]			±Δkeff (1σ)	Parameter Value[(a)]			±Δkeff (1σ)
Reactivity of Critical Configurations	+7.2	±	1.44 ¢	0.00011	+ 3.4	±	0.68 ¢	NEG
Side Reflector Thickness	19.25	±	0.01 cm	0.00016	24.34	±	0.01 cm	0.00016
Side Reflector Inner Diameter	23.07	±	0.01 cm	0.00021	23.07	±	0.01 cm	0.00022
Side Reflector Height	46.63	±	0.01 cm	NEG	46.63	±	0.01 cm	NEG
Top Reflector Height	12.70	±	0.01 cm	NEG	5.08	±	0.01 cm	NEG
Top Reflector Diameter	50.80	±	0.01 cm	NEG	50.80	±	0.01 cm	NEG
Bottom Reflector Height	15.24	±	0.01 cm	NEG	15.24	±	0.01 cm	NEG

a. Personal email communication with J. T. Mihalczo, November 14, 2011.

	Case 1		Case 2	
	Parameter Value[(a)]	±Δkeff (1σ)	Parameter Value[(a)]	±Δkeff (1σ)
Bottom Reflector Diameter	22.87 ± 0.01 cm	NEG	22.87 ± 0.01 cm	NEG
Total Reflector Mass	263.91 ± 0.101 kg	NEG	325.99 ± 0.101 kg	NEG
Plug Diameter	1.11 ± 0.01 cm	NEG	1.11 ± 0.01 cm	NEG
Hole Diameter	1.27 ± 0.01 cm	NEG	1.27 ± 0.01 cm	NEG
Core Tank Side Wall Thickness	0.29 ± 0.01 cm	NEG	0.29 ± 0.01 cm	NEG
Core Tank Bottom Thickness	0.35 ± 0.01 cm	NEG	0.35 ± 0.01 cm	NEG
Core Tank Outside Diameter	22.87 ± 0.01 cm	NEG	22.87 ± 0.01 cm	NEG
Core Tank Outside Length (Height)	31.11 ± 0.01 cm	NEG	31.11 ± 0.01 cm	NEG
Core Tank Mass	2.134 ± 0.001 kg	NEG	2.134 ± 0.001 kg	NEG
Shim Size (Height)	1.91 ± 0.01 cm	NEG	1.91 ± 0.01 cm	NEG
Shim Mass (24 Shims)	185 g ± 1 g	NEG	185 ± 1 g	NEG
Core Placement	Section 2.1.3	NEG	Section 2.1.3	NEG
Fuel-Tube Length	30.48 ± 0.01 cm[(b)]	NEG	30.48 ± 0.01 cm[(b)]	NEG
Fuel-Tube Outside Diameter	1.27 ± 0.007 cm[(b)]	0.00030	1.27 ± 0.007 cm[(b)]	0.00030
Fuel-Tube Thickness	0.051 ± 0.004 cm[(b)]	NEG	0.051 ± 0.004 cm[(b)]	NEG
Fuel Length (26 Pellets)	29.88 ± 0.01 cm[(b)]	NEG	29.88 ± 0.01 cm[(b)]	NEG
Fuel-Pellet Diameter	1.141 ± 0.004 cm[(b)]	NEG	1.141 ± 0.004 cm[(b)]	NEG
Fuel Mass (26 Pellets)	295.8 ± 0.06 g	NEG	295.8 ± 0.06 g	NEG
Fuel-Tube Mass	45.37 ± 0.03 g	0.00013	45.37 ± 0.03 g	0.00012
Fuel Composition	Section 2.1.5.1	NEG	Section 2.1.5.1	NEG
Uranium-to-Oxygen Ratio	2.00 ± 0.02	0.00018	2.00 ± 0.02	0.00012
Uranium Isotopic Distribution	Section 2.1.5.1	NEG	Section 2.1.5.1	NEG
Uranium Isotopic Distribution	Section 2.1.5.1	NEG	Section 2.1.5.1	NEG
Uranium Isotopic Distribution	Section 2.1.5.1	NEG	Section 2.1.5.1	NEG
Uranium Isotopic Distribution	Section 2.1.5.1	NEG	Section 2.1.5.1	NEG
Graphite Composition	Section 2.1.5.2	NEG	Section 2.1.5.2	NEG
Fuel-Tube Composition	Section 2.1.5.3	NEG	Section 2.1.5.3	0.00014
Core-Tank Composition	Section 2.1.5.4	NEG	Section 2.1.5.4	NEG
1.94-cm-Thick Al Plate Thickness	1.74 ± 0.01 cm	NEG	1.74 ± 0.01 cm	NEG

	Case 1		Case 2	
	Parameter Value[(a)]	±Δkeff (1σ)	Parameter Value[(a)]	±Δkeff (1σ)
1.94-cm-Thick Al Plate Diameter	21.60 ± 0.01 cm	NEG	21.60 ± 0.01 cm	NEG
0.63-cm-Thick Al Plate Thickness	0.63 ± 0.01 cm	NEG	0.63 ± 0.01 cm	NEG
0.63-cm-Thick Al Plate Diameter	45.72 ± 0.01 cm	NEG	45.72 ± 0.01 cm	NEG
1.94-cm-Thick Al Plate Mass	1.920 ± 0.001 kg	NEG	1.920 ± 0.001 kg	NEG
0.63-cm-Thick Al Plate Mass	2.787 ± 0.001 kg	NEG	2.787 ± 0.001 kg	NEG
1.94-cm-Thick Al Plate Composition	Section 2.1.6.1	NEG	Section 2.1.6.1	NEG
0.63-cm-Thick Al Plate Composition	Section 2.1.6.1	NEG	Section 2.1.6.1	NEG
Stainless-Steel Plate Thickness	2.38 ± 0.01 cm	NEG	2.38 ± 0.01 cm	NEG
Stainless-Steel Plate Diameter	45.72 ± 0.01 cm	NEG	45.72 ± 0.01 cm	NEG
Stainless-Steel Plate Density	7.9 ± 0.4 g/cm^3	NEG	7.9 ± 0.4 g/cm^3	NEG
Stainless-Steel Plate Composition	Section 2.1.6.2	NEG	Section 2.1.6.2	NEG
Iron Table Thickness	1.27 ± 0.01 cm	NEG	1.27 ± 0.01 cm	NEG
Iron Table Inside Diameter	23.58 ± .01 cm	NEG	23.58 ± .01 cm	NEG
Iron Table Size	121.9 ×121.9 ± 0.1 cm	NEG	121.9 ×121.9 ± 0.1 cm	NEG
Iron Table Mass	137.9 ± 0.1 kg	NEG	137.9 ± 0.1 kg	NEG
Iron Table Composition	Section 2.1.6.3	NEG	Section 2.1.6.3	NEG
Shim Composition	- ± -	NEG	- ± -	NEG
Temperature	22°C ± 1°C	NEG	22°C ± 1°C	NEG
Total	0.00047		0.00046	

(a) Uncertainty is 1σ uncertainty unless stated otherwise.
(b) This uncertainty is 25% systematic and 75% random (see Section 2.1.4).

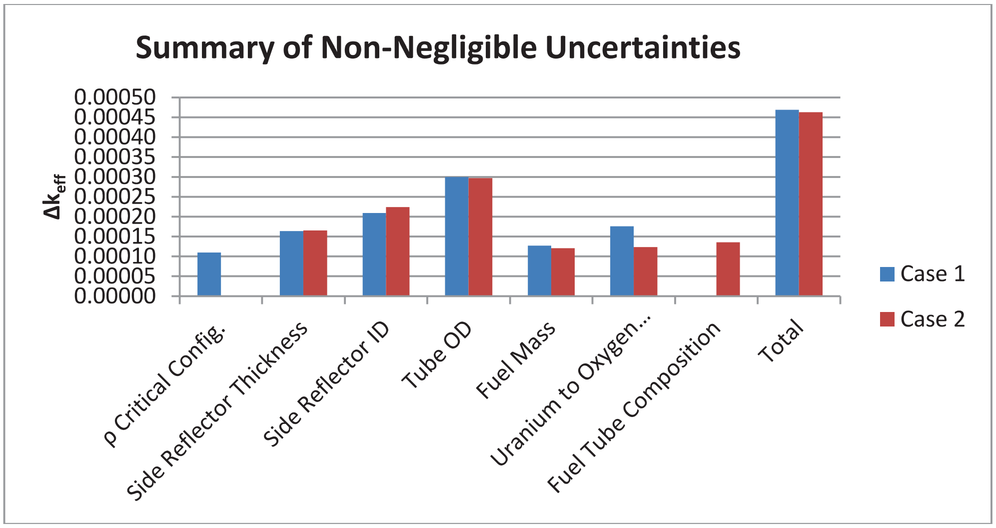

Figure 2.1-1. Summary of Non-Negligible Uncertainties.[a]

2.2 Evaluation of Buckling and Extrapolation Length Data

Buckling and extrapolation-length measurements were not performed.

2.3 Evaluation of Spectral Characteristics Data

Spectral characteristics measurements were not evaluated.

2.4 Evaluation of Reactivity Effects Data

No uncertainty in the worth measurements was reported. A 10% 1σ uncertainty was assumed for the worth measurements.[b] Two plugs were removed when determining the worth of a single plug, and it is believed that six plugs were present in the reflector and two plugs were removed when these measurements were performed. The worth of a radial plug was 2.95 ± 0.295 ¢ for two plugs, or about 1.5 ± 0.15 ¢ per plug, and the center fuel rod was worth 32 ± 3.2 ¢.

2.5 Evaluation of Reactivity Coefficient Data

Reactivity coefficient measurements were not performed.

2.6 Evaluation of Kinetics Measurements Data

Kinetics measurements were not performed

2.7 Evaluation of Reaction-Rate Distributions

2.7.1 Axial Measurements

For the measurement of the axial induced fission in a uranium fission counter, as discussed in Section 1.7.2, about 100,000 counts were collected on the BF_3 monitor and an average of about 10,000 counts on the fission counter. The uncertainty in the measurement can be approximated by adding in

a. The effect of the uncertainty in the reactivity of Case 2 is negligible.

b. A 10% uncertainty was recommended by the experimenter, November 23, 2011.

quadrature the uncertainty of a single measurement ($\sqrt{10{,}000}$) and the uncertainty in the normalization measurement ($\sqrt{10{,}000}$) then dividing by the number of counts taken for the normalization measurement (10,000). This yields a measurement uncertainty of approximately ±1.5%. An uncertainty in the axial location of the detector of ±1 mm yields an average uncertainty of ±0.6% for Case 1 and ±0.7% for Case 2.[a] The measurement, placement, and counter composition uncertainties in the axial distribution of induced fission in a uranium fission counter total ±1.6% for Case 1 and ±1.7% for Case 2 (1.5% and 0.6% or 0.7% added in quadrature). There is also an additional uncertainty in the measurements of ±0.01, bounding with a uniform distribution, due to the rounding of the measured values. These uncertainties, added in quadrature, are given in Table 2.7-1 and shown in Figure 2.7-1. Measurements made in the reflector region are highlighted.

The effect of the fission counter enrichment and purity was evaluated by comparing tallies for a 100 wt.% ^{235}U counter to a 93.2 wt.% ^{235}U counter. It was found that this 6.8 wt.% change in enrichment yields a maximum change in the normalized tally results of 5.0% for Case 1 and 10.4% for Case 2. When scaled to an enrichment uncertainty of 0.005% (see Section 2.1.5.1), the effect of this uncertainty would be negligible.

a. This analysis was based on MCNP results. A smaller uncertainty is obtained if using the experimental results.

Table 2.7-1. Uncertainty in Axial Distribution of the Induced Fission in a Uranium Fission Counter.

Distance from Bottom of Core[(a)] (cm)	Induced Fission[(b)] (Arbitrary Units)					
	Case 1[(c)]			Case 2[(d)]		
3.81	0.81	±	0.01	1.03	±	0.02
6.35	0.82	±	0.01	1.03	±	0.02
8.89	0.84	±	0.01	1.07	±	0.02
11.43	0.88	±	0.02	1.07	±	0.02
12.70	0.86	±	0.01	1.07	±	0.02
13.97	0.88	±	0.02	1.02	±	0.02
14.60		-		1.03	±	0.02
15.24	0.85	±	0.01	1.04	±	0.02
15.87		-		1.02	±	0.02
16.51	0.84	±	0.01	1.00	±	0.02
17.14		-		0.99	±	0.02
17.78	0.82	±	0.01		-	
19.05	0.82	±	0.01	0.95	±	0.02
21.59	0.77	±	0.01	0.89	±	0.02
24.13	0.68	±	0.01	0.75	±	0.01
26.67	0.62	±	0.01	0.63	±	0.01
27.94	0.6	±	0.01		-	
29.21	0.64	±	0.01	0.54	±	0.01
31.75	0.91	±	0.02	0.50	±	0.01
33.02	1.00	±	0.02		-	
34.29	1.06	±	0.02	0.37	±	0.01
36.83	1.04	±	0.02	0.24	±	0.01
38.10	0.93	±	0.02		-	
39.37	0.80	±	0.01		-	
41.91	0.55	±	0.01		-	

(a) Measured from the bottom of the stainless-steel fuel tubes.
(b) The detector was ^{235}U fission counter 2.5 cm long × 0.64 cm diameter.
(c) Uncertainty includes measurement, placement, and counter purity uncertainty (±1.6%) and a ±0.01/√3 round-off uncertainty.
(d) Uncertainty includes measurement and placement uncertainty (±1.7%) and a ±0.01/√3 round-off uncertainty.

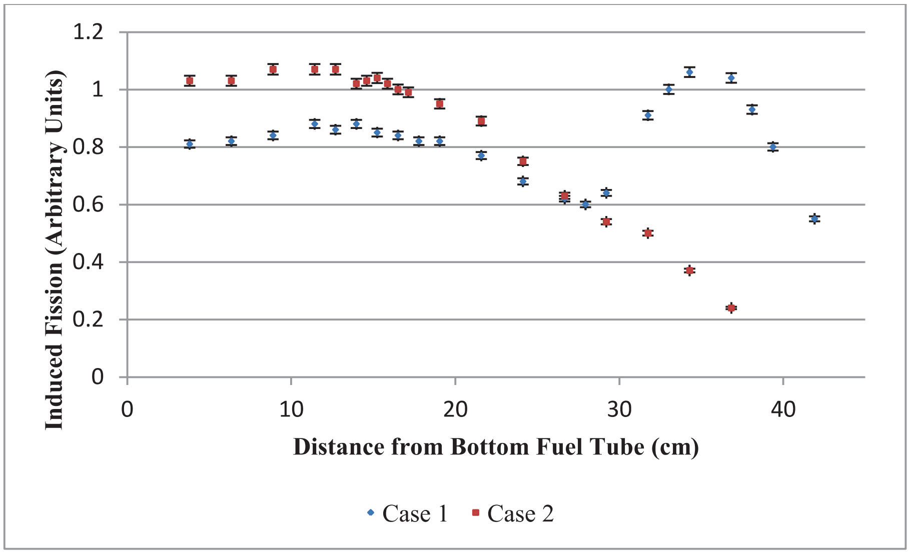

Figure 2.7-1. Uncertainty in Axial Distribution of the Induced Fission in a Uranium Fission Counter.

2.7.2 Radial Measurements

No uncertainty in the radial measurement of the activation of ^{235}U fission foils was reported by the experimenter. However, the logbook showed counts of up to 40,000 per minute. Using similar methods to those used for the axial measurement uncertainties, the uncertainty in the radial measurements would be less than 1%. However, since the 40,000 counts as the upper limit, the uncertainty was arbitrarily increased to ±5%. This is believed to encompass the 2.0% uncertainty associated with the foil placement. There is also an additional uncertainty in the measurements of ±0.01, bounding with a uniform distribution, due to the rounding of the measured values. These uncertainties, added in quadrature, are given in Table 2.7-2 and shown in Figure 2.7-2.

The effect of foil enrichment and purity was evaluated by comparing tallies for 100 wt.% ^{235}U foils to 93.2 wt.% ^{235}U foils. It was found that this 6.8 wt.% change in enrichment yields a maximum change in the normalized tally results of only 0.6%. Based on these results, it is assumed that the effect of uncertainty in the foil enrichment and purity would be negligible.

The relative radial activation of the ^{235}U fission foils was measured from the core-reflector interface; however, there was a 0.1-cm gap between the outside of the core and the inside of the side reflector. The zero point for these measurements was assumed to be at the inside surface of the side reflector. Radial plugs were in place when the activation of ^{235}U fission foils measurements were made.[a]

a. Personal email communication with J. T. Mihalczo, September 13, 2011.

Table 2.7-2. Uncertainty in Relative Radial Activation of ^{235}U Fission Foils Distribution (Case 1).

Distance from Core (cm)[(a)]	Radial Distribution[(b)(c)(d)]
0.0	1.68 ± 0.08
0.5	1.92 ± 0.10
1.0	2.25 ± 0.11
2.0	2.43 ± 0.12
3.5	2.84 ± 0.14
5.5	3.19 ± 0.16
6.5	3.19 ± 0.16
8.0	3.08 ± 0.15
10.5	2.92 ± 0.15
13.0	2.25 ± 0.11
16.0	1.54 ± 0.08

(a) Measured from the core-reflector interface. This was assumed to be the inside surface of the side reflector.
(b) Normalized to same arbitrary units as axial activation distribution.
(c) Measured through 19.25-cm-thick side reflector of the first assembly.
(d) Uncertainty includes measurement, foil placement, foil enrichment, and round-off uncertainty.

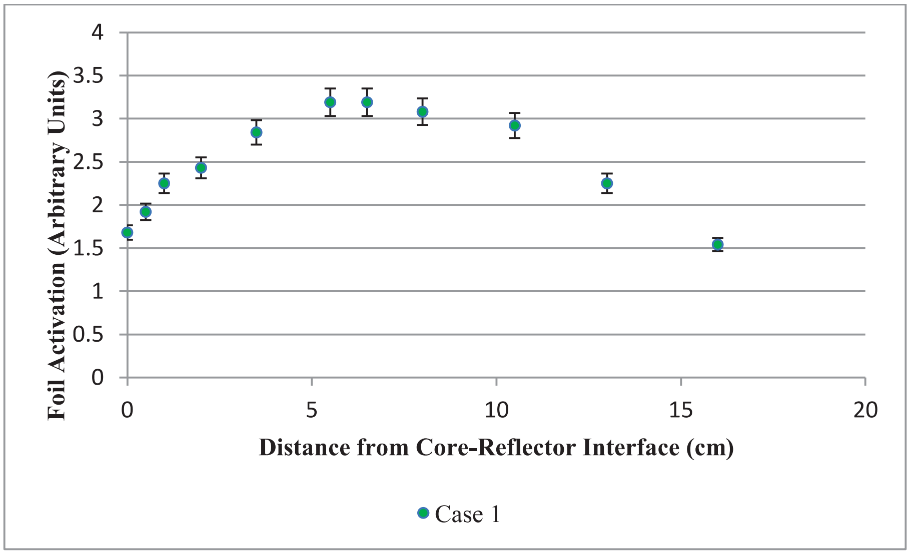

Figure 2.7-2. Uncertainty in Relative Radial Distribution of Activation of ^{235}U Fission Foils.

2.8 Evaluation of Power Distribution Data

The axial relative power distribution in the core is the same as the relative fission rate as was measured in the core region of Assembly 1 (see Section 2.7).

2.9 Evaluation of Isotopic Measurements

Isotopic measurements were not performed.

2.10 Evaluation of Other Miscellaneous Types of Measurements

Other miscellaneous types of measurements were not performed.

3.0 BENCHMARK SPECIFICATIONS

3.1 Benchmark-Model Specifications for Critical and/or Subcritical Measurements

Models of the experiments were created using MCNP5 with ENDF.B-VII.0 neutron cross section libraries. All models were run in MCNP5 such that the statistical uncertainty (1σ) of k_{eff} was not more than 0.00006.

The method for determining the simplification bias was as follows. First, a base model of only the configuration described in Reference 1 was created with void in place of air. Next, additional details such as air and room walls were added step by step, calculating the bias each time, until the detailed model was obtained. Next, simplifications were made to the base model one at a time, calculating the bias for each. Finally, all simplifications were added to the model simultaneously to get the simple model. The overall simplification bias was found by comparing the simple model to the detailed model. Figure 3.1-1 depicts this process. A simplification is considered negligible if the effect on k_{eff} is ≤0.00010. Sample input listings and results of the detailed model are provided in Appendix C for reference.

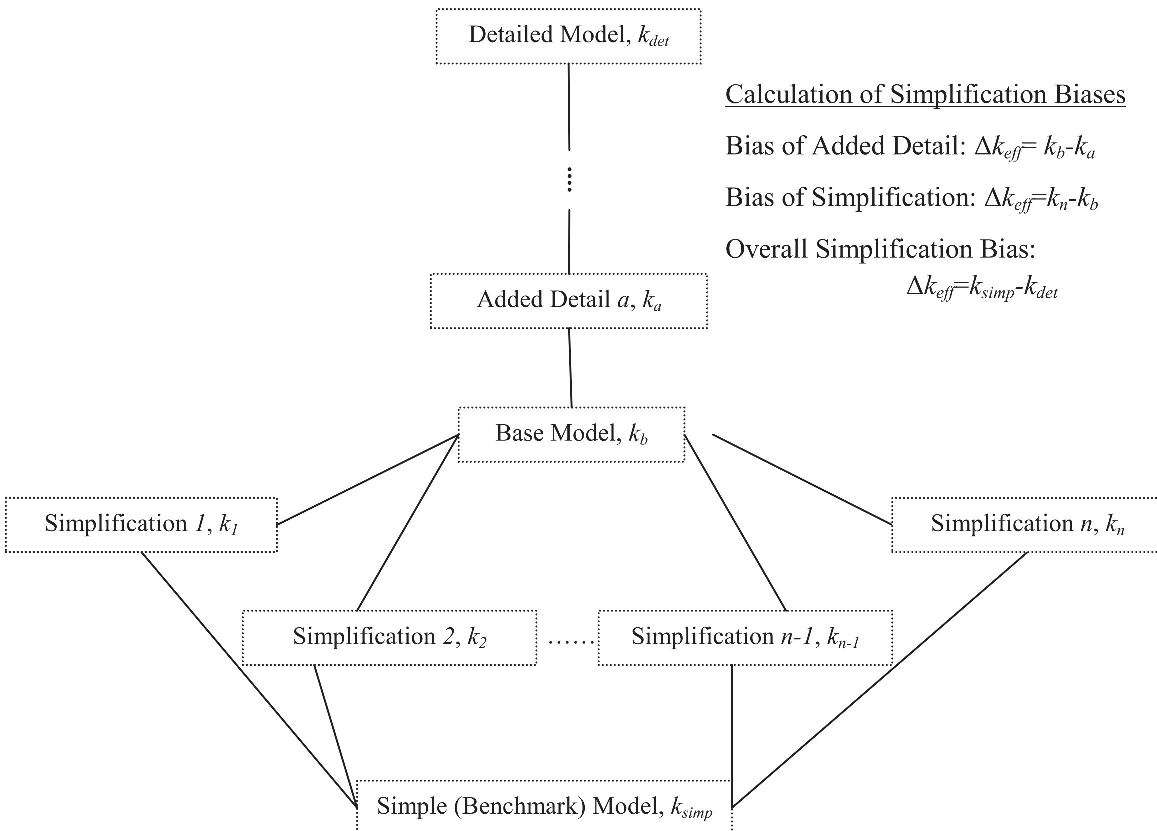

Figure 3.1-1. Bias Analysis Flow Diagram.

Sample input decks for the detailed model can be found in Appendix C. The calculated k_{det} using these input decks were 1.00551 and 1.00484.[a]

a. Found using MCNP5 and ENDF/B-VII.0 neutron cross section libraries.

3.1.1 Description of the Benchmark-Model Simplifications

3.1.1.1 Room Return and Effect of Air

As stated in Reference 2, the vertical assembly machine was located in the experiment cell such that the center of the core was 12.336 ft from the 4.92-ft-thick west wall, 12.79 ft from the 1.97-ft-thick north wall, and 9.19 ft above the concrete floor in the 35.10 × 35.10-ft-square 29.86-ft-tall room. The walls were modeled as described (the east and south walls were modeled as being 2 ft thick) with a 2-ft-thick concrete floor and ceiling, using Oak Ridge concrete.[a] The results of this simplification bias are in Table 3.1-2.

The simplification bias of removing air (density of 1.19 kg/m^3) from the model and replacing it with void is summarized in Table 3.1-2.

3.1.1.2 Homogenization of Reflectors

Two different homogenizations of the reflectors were performed independently. First, the holes and plugs were homogenized into the reflector, and second, the reflector mass was averaged over the entire volume of reflector. When both of these simplifications were performed simultaneously for the benchmark model, the total reflector masses and volumes in Table 3.1-1 were used. The results of these two homogenizations can be found in Table 3.1-2.

Table 3.1-1. Benchmark-Model Reflector Mass and Volume.

	Case 1		Case 2	
Total Reflector Mass	263.91	kg	325.99	kg
Total Reflector Volume	151342.8	cm^3	185603.1	cm^3

3.1.1.3 Simplification of Core Region

Three simplifications were made to the core: the aluminum shims were removed, the fuel-tube geometry was simplified, and the fuel pellet mass was homogenized over the total fuel length. The fuel-tube geometry was simplified by homogenizing the mass of the fuel tube and two end caps (46.0114 g) over the entire fuel-tube volume rather than having separate material densities for the fuel tube and the two end caps. The fuel region of the fuel tubes was simplified by homogenizing the fuel mass per tube (295.818 g[b]) over the total fuel length (30.55215 cm^3) rather than model each individual fuel pellet and void region between pellets. The biases associated with these simplifications can be found in Table 3.1-2.

3.1.1.4 Removal of Impurities

The impurities as given in Table 1.1-5 and Table 1.1-7 were replaced with void in the fuel and the graphite. This reduced the total material weight percentage for the fuel and graphite. The effect on k_{eff} of removing these impurities is given in Table 3.1-2.

---

a. *SCALE: A Modular Code System for Performing Standardized Computer Analyses for Licensing Evaluation*, ORNL/TM-2005/39 Version 5, Volume III, Section M.8, Oak Ridge National Laboratory, April 2005.

b. This mass was not reduced when impurities were replaced with void (Section 3.1.1.5); rather, the total weight percentage was reduced.

3.1.1.5 Temperature

The experiments were performed at 22°C, or 295.15 K. The model temperature was 293.6 K. The bias of this temperature change is negligible.

3.1.1.6 Summary of Simplification Biases

The overall simplification bias was found by comparing the detailed model to the simple/benchmark model. The overall simplification bias is given in Table 3.1-2. The biases associated with individual simplifications are also given in Table 3.1-2 for reference. The simplification with the largest contribution was the homogenization of the reflectors. The overall simplification bias was also calculated using JEFF3.1 and JENDL-3.3 neutron cross section libraries to assess the effect of cross sections on the bias. The simplification bias used for the benchmark model was the average of the results of the three cross section libraries.

Table 3.1-2. Summary of Simplification Biases.

	Case 1			Case 2		
Room Return	-0.00032	±	0.00008	-0.00027	±	0.00008
Replacing Air with Void	-0.00012	±	0.00008	-0.00027	±	0.00008
Homogenizing Holes and Plugs in Reflector	-0.00080	±	0.00008	0.00094	±	0.00008
Averaging Total Reflector Mass	0.00022	±	0.00008	0.00024	±	0.00008
Removing Shims	-0.00069	±	0.00008	-0.00042	±	0.00008
Simplification of Fuel Tube	-0.00061	±	0.00008	-0.00049	±	0.00008
Homogenization of Fuel	NEG			0.00013	±	0.00008
Removing of Fuel Impurities	-0.00046	±	0.00008	-0.00015	±	0.00008
Removing of Graphite Impurities	NEG			0.00052	±	0.00008
Temperature Bias	NEG			NEG		
Overall Simplification Bias[(a)(b)]	**-0.00248**	**±**	**0.00048**	**-0.00051**	**±**	**0.00043**
ENDF/B-VII.0	-0.00222	±	0.00006	-0.00019	±	0.00006
JEFF3.1	-0.00219	±	0.00006	-0.00035	±	0.00006
JENDL-3.3	-0.00303	±	0.00006	-0.00100	±	0.00006

(a) Found by comparing detailed model with simple/benchmark model.
(b) Overall simplification bias found by averaging of the three cross section libraries. Uncertainty is the standard deviation of the results.

3.1.1.7 Summary of Biases

There are two different biases for these experiments: the bias of the measured reactivity of the critical configuration and the overall simplification bias. The first was found using the measured reactivities given in Section 1.1.2.4. The second was found by comparing the detailed model and the simple/benchmark model. The excess reactivity and simplification biases were added to obtain the total bias. The total bias of the benchmark model is given in Table 3.1-3.

Table 3.1-3. Summary of Benchmark-Model Bias.

	Case 1	Case 2
Bias of Measured Reactivity of Critical Configuration (see Table 2.1-1)	0.00052 ± 0.00011[b]	0.00025 ± 0.00005[b]
Overall Simplification Bias[a]	-0.00248 ± 0.00048	-0.00051 ± 0.00043
Total Bias[b]	-0.00196 ± 0.00048	-0.00026 ± 0.00043

(a) Found by comparing detailed model with simple/benchmark model.
(b) The uncertainty in the measured reactivity of the critical configuration was included in the measurement uncertainty given in Section 2.1 (see Table 2.1-31).

3.1.1.8 Additional Evaluated Biases

Two Type 1100 aluminum support plates, a Type 304 stainless-steel plate, and an iron table were used to support the assembly on the vertical assembly machine. (Dimensions of these plates are given in Table 1.1-4 and the compositions are given in Tables 2.1-19, 2.1-26, and 2.1-29. Masses given in Table 1.1-4 were used for the aluminum plates and iron table but a mass of 31.2 kg was used for the stainless-steel plate.) They also provide some additional reflection. These plates and table are present in the benchmark model. The effect of removing these from the model was evaluated and is summarized in Table 3.1-4, but is not included in the experimental bias. Table 3.1-4 also contains the total simplification bias if these simplifications had been included.

Table 3.1-4. Additional Evaluated Biases.

	Case 1	Case 2
Removing of 1.94-cm-Thick Al Plate	-0.00043 ± 0.00008	-0.00039 ± 0.00008
Removing of 0.63-cm-Thick Al Plate	-0.00024 ± 0.00008	-0.00030 ± 0.00008
Removing Stainless-Steel Plate	-0.00309 ± 0.00008	-0.00384 ± 0.00008
Removing Iron Table	-0.00170 ± 0.00008	-0.00224 ± 0.00008
Total Simplification Bias[a]	-0.00759 ± 0.00008	-0.00743 ± 0.00008

(a) Comparing detailed model to simple model without support plates and table.

3.1.2 Dimensions

3.1.2.1 Fuel Tubes

Fuel rods were modeled as a cylinder of fuel homogenized with void between the fuel and the fuel tube. The end caps were modeled as solid plugs. The height of each plug was found by taking half the difference between the fuel-tube length (30.48 cm) and the length of 26 pellets (29.88 cm). Figures 3.1-2 and 3.1-3 give the dimensions of the fuel tubes.

3.1.2.2 The Core

The core consisted of 253 fuel tubes tightly packed into a 22.87-cm-diameter Type 1100 aluminum core tank with the center fuel tube removed thus only 252 fuel tubes were present. The 1.27-cm-diameter fuel tubes in a tightly packed array resulted in a hexagonal lattice with a 1.27-cm pitch. There is no fuel rod in the centermost position. The array and core tank are shown in Figures 3.1-2 and 3.1-3.

3.1.2.3 Reflectors

Two different reflector configurations were used for Case 1 and Case 2. The dimensions for both cases can be seen in Figures 3.1-2 and 3.1-3. The top of the core was in contact with the bottom of the top reflector in the models.

3.1.2.4 Support Plates and Table

Three support plates were under the bottom reflector and core, and the side and top reflector were placed on the support table. The dimensions of the support plates and table are given in Table 3.1-5.

Table 3.1-5. Support Plate Dimensions.

1.94-cm-Thick Type 1100 Aluminum Plate	21.60-cm Diameter
0.63-cm-Thick Type 1100 Aluminum Plate	45.72-cm Diameter
2.38-cm-Thick Type 304 Stainless-Steel Plate	45.72-cm Diameter
1.27-cm-Thick Iron Table	121.9 × 121.9-cm square table with 23.58-cm diameter cutout[(a)]

(a) A cutout in the middle of the table allowed the core and bottom reflector to be lifted into the side reflector.

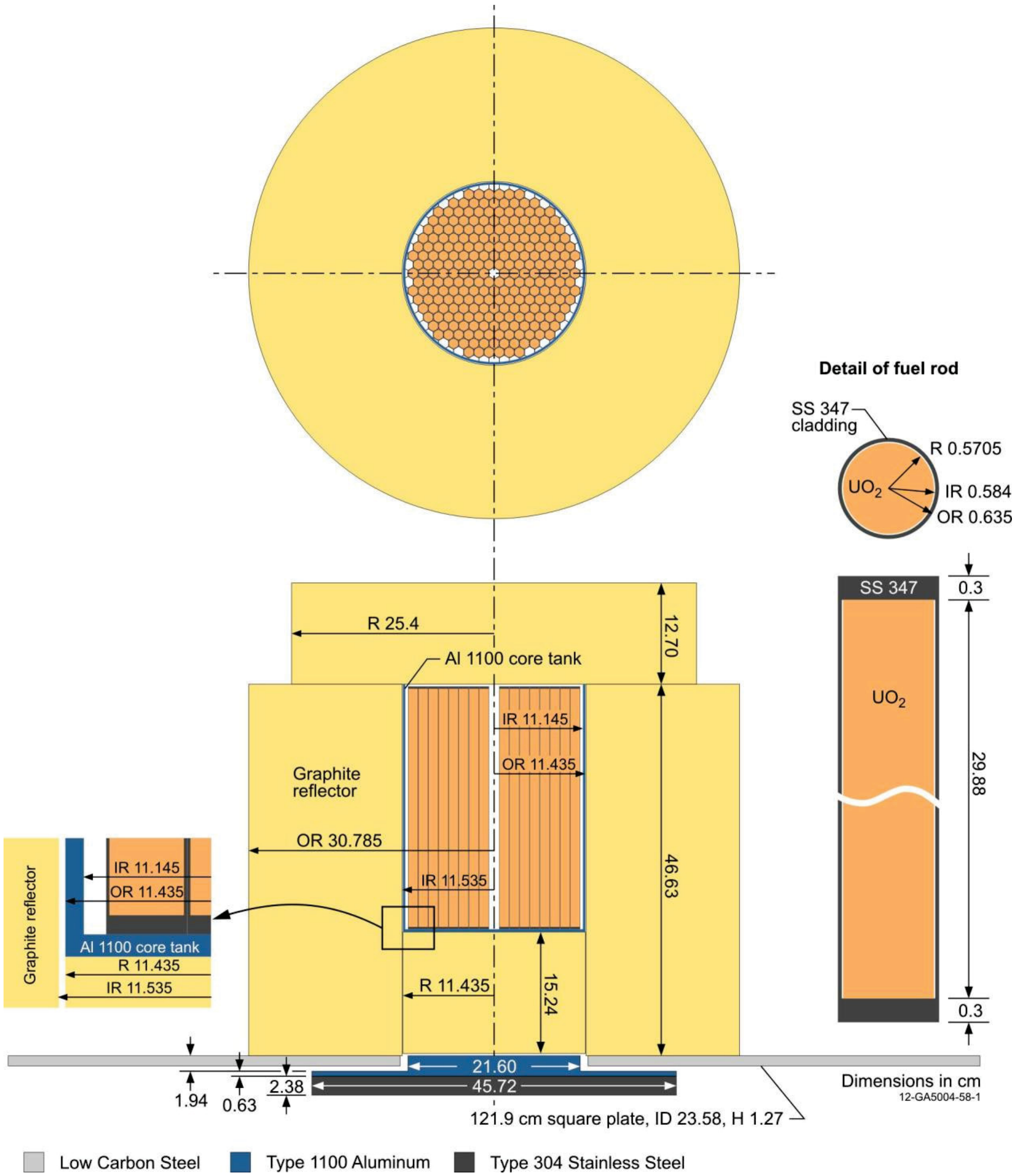

Figure 3.1-2. Dimensions of Case 1.

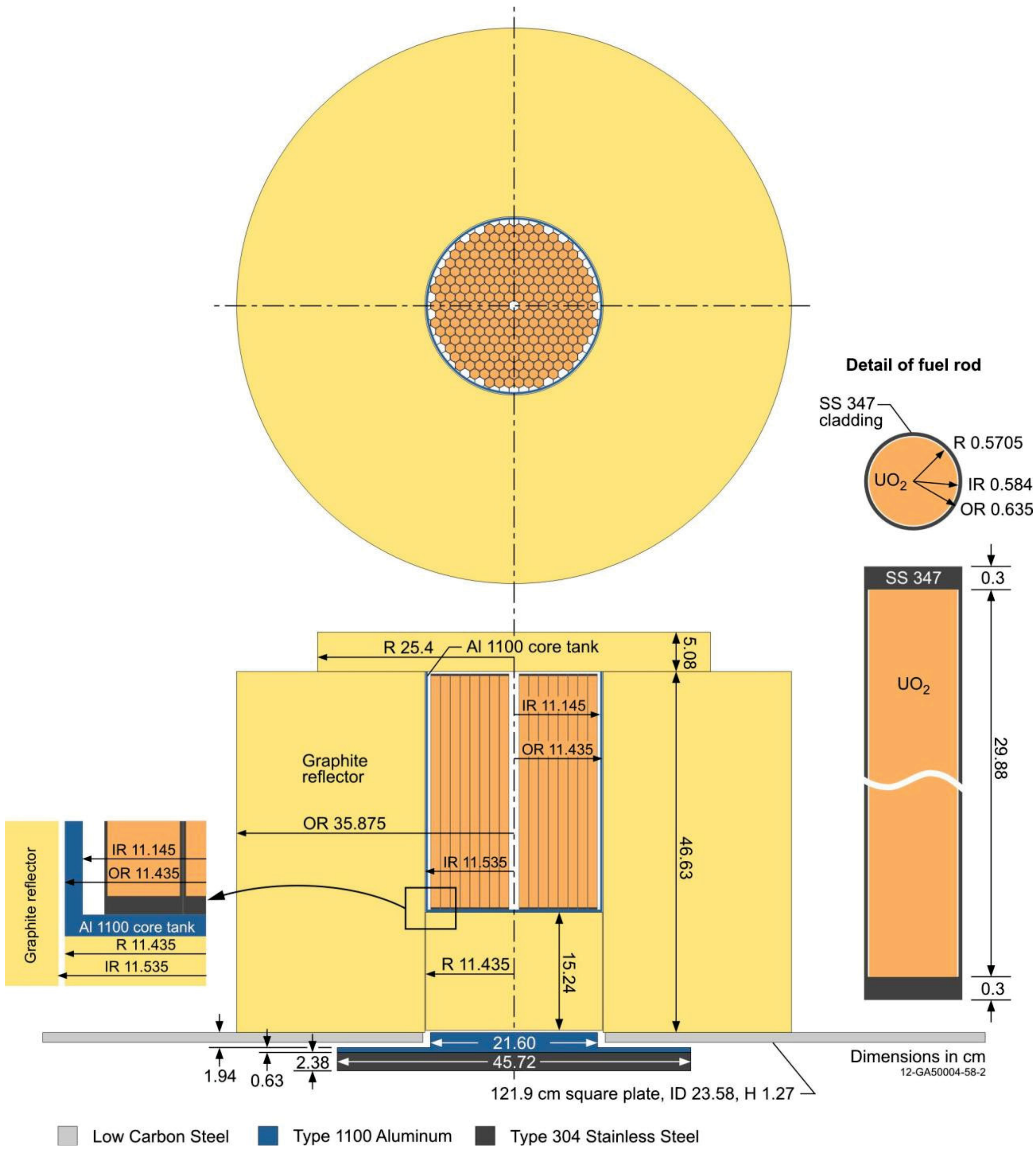

Figure 3.1-3. Dimensions of Case 2.

3.1.3 Material Data

Atomic masses from the *International Criticality Safety Benchmark Evaluation Project (ICSBEP) Document Content and Format Guide* were used to derive atom densities for all materials.

3.1.3.1 Uranium Dioxide

All impurities were replaced with void for the benchmark model by reducing the total material weight percentage. The composition of the fuel is given in Table 3.1-6.

Table 3.1-6. UO_2 Composition.

Isotope/Element	wt.%	Atoms/barn-cm
^{234}U	0.8887	2.2140E-04
^{235}U	81.9608	2.0332E-02
^{236}U	0.4135	1.0215E-04
^{238}U	4.7250	1.1573E-03
O	11.9708	4.3627E-02
Total	99.9588 [(a)]	6.5440E-02

(a) Weight fractions do not add up to 100% due to the removal of impurities.

3.1.3.2 Fuel Tube

The fuel tube was made of Type 347 stainless steel. The composition of the fuel tube is given in Table 3.1-7.

Table 3.1-7. Fuel-Tube Composition.

Isotope/Element	wt.%	Atoms/barn-cm
Fe	68.7225	5.1693E-02
C	0.04	1.3990E-04
Mn	1.00	7.6465E-04
Si	0.50	7.4787E-04
Cr	18.0	1.4542E-02
Ni	11.0	7.8734E-03
P	0.0225	3.0516E-05
S	0.0150	1.9648E-05
Nb	0.644	2.9104E-04
Ta	0.056	1.3076E-05
Total	100.0	7.61160E-02

3.1.3.3 Core Tank

The core tank was made of Type 1100 aluminum, weighed 2.134 kg, and had a volume of 776.565 cm^3. The core tank composition is summarized in Table 3.1-8.

Table 3.1-8. Core Tank Composition

Isotope/Element	wt.%	Atoms/barn-cm
Al	99.37	6.0920E-02
Cu	0.125	3.2553E-05
Si	0.2375	1.3994E-04
Fe	0.2375	7.0377E-05
Mn	0.025	7.5306E-06
Zn	0.05	1.2654E-05
Total	100.00	6.1183E-02

3.1.3.4 Reflectors

Impurities were replaced with void in the graphite for the benchmark model. The graphite compositions are given in Table 3.1-9.

Table 3.1-9. Reflector Composition.

Element	wt.%	Case 1 Atoms/barn-cm	Case 2 Atoms/barn-cm
C	99.4536[(a)]	8.6953E-02	8.7581E-02

(a) Total weight percent is reduced when impurities are replaced with void.

3.1.3.5 Support Plates and Table

The two aluminum support plates were Type 1100 aluminum. They weighed 1.920 and 2.787 kg. The compositions of these plates are given in Table 3.1-10.

Table 3.1-10. Aluminum Plate Composition.

Isotope/Element	wt.%	1.94-cm-Thick Al Reflector Atoms/barn-cm	0.63-cm-Thick Al Reflector Atoms/barn-cm
Al	99.37	5.9875E-02	5.9736E-02
Cu	0.125	3.1994E-05	3.1920E-05
Si	0.2375	1.3754E-04	1.3722E-04
Fe	0.2375	6.8974E-05	6.8814E-05
Mn	0.025	7.4015E-06	7.3843E-06
Zn	0.05	1.2437E-05	1.2408E-05
Total	100.00	6.0133E-02	5.9994E-02

A mass of 31.2 kg was used in the benchmark model for the stainless-steel plate (see Section 2.1.6.2). The stainless-steel plate composition is given in Table 3-1.11.

Table 3.1-11. Stainless-Steel Plate Composition.

Element	wt.%	Atoms/barn-cm
Fe	69.9225	6.0206E-02
C	0.04	1.6014E-04
Mn	1.00	8.7529E-04
Si	0.50	8.5607E-04
Cr	19.00	1.7571E-02
Ni	9.50	7.7836E-03
P	0.0225	3.4931E-05
S	0.015	2.2491E-05
Total	100.00	8.7510E-02

The iron table was low-carbon steel and had a mass of 137.9 kg. The composition is given in Table 3.1-12.

Table 3.1-12. Iron Table Composition.

Element	wt.%	Atoms/barn-cm
Fe	98.305	7.9805E-02
C	0.25	9.4366E-04
Mg	1.00	1.8653E-03
P	0.02	2.9275E-05
S	0.025	3.5342E-05
Si	0.20	3.2285E-04
Cu	0.20	1.4269E-04
Total	100.00	8.3144E-02

3.1.4 Temperature Data

The benchmark-model temperature is 293.6 K.

3.1.5 Experimental and Benchmark-Model k_{eff} Values and/or Subcritical Parameter Values

The experimental configurations had an excess reactivity of +7.2 and +3.4 ¢. This bias and the simplification bias were applied to obtain the benchmark-model experiment k_{eff} values found in Table 3.1-13. The uncertainty in the benchmark model was found by adding in quadrature the uncertainty derived in Section 2.1 and the uncertainty in the bias derived in Section 3.1.1

Table 3.1-13. Benchmark Experiment Eigen Values.

	Case 1	Case 2
Benchmark $k_{eff} \pm 1\sigma$	0.9980 ± 0.0007	0.9997 ± 0.0006

3.2 Benchmark-Model Specifications for Buckling and Extrapolation-Length Measurements

Buckling and extrapolation-length measurements were not performed.

3.3 Benchmark-Model Specifications for Spectral Characteristics Measurements

Spectral characteristics measurements were not evaluated.

3.4 Benchmark-Model Specifications for Reactivity Effects Measurements

3.4.1 Description of the Benchmark-Model Simplifications

The models used to determine the center fuel rod and radial graphite plug worth were run using MCNP5 and ENDF/B-VII.0 neutron cross section libraries. They were run until the statistical uncertainty of k_{eff} was 0.00002. Thus, the statistical uncertainty in all bias calculations was 0.00003, or approximately 0.42 ¢ for the plug worth measurements and 2.11¢ for the center fuel rod worth measurements (1σ). Biases were considered negligible if they were less than 0.00006 Δk_{eff} .

3.4.1.1 Center Fuel Rod Worth

The model used for the reactivity effect calculation for the worth of the extra fuel rod was identical to the benchmark model (see Section 3.1) except with an additional fuel rod, identical to all other fuel rods, inserted into the center of the core. The simplifications in the geometry from the detailed to the benchmark model had a negligible bias for the calculation of the central fuel rod worth. The associated bias uncertainty was 2.11 ¢. The benchmark worth of the center fuel rod is given in Table 3.4-1.

3.4.1.2 Graphite Plug Worth

Because two plugs were removed during the experiment, 2.95 ¢ for two radial graphite plugs was used as the benchmark value, rather than 1.5 ¢ per plug.

The model used for the reactivity effect calculation for the plug worth differed from the benchmark model. The total reflector mass was not averaged over the total volume of reflector. The simplifications in the geometry from the detailed to the benchmark model had a negligible bias for the calculation of the graphite plug worth. The associated bias uncertainty was 0.39 ¢. The benchmark worth of two radial graphite plugs is given in Table 3.4-1.

Table 3.4-1. Benchmark Experiment Worth Values.

	Case 1[(a)]
Center Fuel Rod Worth	32 ± 3.8 ¢[(b)]
Worth of Two Radial Graphite Plugs	2.95 ± 0.51 ¢[(c)]

(a) Worth measurements were only performed using the Case 1 configuration.
(b) Total uncertainty was found by adding in quadrature the measurement uncertainty in Section 2.4 and the bias uncertainty of ±2.11 ¢.
(c) Total uncertainty was found by adding in quadrature the measurement uncertainty in Section 2.4 and the bias uncertainty of ±0.42 ¢.

3.4.2 Dimensions

3.4.2.1 The Core and Support Structure

3.4.2.1.1 Center Fuel Rod Worth

The core region of the assemblies was identical to those described in Sections 3.1.2.1 and 3.1.2.2. To determine the worth of the center fuel rod, the benchmark model was perturbed by adding the center fuel rod and calculating the resulting k_{eff}. The results are given in Section 3.4.4.

The support plates and table were identical to those described in Section 3.1.2.4.

3.4.2.1.2 Graphite Plug Worth

The core region of the assemblies was identical to those described in Sections 3.1.2.1 and 3.1.2.2.

The support plates and table were identical to those described in Section 3.1.2.4.

3.4.2.2 The Reflectors

3.4.2.2.1 Center Fuel Rod Worth

The reflectors of the assemblies were identical to those described in Section 3.1.2.3.

3.4.2.2.2 Graphite Plug Worth

The dimensions of the bottom, side, and top reflectors were the same as those described in Section 3.1.2.3 except the radial and axial 1.27-cm-diameter holes and 1.11-cm-diameter plugs were also included in the model for the evaluation reactivity effect measurements. The six equally spaced radial holes extended through the side reflector at the core midplane and had a diameter of 1.27 cm. Plugs were present in five of the holes. The axial hole in the top reflector was centered above the core and was plugged. The measured reflector masses included the masses of these plugs.

To determine the worth of the radial plugs, the base model was perturbed by adding a plug to the sixth radial hole and then by removing all two plugs from the radial holes. The results are given in Section 3.4.4.

3.4.3 Material Data

3.4.3.1 Core and Support Structure

3.4.3.1.1 Center Fuel Rod Worth

The material data for the core region of the model is the same as those described in Sections 3.1.3.1, 3.1.3.2, and 3.1.3.3.

The support plates and table were identical to those described in Section 3.1.3.5.

3.4.3.1.2 Graphite Plug Worth

The material data for the core region of the model is the same as those described in Sections 3.1.3.1, 3.1.3.2, and 3.1.3.3.

The support plates and table were identical to those described in Section 3.1.3.5.

3.4.3.2 Reflectors

3.4.3.2.1 Center Fuel Rod Worth

The material data for the reflectors is the same as those described in Section 3.1.3.4.

3.4.3.2.2 Graphite Plug Worth

The reflector mass was not averaged over the total reflector volume as was done for the benchmark model. The atom densities for the reflectors and plugs are given in Table 3.4-2. The atom densities were not changed when the plugs were removed.

Table 3.4-2. Reflector Composition.

	Case 1	Case 2
	Carbon Atom Density (Atoms/barn-cm)	
Bottom Reflector	8.8013E-02	
Side Reflector Radial Plugs	8.7992E-02	8.7937E-02
Top Reflector Axial Plugs	8.2071E-02	8.2051E-02

3.4.4 Temperature Data

The temperature was the same as the benchmark model (see Section 3.1.4).

3.4.5 Experimental and Benchmark-Model Reactivity Effect Values

The center fuel rod was worth 32 ± 3.8 ¢ and the worth of a two radial plugs was 2.95 ± 0.51 ¢.

3.5 Benchmark-Model Specifications for Reactivity Coefficient Measurements

Reactivity coefficient measurements were not performed.

3.6 Benchmark-Model Specifications for Kinetics Measurements

Kinetics measurements were not performed.

3.7 Benchmark-Model Specifications for Reaction-Rate Distribution Measurements

3.7.1 Description of the Benchmark-Model Simplifications

The model for the evaluation of the reaction-rate distribution was the same as the model used for the evaluation of the radial plug worth (see Section 3.4.1.2).

A bias in the reaction-rate distribution measurements in considered negligible if it is less than the statistical uncertainty of the Monte Carlo calculation. For biases that are negligible the bias uncertainty is preserved as can be seen in Table 3.7-1, 3.7-2, and 3.7-3.

3.7.1.1 Axial Measurement

Tallies were modeled using a mesh of cells superimposed over the geometry. The cells had a radius of 0.32 cm and extended from the bottom of the core tank to the top of the top reflector. Each cell had a height of 0.01 cm. Cell-averaged flux tallies were used. A tally multiplier for the ^{235}U fission cross section was also used. It is believed that this method for modeling the reaction-rate distribution would have a negligible bias. The simplification bias on the measurement due to geometry simplifications is given in Table 3.7-1. Statistically insignificant biases were not included in Table 3.7-1 but the associated bias uncertainty was preserved.

Table 3.7-1. Simplification Bias of Relative Axial Distribution of the Induced Fission in a Uranium Fission Counter.

Distance from Bottom of Core (cm)	Simplification Bias[(a)]					
	Case 1			Case 2		
3.81	-0.042	±	0.006	0.009	±	0.002
6.35	-0.048	±	0.006	0.009	±	0.002
8.89	-0.053	±	0.006	-	±	0.002
11.43	-0.054	±	0.007	-	±	0.001
12.70	-0.054	±	0.007	-0.002	±	0.001
13.97	-0.053	±	0.007	-	±	0.001
14.60		-		-	±	0.001
15.24	-0.054	±	0.007	-	±	0.001
15.87		-		-	±	0.001
16.51	-0.054	±	0.007	-	±	0.001
17.14		-		0.002	±	0.001
17.78	-0.053	±	0.007		-	
19.05	-0.051	±	0.006	0.001	±	0.001
21.59	-0.048	±	0.006	-	±	0.001
24.13	-0.045	±	0.006	0.003	±	0.001
26.67	-0.037	±	0.005	0.009	±	0.001
27.94	-0.035	±	0.005		-	
29.21	-0.032	±	0.005	-	±	
31.75	0.015	±	0.011	-0.014	±	0.006
33.02	-	±	0.012		-	
34.29	0.015	±	0.013	-0.036	±	0.006
36.83	-0.005	±	0.013	-0.060	±	0.005
38.10	-0.003	±	0.013		-	
39.37	-0.020	±	0.012		-	
41.91	-0.038	±	0.008		-	

(a) Calculated by comparing detailed model results to simple/benchmark-model results.

3.7.1.2 Radial Measurement

A superimposed mesh was also used to model the radial reaction-rate distributions. The cells had a radius of 0.375 cm and extended from the core tank out through the side reflector. Each cell had a height of 0.01 cm. An identically sized fmesh tally was also used to model the activation of the foil that was placed at the midpoint of the top reflector (36.79 cm above to bottom of the core) for normalization of the radial measurements to axial measurements. A tally multiplier for the uranium fission cross section (93.2 wt.% ^{235}U, 6.8 wt.% ^{238}U) was used. It is believed that this method for modeling the reaction-rate distribution would have a negligible bias. The simplification bias on the measurement due to geometry simplifications is given in Table 3.7-2. Statistically insignificant biases were not included in Table 3.7-2 but the associated bias uncertainty was preserved.

Table 3.7-2. Simplification Bias of Distribution of Relative Radial Activation of ^{235}U Fission Foils.

Distance from Core (cm)(a)	Simplification Bias(b)		
	Case 1		
0.0	-0.020	±	0.014
0.5	-0.108	±	0.016
1.0	-0.129	±	0.017
2.0	-0.210	±	0.020
3.5	-0.257	±	0.023
5.5	-0.261	±	0.025
6.5	-0.312	±	0.025
8.0	-0.300	±	0.026
10.5	-0.270	±	0.024
13.0	-0.246	±	0.020
16.0	-0.141	±	0.015

(a) Measured from the core-reflector interface.
(b) Calculated by comparing detailed model results to simple/benchmark-model results.

3.7.2 Dimensions

The dimensions were the same as those used for the evaluation of the radial plug worth (see Sections 3.4.2.1.2 and 3.4.2.2.2).

3.7.3 Material Data

The material data were the same as those used for the evaluation of the radial plug worth (see Sections 3.4.3.1.2 and 3.4.3.2.2).

3.7.4 Temperature Data

The temperature was the same as the benchmark model (see Section 3.1.4).

3.7.5 Experimental and Benchmark-Model Reaction-Rate Distribution Values

3.7.5.1 Axial Measurement

The benchmark values of the induced fission in uranium-fission-counter measurements are found by applying the biases in Table 3.7-1 to the experimental results. The uncertainty in the benchmark model is found by adding in quadrature the uncertainty in the experimental results, discussed in Section 2.7, and the bias uncertainty given in Table 3.7-1. The benchmark results are given in Table 3.7-3 and Figure 3.7-1. Measurements in the core region are fission rates. Measurements above the top of the core region are highlighted.

Table 3.7-3. Benchmark Relative Axial Distribution of the Induced Fission in a Uranium Fission Counter.[a]

Distance from Bottom of Core[b] (cm)	Induced Fission[c] (Arbitrary Units)					
	Case 1 (±1.6%)			Case 2 (±1.7%)		
3.81	0.77	±	0.02	1.04	±	0.02
6.35	0.77	±	0.02	1.04	±	0.02
8.89	0.79	±	0.02	1.07	±	0.02
11.43	0.83	±	0.02	1.07	±	0.02
12.70	0.81	±	0.02	1.07	±	0.02
13.97	0.83	±	0.02	1.02	±	0.02
14.60		-		1.030	±	1.03
15.24	0.80	±	0.02	1.04	±	0.02
15.87				1.02	±	1.02
16.51	0.79	±	0.02	1.00	±	0.02
17.14		-		0.99	±	0.99
17.78	0.77	±	0.02		-	
19.05	0.77	±	0.02	0.95	±	0.02
21.59	0.72	±	0.01	0.89	±	0.02
24.13	0.64	±	0.01	0.75	±	0.01
26.67	0.58	±	0.01	0.63	±	0.01
27.94	0.56	±	0.01		-	
29.21	0.61	±	0.01	0.54	±	0.01
31.75	0.93	±	0.02	0.49	±	0.01
33.02	1.00	±	0.02		-	
34.29	1.08	±	0.02	0.33	±	0.01
36.83	1.04	±	0.02	0.18	±	0.01
38.10	0.93	±	0.02		-	
39.37	0.78	±	0.02		-	
41.91	0.51	±	0.01		-	

(a) These are relative fission rates in the core and relative activation of ^{235}U in the reflector.
(b) Measured from the bottom of the stainless-steel fuel tubes.
(c) The detector was a ^{235}U fission counter 2.5 cm long × 0.64 cm in diameter.

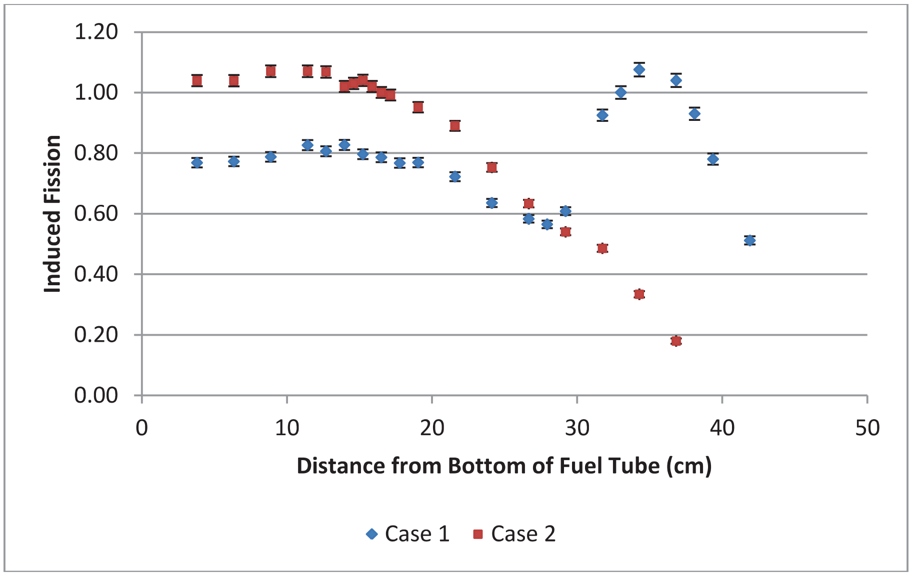

Figure 3.7-1. Benchmark Relative Axial Distribution of the Induced Fission in a Uranium Fission Counter.

3.7.5.2 Radial Measurement

The radial distribution of the activation of ^{235}U fission foils and the associated uncertainties, as discussed in Section 2.7, are given in Table 3.7-4 and Figure 3.7-2.

Table 3.7-4. Benchmark Distribution of Relative Radial Activation of ^{235}U Fission Foils.

Distance from Core (cm)[(a)]	Foil Activation[(b)(c)]		
0.0	1.66	±	0.09
0.5	1.81	±	0.10
1.0	2.12	±	0.11
2.0	2.22	±	0.12
3.5	2.58	±	0.14
5.5	2.93	±	0.16
6.5	2.88	±	0.16
8.0	2.78	±	0.16
10.5	2.65	±	0.15
13.0	2.00	±	0.11
16.0	1.40	±	0.08

(a) Measured from the core-reflector interface.
(b) Normalized to same arbitrary units as axial measurement.
(c) Measured through 19.25-cm-thick side reflector of Case 1.

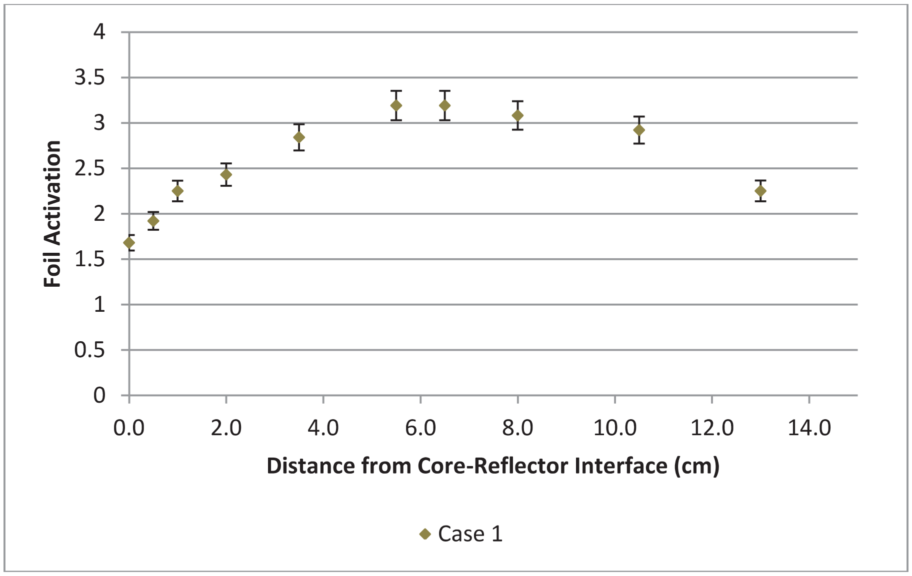

Figure 3.7-2. Benchmark Relative Radial Distribution of Activation of ^{235}U Fission Foils.[a]

3.8 Benchmark-Model Specifications for Power Distribution Measurements

The axial relative power distribution is the same as the relative fission rate as was measured in the core region of Assembly 1 (see Section 3.7).

3.9 Benchmark-Model Specifications for Isotopic Measurements

Isotopic measurements were not performed.

3.10 Benchmark-Model Specifications for Other Miscellaneous Types of Measurements

Other miscellaneous types of measurements were not performed.

[a] The zero point was assumed to be at the inside surface of the side reflector.

4.0 RESULTS OF SAMPLE CALCULATIONS

4.1 Results of Calculations of the Critical or Subcritical Configurations

Models were created with MCNP5 and KENO-VI using the ENDF/B-VII.0 continuous energy neutron cross section libraries. Thermal scattering treatments, S(α,β), were used for the uranium dioxide fuel, the aluminum, and the graphite reflectors. Example input files for the benchmark model can be found in Appendix A. Results of the MCNP5 and KENO-VI sample calculations are approximately 0.5%, or about 7-8σ greater than the benchmark. Results are summarized in Table 4.1-1.

Table 4.1-1. Sample Results for the Benchmark Model, ENDF/B-VII.0.

	Benchmark			Calculated							
				MCNP5 ENDF/B-VII.0[a]			$\frac{C-E}{E}$	KENO-VI ENDF/B-VII.0[b,c]			$\frac{C-E}{E}$[d]
	k_{eff}	±	σ	k_{eff}	±	σ		k_{eff}	±	σ	
Case 1	0.9980	±	0.0007	1.00329	±	0.00002	0.53%	1.00312	±	0.00006	0.51%
Case 2	0.9997	±	0.0006	1.00465	±	0.00002	0.49%	1.00442	±	0.00006	0.47%

(a) Results obtained using 100,000 histories for 2000 cycles, skipping the first 150 cycles.
(b) Results provided by John D. Bess from Idaho National Laboratory.
(c) Results obtained using 100,000 histories for 2150 cycles, skipping the first 150 cycles.
(d) "E" is the expected or benchmark value. "C" is the calculated value.

A second experimental configuration was evaluated in HEU-COMP-FAST-002.[a] The calculational bias for part two of the experimental series was only 0.2% with ENDF/B-VII.0 cross section libraries. The reason for the large difference in the calculation bias between these two highly correlated experiments is unknown.

Models were also run with MCNP5 using the JEFF-3.1 and JENDL-3.3 libraries. The JEFF-3.1 results are within 0.05 and 0.02%, or within 1σ, of the benchmark model. JENDL-3.3 results are within 0.30 and 0.28%, or ~4.5σ, of the benchmark model. The JENDL-3.3 libraries did not have the needed S(α,β), so ENDF/B-VII.0 treatments were used instead.[b] Results are summarized in Table 4.1-2.

---

a. International Handbook of Evaluated Criticality Safety Benchmark Experiments, NEA/NSC/DOC(95)03, OECD-NEA, Paris, 2012

b. Certain isotopes were not available in JENDL-3.3; thus, they were replaced with void. Such isotopes are: oxygen-17, lutetium-75 and -76, and strontium-84.

Table 4.1-2. Sample Results for the Benchmark Model, JEFF-3.1 and JENDL-3.3.

	Benchmark			Calculated							
				MCNP5 JEFF-3.1[a,b]			$\frac{C-E}{E}$	MCNP5 JENDL-3.3[a,b,c]			$\frac{C-E}{E}$[d]
	k_{eff}	±	σ	k_{eff}	±	σ		k_{eff}	±	σ	
Case 1	0.9980	±	0.0007	0.99850	±	0.00002	0.05%	1.00107	±	0.00002	0.30%
Case 2	0.9997	±	0.0006	0.99990	±	0.00002	0.02%	1.00252	±	0.00002	0.28%

(a) Results obtained using 1,000,000 histories for 2000 cycles, skipping the first 150 cycles.
(b) Results provided by John D. Bess from Idaho National Laboratory.
(c) S(α,β) treatment from ENDF/B-VII.0.
(d) "E" is the expected or benchmark value. "C" is the calculated value.

Models were also run with MCNP5 using ENDF/B-V.2 cross section libraries. These results are given in Table 4.1-3.

Table 4.1-3. Sample Results for the Benchmark Model, ENDF/B-V.2.

	Benchmark			Calculated			
				MCNP5 ENDF/B-V.2[a]			$\frac{C-E}{E}$
	k_{eff}	±	σ	k_{eff}	±	σ	
Case 1	0.9980	±	0.0007	0.99839	±	0.00002	0.04%
Case 2	0.9997	±	0.0006	0.99994	±	0.00002	0.02%

(a) Results obtained using 100,000 histories for 2000 cycles, skipping the first 150 cycles.

4.2 Results of Buckling and Extrapolation Length Calculations

Buckling and extrapolation-length measurements were not performed.

4.3 Results of Spectral-Characteristics Calculations

Spectral characteristics measurements were not evaluated.

4.4 Results of Reactivity-Effects Calculations

Worth measurements were evaluated by adding or removing graphite plugs and the center fuel rod from the model described in Section 3.4. The models were run using MCNP5-1.60 and ENDF/B-VII.0 neutron cross section libraries. The models were run until the Monte Carlo statistical uncertainty was 0.00002; this required 1,000,000 histories per cycle for 2,000 cycles, skipping the first 150 cycles. The benchmark values and sample calculation results are given in Table 4.4-1.

Table 4.4-1. Worth Measurement Sample Calculation Results.

	Benchmark Results	MCNP5 ENDF/B-VII.0[a]	$\frac{C-E}{E}$[c]
Center Fuel Rod Worth (Δk_{eff})	-	0.00298 ± 0.00003	-
Center Fuel Rod Worth (¢)	32 ± 3.8 ¢[b]	41.39 ± 2.11 ¢	29.35%
Worth of Two Radial Graphite Plugs (Δk_{eff})	-	0.00019 ± 0.00003	-
Worth of Two Radial Graphite Plugs (¢)	2.95 ± 0.51 ¢[b]	2.63 ± 0.42 ¢	-10.88%

(a) Worth measurements were only performed using the Case 1 configuration.
(b) Total uncertainty was found by adding in quadrature the measurement uncertainty in Section 2.4 and the bias uncertainty in Section 3.4.
(c) "E" is the expected or benchmark value. "C" is the calculated value.

4.5 Results of Reactivity Coefficient Calculations

Reactivity coefficient measurements were not performed.

4.6 Results of Kinetics Parameter Calculations

Kinetics measurements were not performed.

4.7 Results of Reaction-Rate Distribution Calculations

The relative axial induced fission in uranium fission counter distributions and the relative radial activation of 235U fission foils distribution were evaluated using models as described in Section 3.7 in MCNP5-1.60 and ENDF/B-VII.0 neutron cross section libraries. An fmesh cell flux tally and a fission cross section tally multiplier were used to simulate the measurements. An fmesh mesh of cells was superimposed over a geometry for the purpose of performing tallies. A total of 2,000 cycles were run, skipping the first 150 cycles, with 1,000,000 histories per cycle. Seven different random numbers were used for each calculation. The variance weighted average of the seven tally results was taken for the calculated distributions.

4.7.1 Axial Measurements

The fmesh extended from the bottom of the core to the top of the top reflector for the axial measurements and had a radius of 0.32 cm. The tally multiplier was for ^{235}U. It can be seen in Tables 4.7-1, 4.7-2, and 4.7-3, and in Figures 1.7-1, 4.7-2, and 4.7-3 that for Case 1, the axial measurements calculate a little low through the lower region of the core: 6.7σ at the lowest measured point. Case 2 calculated fairly accurately: 3.7σ at the lowest point. It is not known why the models calculate low near the bottom of the core region. The sharp increase at the bottom of the core is due to the effect of the bottom reflector.[a] The tally multiplier was for a ^{235}U fission cross section.

a. Personal communication with the experimenter J. T. Mihalczo, November 23, 2011.

Table 4.7-1. Relative Axial Distribution of the Induced Fission in a Uranium Fission Counter, Case 1.

Distance from Bottom of Core[a]	Induced Fission[a] (Arbitrary Units) Benchmark Values			Calculated Values			(C-E)/E[b]	C/E Ratio[b]
3.81	0.77	±	0.02	0.664	±	0.004	-13.58%	0.864
6.35	0.77	±	0.02	0.682	±	0.004	-11.73%	0.883
8.89	0.79	±	0.02	0.715	±	0.004	-9.26%	0.907
11.43	0.83	±	0.02	0.739	±	0.005	-10.52%	0.895
12.7	0.81	±	0.02	0.747	±	0.005	-7.37%	0.926
13.97	0.83	±	0.02	0.749	±	0.005	-9.40%	0.906
15.24	0.80	±	0.02	0.747	±	0.005	-6.17%	0.938
16.51	0.79	±	0.02	0.740	±	0.005	-5.87%	0.941
17.78	0.77	±	0.02	0.730	±	0.004	-4.83%	0.952
19.05	0.77	±	0.02	0.715	±	0.004	-7.02%	0.930
21.59	0.72	±	0.01	0.673	±	0.004	-6.78%	0.932
24.13	0.64	±	0.01	0.619	±	0.004	-2.55%	0.975
26.67	0.58	±	0.01	0.563	±	0.003	-3.36%	0.966
27.94	0.56	±	0.01	0.548	±	0.003	-2.97%	0.970
29.21	0.61	±	0.01	0.581	±	0.004	-4.53%	0.955
31.75	0.93	±	0.02	0.915	±	0.008	-1.13%	0.989
33.02	1.00	±	0.02	1.000	±	0.009	0.00%	1.000
34.29	1.08	±	0.02	1.071	±	0.010	-0.37%	0.996
36.83	1.04	±	0.02	1.042	±	0.009	0.21%	1.002
38.1	0.93	±	0.02	0.967	±	0.009	3.93%	1.039
39.37	0.78	±	0.02	0.854	±	0.009	9.47%	1.095
41.91	0.51	±	0.01	0.527	±	0.006	3.06%	1.031

(a) Measured from bottom of fuel tube. Measurements above the top of the core region are highlighted.
(b) "E" is the expected or benchmark value. "C" is the calculated value.

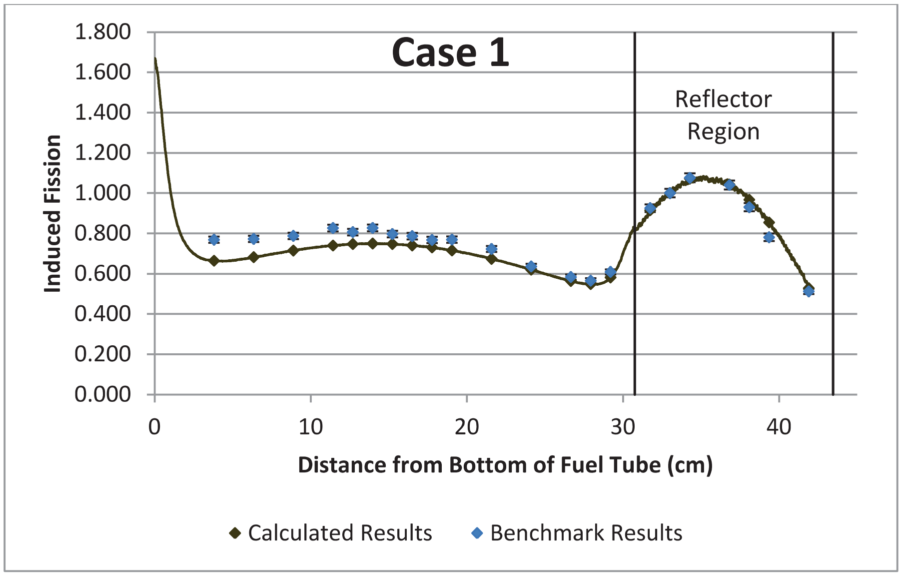

Figure 4.7-1. Relative Axial Uranium Fission Counter Count Rate Distribution, Case 1.

Table 4.7-2. Relative Axial Distribution of the Induced Fission in a Uranium Fission Counter, Case 2.

Distance from Bottom of Core	Induced Fission[a] (Arbitrary Units)						(C-E)/E[b]	C/E[b] Ratio
	Benchmark Values			Calculated Values				
3.81	1.04	±	0.02	0.970	±	0.002	-6.65%	0.933
6.35	1.04	±	0.02	0.972	±	0.002	-6.41%	0.936
8.89	1.07	±	0.02	1.011	±	0.001	-5.51%	0.945
11.43	1.07	±	0.02	1.032	±	0.001	-3.59%	0.964
12.7	1.07	±	0.02	1.032	±	0.001	-3.36%	0.966
13.97	1.02	±	0.02	1.029	±	0.001	0.90%	1.009
14.6	1.03	±	0.02	1.024	±	0.001	-0.58%	0.994
15.24	1.04	±	0.02	1.018	±	0.001	-2.14%	0.979
15.87	1.02	±	0.02	1.010	±	0.001	-1.01%	0.990
16.51	1.00	±	0.02	1.000	±	0.001	0.00%	1.000
17.14	0.99	±	0.02	0.990	±	0.001	-0.20%	0.998
19.05	0.95	±	0.02	0.946	±	0.001	-0.61%	0.994
21.59	0.89	±	0.02	0.864	±	0.001	-2.89%	0.971
24.13	0.75	±	0.01	0.764	±	0.001	1.49%	1.015
26.67	0.63	±	0.01	0.645	±	0.001	1.86%	1.019
29.21	0.54	±	0.01	0.528	±	0.001	-2.19%	0.978
31.75	0.49	±	0.01	0.496	±	0.004	2.19%	1.022
34.29	0.33	±	0.01	0.354	±	0.004	5.83%	1.058
36.83	0.18	±	0.01	0.215	±	0.003	19.62%	1.196

(a) Measured from bottom of fuel tube. Measurements above the top of the core region are highlighted.
(b) "E" is the expected or benchmark value. "C" is the calculated value.

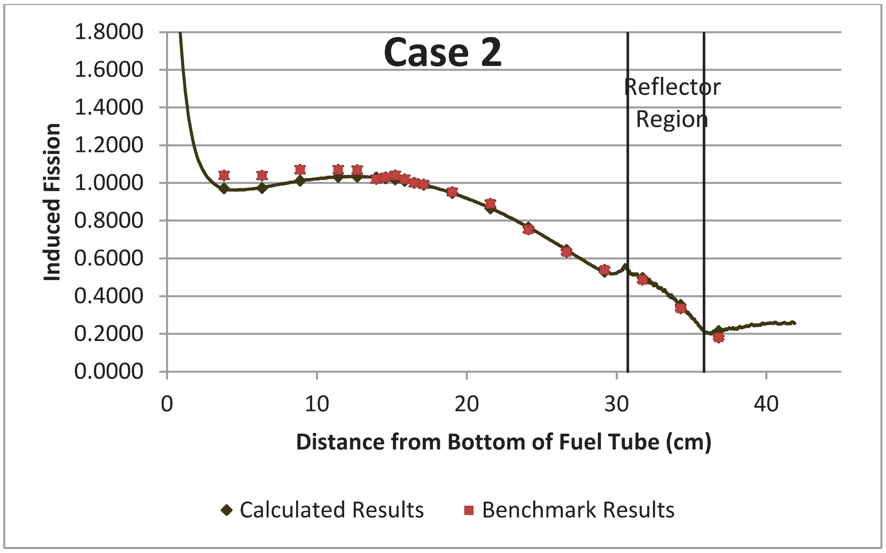

Figure 4.7-2. Relative Axial Uranium Fission Counter Count Rate Distribution, Case 2.

4.7.2 Radial Measurements

For the radial measurements, the fmesh extended from a radius of 11.485 cm (halfway between the core tank wall and the inside surface of the side reflector) through a plugged radial hole to the outside of the side reflector and had a radius of 0.375 cm. The normalization value was modeled using an identically sized fmesh spanning the height of the top reflector. The midpoint of the reflector, 36.79 cm, was used as the normalization point. The tally multiplier was for 93.2 wt.% ^{235}U (6.8 wt.% ^{238}U) fission cross sections. Results are given in Table 4.7-3 and plotted in Figure 4.7-3. The calculated results are lower than the benchmark values.

Table 4.7-3. Radial Activation of ^{235}U Fission Foils, Case 1.

Distance from Core (cm)[a]	Foil Activation[b]		(C-E)/E[c]	C/E[c] Ratio
	Benchmark Value	Calculated Value		
0.0	1.66 ± 0.09	1.499 ± 0.010	-9.75%	0.903
0.5	1.81 ± 0.10	1.656 ± 0.011	-8.63%	0.914
1.0	2.12 ± 0.11	1.826 ± 0.012	-13.93%	0.861
2.0	2.22 ± 0.12	2.080 ± 0.013	-6.30%	0.937
3.5	2.58 ± 0.14	2.443 ± 0.016	-5.43%	0.946
5.5	2.93 ± 0.16	2.721 ± 0.017	-7.12%	0.929
6.5	2.88 ± 0.16	2.748 ± 0.017	-4.51%	0.955
8.0	2.78 ± 0.16	2.765 ± 0.017	-0.53%	0.995
10.5	2.65 ± 0.15	2.539 ± 0.016	-4.19%	0.958
13.0	2.00 ± 0.11	2.100 ± 0.014	4.75%	1.047
16.0	1.40 ± 0.08	1.398 ± 0.011	-0.06%	0.999

(a) Zero point assumed to be inside surface of side reflector.
(b) Normalized to the midpoint of the top reflector of Case 1.
(c) "E" is the expected or benchmark value. "C" is the calculated value.

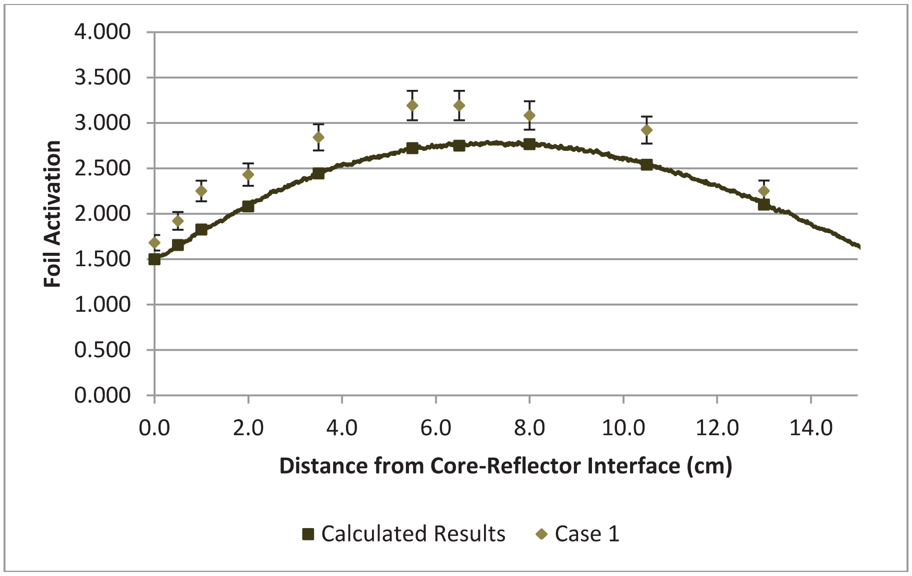

Figure 4.7-3. Relative Activation of ^{235}U Fission Foils in the Radial Reflector of Case 1.

4.8 Results of Power Distribution Calculations

Power density distribution measurements were not performed in the radial direction, but axial relative power density distribution measurements were performed in the central fuel pin location. Power density is proportional to the fission rate in a fission counter traversed axially through the core (see Section 4.7).

4.9 Results of Isotopic Calculations

Isotopic measurements were not performed.

4.10 Results of Calculations for Other Miscellaneous Types of Measurements

Other miscellaneous types of measurements were not performed.

5.0 REFERENCES

1. J. T. Mihalczo, "A Small Graphite-Reflected UO_2 Critical Assembly," ORNL-TM-450, Oak Ridge National Laboratory (1962).

2. J. T. Mihalczo, "A Small Graphite-Reflected UO_2 Assembly," *Proc. 5th Int. Conf. Nucl. Crit. Safety*, Albuquerque, NM, September 17-21 (1995).

APPENDIX A: COMPUTER CODES, CROSS SECTIONS, AND TYPICAL INPUT LISTINGS

Models were creating using Monte Carlo n-Particle (MCNP), Versions 5-1.51 and 5-1.60, and ENDF/B-VII.0 neutron cross section libraries. Isotopic abundances for all elements except uranium were taken from "Nuclides and Isotopes: Chart of the Nuclides," Sixteenth Edition, KAPL, 2002.

A.1 Critical/Subcritical Configurations

A.1.1 Name(s) of Code System(s) Used

1. Monte Carlo n-Particle, Versions 5.1.51 and 5.1.60 (MCNP5).

2. KENO-VI (SCALE 6.0).

A.1.2 Bibliographic References for the Codes Used

1. F. B. Brown, R. F. Barrett, T. E. Booth, J. S. Bull, L. J. Cox, R. A. Forster, T. J. Goorley, R. D. Mosteller, S. E. Post, R. E. Prael, E. C. Selcow, A. Sood, and J. Sweezy, "MCNP Version 5," LA-UR-02-3935, Los Alamos National Laboratory (2002).

2. D. F. Hollenbach, L. M. Petrie, S. Goluoglu, N. F. Landers, and M. E. Dunn, "KENO-VI: A General Quadratic Version of the KENO Program," ORNL/TM-2005/39 Version 6 Vol. II, Sect. F17, Oak Ridge National Laboratory (January 2009).

A.1.3 Origin of Cross-section Data

The evaluated neutron data file library ENDF/B-VII.0[a] was utilized in the benchmark-model analysis.

A.1.4 Spectral Calculations and Data Reduction Methods Used

Not applicable.

A.1.5 Number of Energy Groups or If Continuous-energy Cross Sections are Used in the Different Phases of Calculation

1. Continuous-energy cross sections.

2. Continuous-energy cross sections.

A.1.6 Component Calculations

- Type of cell calculation – reactor core and reflectors

- Geometry – fuel pin and assembly lattice

- Theory used – Not applicable

---

a. M. B. Chadwick, et al., "ENDF/B-VII.0: Next Generation Evaluated Nuclear Data Library for Nuclear Science and Technology," *Nucl. Data Sheets*, **107**: 2931-3060 (2006).

- Method used – Monte Carlo

- Calculation characteristics

  - MCNP5 – histories/cycles/cycles skipped = 100,000/2,000/150
    continuous-energy cross sections

  - KENO-VI – histories/cycles/cycles skipped = 100,000/2,000/150
    continuous-energy cross sections

A.1.7 Other Assumptions and Characteristics

Not applicable.

A.1.8 Typical Input Listings for Each Code System Type

MCNP5 Input Deck for Benchmark Models:
<u>*Case 1*</u>

```
SCCA-FUND-EXP-001-001
C
C
C   Cell Cards
C     Fuel Rod
4   1   6.5440E-02  -19 22 -23   u=1  imp:n=1 $ fuel rod
2   0             19 -21 22 -23  imp:n=1 u=1 $void around fuel
5   15  7.6116E-02  (-21 1 -22):(1 -24 -20 21):(23 -24 -21) u=1 imp:n=1 $ clad
9   0  -1:(1 -24 20):24 u=1 imp:n=1
10   0  -999 u=9 imp:n=1
C   Core Assembly
12   0  -11  lat=2 imp:n=1 u=2 fill= -10:10  -10:10  0:0
     2 2 2 2 2 2 2 2 2 2  2  2 2 2 2 2 2 2 2 2 2
     2 2 2 2 2 2 2 2 2 2  2  2 1 1 1 1 1 1 2 2 2
     2 2 2 2 2 2 2 2 2 2  1  1 1 1 1 1 1 1 1 2 2
     2 2 2 2 2 2 2 2 1 1  1  1 1 1 1 1 1 1 1 1 2
     2 2 2 2 2 2 2 1 1 1  1  1 1 1 1 1 1 1 1 1 2
     2 2 2 2 2 2 1 1 1 1  1  1 1 1 1 1 1 1 1 1 2
     2 2 2 2 2 1 1 1 1 1  1  1 1 1 1 1 1 1 1 1 2
     2 2 2 2 1 1 1 1 1 1  1  1 1 1 1 1 1 1 1 1 2
     2 2 2 1 1 1 1 1 1 1  1  1 1 1 1 1 1 1 1 1 2
     2 2 2 1 1 1 1 1 1 1  1  1 1 1 1 1 1 1 1 2 2
C
     2 2 1 1 1 1 1 1 1 1  9  1 1 1 1 1 1 1 1 2 2
C
     2 2 1 1 1 1 1 1 1 1  1  1 1 1 1 1 1 1 2 2 2
     2 1 1 1 1 1 1 1 1 1  1  1 1 1 1 1 1 1 2 2 2
     2 1 1 1 1 1 1 1 1 1  1  1 1 1 1 1 1 2 2 2 2
     2 1 1 1 1 1 1 1 1 1  1  1 1 1 1 1 2 2 2 2 2
     2 1 1 1 1 1 1 1 1 1  1  1 1 1 1 2 2 2 2 2 2
     2 1 1 1 1 1 1 1 1 1  1  1 1 1 2 2 2 2 2 2 2
     2 1 1 1 1 1 1 1 1 1  1  1 1 2 2 2 2 2 2 2 2
     2 2 1 1 1 1 1 1 1 1  1  2 2 2 2 2 2 2 2 2 2
     2 2 2 1 1 1 1 1 1 2  2  2 2 2 2 2 2 2 2 2 2
     2 2 2 2 2 2 2 2 2 2  2  2 2 2 2 2 2 2 2 2 2
13  0    -151 1 -153   fill=2 imp:n=1
C    Core Tank
20  2  6.1183E-02  (-153 1 151 -150):(-1 152 -150)  imp:n=1  $Core Tank
C   Reflectors
50  10   8.6953E-02  (-200 201 202 -203) imp:n=1  $Side Reflector
C
51  10   8.6953E-02  -210 211 -212 imp:n=1  $Bottom
C
```

```
52  10   8.6953E-02  -220 221 -222 imp:n=1  $Top
C
53  0  (211 -152 -201 210):(152 -153 -201 150):(-211 202 -201 300) imp:n=1
C
60  4  6.01329E-02  -300  imp:n=1  $Al 1100 reflector 1
61  5  5.99935E-02  -301  imp:n=1  $Al 1100 reflector 2
62  6  8.75101E-02  -302  imp:n=1  $SS304 lift
63  7  8.31444E-02  -303 304 imp:n=1
C
998  0 300 301 302 #63  (-202 -999):(202 -203 200 -999):
          (203 -222 220 -999):(222 -999)  imp:n=1
999  0  999 imp:n=0

C   Surface Cards
1    pz  0
10   rcc  0 0 0  0 0 30.48  0.635
11   rhp  0 0 -10  0 0 50  0.635001 0 0
12   rcc  0 0 0  0 0 30.76  11.145
C
19   cz  0.5705  $IR of Fuel
20   cz  0.635  $ OR Clad
21   cz  0.584  $IR Clad
22   pz  0.3    $ Top of bottom cap
23   pz  30.18  $ Bottom of Top cap
24   pz  30.48  $ Top of Tube
28   rpp -.9 .9  -.9 .9  0.2978 1.4472
C
C
150   cz  11.435 $ OR Core Tank
151   cz  11.145  $ IR Core Tank
152   pz    -0.35  $ Bottom Core Tank
153   pz    30.76  $ Top of Core Tank
C
C
200   cz  30.785  $OR Side Reflector
201   cz  11.535  $IR side reflector
202   pz  -15.87  $Bottom side reflector
203   pz  30.76   $Top of side reflector
C
210   cz  11.435  $OR Bottom Reflector
211   pz  -15.59  $Bottom of Bottom Reflector
212   pz  -0.35   $Top of Bottom Reflector
C
220   cz  25.40  $OR Top Reflector
221   pz  30.76  $Bottom of Top Reflector
222   pz  43.46  $Top of Top Reflector
C
300   rcc  0 0 -17.53  0 0 1.94  10.8
301   rcc  0 0 -18.16  0 0 0.63  22.86
302   rcc  0 0 -20.54  0 0 2.38  22.86
303   rpp  -60.95 60.95  -60.95 60.95  -17.14 -15.87
304   cz  11.79
C
C
999   rpp  -367 703   -680 390  -280 630

C   Data Cards
C     UO2
m1       92234.70c   2.2140E-04
      92235.70c   2.0332E-02
      92236.70c   1.0215E-04
      92238.70c   1.1573E-03
      8016.70c   4.3521E-02
      8017.70c   1.0601E-04   $ TOT   6.5440E-02
C
C    Core Tank - Al 1100
```

```
m2   13027.70c   6.0920E-02
      29063.70c   2.2517E-05
      29065.70c   1.0036E-05
      14028.70c   1.2907E-04
      14029.70c   6.5537E-06
      14030.70c   4.3203E-06
      26054.70c   4.1135E-06
      26056.70c   6.4573E-05
      26057.70c   1.4913E-06
      26058.70c   1.9846E-07
      25055.70c   7.5306E-06
      30000.70c   1.2654E-05   $ Tot   6.1183E-02
C
C    ATL  Reflector
m10   6000.70c   8.6953E-02
C   Fuel Clad- SS347
m15       26054.70c   3.0215E-03
      26056.70c   4.7431E-02
      26057.70c   1.0954E-03
      26058.70c   1.4578E-04
      6000.70c   1.3990E-04
      25055.70c   7.6465E-04
      14028.70c   6.8975E-04
      14029.70c   3.5024E-05
      14030.70c   2.3088E-05
      24050.70c   6.3187E-04
      24052.70c   1.2185E-02
      24053.70c   1.3817E-03
      24054.70c   3.4393E-04
      28058.70c   5.3600E-03
      28060.70c   2.0647E-03
      28061.70c   8.9749E-05
      28062.70c   2.8616E-04
      28064.70c   7.2877E-05
      15031.70c   3.0516E-05
      16032.70c   1.8652E-05
      16033.70c   1.4933E-07
      16034.70c   8.4292E-07
      16034.70c   3.9297E-09
      41093.70c   2.9104E-04
      73181.70c   1.3076E-05   $ tot   7.6116E-02
C    bot. reflt. 1 - Al 1100
m4   13027.70c   5.98746E-02
      29063.70c   2.21304E-05
      29065.70c   9.86383E-06
      14028.70c   1.26853E-04
      14029.70c   6.44131E-06
      14030.70c   4.24616E-06
      26054.70c   4.04295E-06
      26056.70c   6.34657E-05
      26057.70c   1.46570E-06
      25055.70c   7.40146E-06
      30000.70c   1.24368E-05   $ Tot   6.01329E-02
C    bot. reflt. 2 - Al 1100
m5   13027.70c   5.97358E-02
      29063.70c   2.20791E-05
      29065.70c   9.84096E-06
      14028.70c   1.26559E-04
      14029.70c   6.42638E-06
      14030.70c   4.23632E-06
      26054.70c   4.03358E-06
      26056.70c   6.33185E-05
      26057.70c   1.46230E-06
      25055.70c   7.38430E-06
      30000.70c   1.24080E-05   $ Tot   5.99935E-02
C    lift SS 304
```

```
m6   26054.70c   3.51905E-03
      26056.70c   5.52415E-02
      26057.70c   1.27577E-03
      26058.70c   1.69781E-04
      6000.70c   1.60142E-04
      25055.70c   8.75287E-04
      14028.70c   7.89554E-04
      14029.70c   4.00916E-05
      14030.70c   2.64287E-05
      24050.70c   7.63478E-04
      24052.70c   1.47229E-02
      24053.70c   1.66946E-03
      24054.70c   4.15564E-04
      28058.70c   5.29886E-03
      28060.70c   2.04111E-03
      28061.70c   8.87257E-05
      28062.70c   2.82896E-04
      28064.70c   7.20454E-05
      15031.70c   3.49310E-05
      16032.70c   2.13510E-05
      16033.70c   1.70934E-07
      16034.70c   9.64879E-07
      16034.70c   4.49827E-09   $ tot   8.75101E-02
C    Fe table
m7   26054.70c   4.66461E-03
      26056.70c   7.32245E-02
      26057.70c   1.69107E-03
      26058.70c   2.25051E-04
      6000.70c   9.43662E-04
      12024.70c   1.47344E-03
      12025.70c   1.86535E-04
      12026.70c   2.05375E-04
      15031.70c   2.92746E-05
      16032.70c   3.35506E-05
      16033.70c   2.68603E-07
      16034.70c   1.51619E-06
      16036.70c   7.06849E-09
      14028.70c   2.97765E-04
      14029.70c   1.51198E-05
      14030.70c   9.96708E-06
      29063.70c   9.86995E-05
      29065.70c   4.39917E-05   $ tot   8.31444E-02
mt1   o2/u.10t  u/o2.10t
mt2   al27.12t
mt4   al27.12t
mt5   al27.12t
mt10  grph.10t
kcode  1000000 1 150 2000
C  kcode  100 1 10 150
ksrc   0.0692  4.5245 0.77787  0  8.8072 0.7787
       0.0692 -4.3864 0.77787  0 -8.7382 0.7787
       3.8736 0 0.7787   7.6780 0 0.7787
      -3.7353 0 0.7787  -7.8510 0 0.7787
```

<u>*Case 2*</u>

```
SCCA-FUND-EXP-001-002
C
C
C   Cell Cards
C     Fuel Rod
4   1   6.5440E-02  -19 22 -23   u=1  imp:n=1 $ fuel rod
2   0             19 -21 22 -23  imp:n=1 u=1 $void around fuel
5   15  7.6116E-02  (-21 1 -22):(1 -24 -20 21):(23 -24 -21) u=1 imp:n=1 $ clad
9   0  -1:(1 -24 20):24 u=1 imp:n=1
10   0  -999 u=9 imp:n=1
```

```
C   Core Assembly
12   0  -11  lat=2 imp:n=1 u=2 fill= -10:10  -10:10  0:0
     2 2 2 2 2 2 2 2 2 2  2  2 2 2 2 2 2 2 2 2 2
     2 2 2 2 2 2 2 2 2 2  2  2 1 1 1 1 1 1 2 2 2
     2 2 2 2 2 2 2 2 2 2  1  1 1 1 1 1 1 1 1 2 2
     2 2 2 2 2 2 2 2 1 1  1  1 1 1 1 1 1 1 1 1 2
     2 2 2 2 2 2 2 1 1 1  1  1 1 1 1 1 1 1 1 1 2
     2 2 2 2 2 2 1 1 1 1  1  1 1 1 1 1 1 1 1 1 2
     2 2 2 2 2 1 1 1 1 1  1  1 1 1 1 1 1 1 1 1 2
     2 2 2 2 1 1 1 1 1 1  1  1 1 1 1 1 1 1 1 1 2
     2 2 2 1 1 1 1 1 1 1  1  1 1 1 1 1 1 1 1 1 2
     2 2 2 1 1 1 1 1 1 1  1  1 1 1 1 1 1 1 1 2 2
C
     2 2 1 1 1 1 1 1 1 1  9  1 1 1 1 1 1 1 1 2 2
C
     2 2 1 1 1 1 1 1 1 1  1  1 1 1 1 1 1 1 2 2 2
     2 1 1 1 1 1 1 1 1 1  1  1 1 1 1 1 1 1 2 2 2
     2 1 1 1 1 1 1 1 1 1  1  1 1 1 1 1 1 2 2 2 2
     2 1 1 1 1 1 1 1 1 1  1  1 1 1 1 1 2 2 2 2 2
     2 1 1 1 1 1 1 1 1 1  1  1 1 1 1 2 2 2 2 2 2
     2 1 1 1 1 1 1 1 1 1  1  1 1 1 2 2 2 2 2 2 2
     2 1 1 1 1 1 1 1 1 1  1  1 1 2 2 2 2 2 2 2 2
     2 2 1 1 1 1 1 1 1 1  1  2 2 2 2 2 2 2 2 2 2
     2 2 2 1 1 1 1 1 1 2  2  2 2 2 2 2 2 2 2 2 2
     2 2 2 2 2 2 2 2 2 2  2  2 2 2 2 2 2 2 2 2 2
13  0    -151 1 -153  fill=2 imp:n=1
C    Core Tank
20  2  6.1183E-02  (-153 1 151 -150):(-1 152 -150)  imp:n=1  $Core Tank
C   Reflectors
50  10  8.7581E-02  (-200 201 202 -203)  imp:n=1  $Side Reflector
C
51  10  8.7581E-02  -210 211 -212 imp:n=1  $Bottom
C
52  10  8.7581E-02  -220 221 -222 imp:n=1  $Top
C
53  0  (211 -152 -201 210):(152 -153 -201 150):(-211 202 -201 300) imp:n=1
C
60  4  6.01329E-02  -300  imp:n=1  $Al 1100 reflector 1
61  5  5.99935E-02  -301  imp:n=1  $Al 1100 reflector 2
62  6  8.75101E-02  -302  imp:n=1  $SS304 lift
63  7  8.31444E-02  -303 304 imp:n=1
C
998  0  300 301 302 #63 (-202 -999):(202 -203 200 -999):
           (203 -222 220 -999):(222 -999)  imp:n=1
999  0  999 imp:n=0

C   Surface Cards
1    pz  0
C  10   rcc  0 0 0  0 0 30.48  0.635
11   rhp  0 0 -10  0 0 50  0.635001 0 0
C 12   rcc  0 0 0  0 0 30.76  11.145
C
19   cz  0.5705  $IR of Fuel
20   cz  0.635  $ OR Clad
21   cz  0.584  $IR Clad
22   pz  0.3    $ Top of bottom cap
23   pz  30.18  $ Bottom of Top cap
24   pz  30.48  $ Top of Tube
C 28   rpp -.9 .9  -.9 .9  0.2978 1.4472
C
C
150   cz  11.435 $ OR Core Tank
151   cz  11.145  $ IR Core Tank
152   pz    -0.35  $ Bottom Core Tank
153   pz    30.76  $ Top of Core Tank
C
```

```
155   pz    1.91  $top of bottom shims
156   pz    28.82 $bottom of top shims
C
200   cz  35.875  $OR Side Reflector
201   cz  11.535  $IR side reflector
202   pz  -15.87  $Bottom side reflector
203   pz  30.76   $Top of side reflector
C
210   cz  11.435  $OR Bottom Reflector
211   pz  -15.59  $Bottom of Bottom Reflector
212   pz  -0.35   $Top of Bottom Reflector
C
220   cz  25.40  $OR Top Reflector
221   pz  30.76  $Bottom of Top Reflector
222   pz  35.84  $Top of Top Reflector
C
300   rcc  0 0 -17.53  0 0 1.94  10.8
301   rcc  0 0 -18.16  0 0 0.63  22.86
302   rcc  0 0 -20.54  0 0 2.38  22.86
303   rpp  -60.95 60.95  -60.95 60.95  -17.14 -15.87
304   cz  11.79
C
C 310   c/x 0 15.555 0.635
C 311   px  0
C
999   rpp  -367 703   -680 390  -280 630

C   Data Cards
C     UO2
m1      92234.70c   2.2140E-04
      92235.70c   2.0332E-02
      92236.70c   1.0215E-04
      92238.70c   1.1573E-03
      8016.70c   4.3521E-02
      8017.70c   1.0601E-04   $ TOT   6.5440E-02
C
C    Core Tank - Al 1100
m2   13027.70c   6.0920E-02
      29063.70c   2.2517E-05
      29065.70c   1.0036E-05
      14028.70c   1.2907E-04
      14029.70c   6.5537E-06
      14030.70c   4.3203E-06
      26054.70c   4.1135E-06
      26056.70c   6.4573E-05
      26057.70c   1.4913E-06
      26058.70c   1.9846E-07
      25055.70c   7.5306E-06
      30000.70c   1.2654E-05   $ Tot   6.1183E-02
C
C    ATL  Reflector
m10   6000.70c   8.7581E-02
C   Fuel Clad- SS347
m15       26054.70c   3.0215E-03
      26056.70c   4.7431E-02
      26057.70c   1.0954E-03
      26058.70c   1.4578E-04
      6000.70c   1.3990E-04
      25055.70c   7.6465E-04
      14028.70c   6.8975E-04
      14029.70c   3.5024E-05
      14030.70c   2.3088E-05
      24050.70c   6.3187E-04
      24052.70c   1.2185E-02
      24053.70c   1.3817E-03
      24054.70c   3.4393E-04
```

```
      28058.70c   5.3600E-03
      28060.70c   2.0647E-03
      28061.70c   8.9749E-05
      28062.70c   2.8616E-04
      28064.70c   7.2877E-05
      15031.70c   3.0516E-05
      16032.70c   1.8652E-05
      16033.70c   1.4933E-07
      16034.70c   8.4292E-07
      16034.70c   3.9297E-09
      41093.70c   2.9104E-04
      73181.70c   1.3076E-05   $ tot   7.6116E-02
C    bot. reflt. 1 - Al 1100
m4   13027.70c   5.98746E-02
      29063.70c   2.21304E-05
      29065.70c   9.86383E-06
      14028.70c   1.26853E-04
      14029.70c   6.44131E-06
      14030.70c   4.24616E-06
      26054.70c   4.04295E-06
      26056.70c   6.34657E-05
      26057.70c   1.46570E-06
      25055.70c   7.40146E-06
      30000.70c   1.24368E-05   $ Tot   6.01329E-02
C    bot. reflt. 2 - Al 1100
m5   13027.70c   5.97358E-02
      29063.70c   2.20791E-05
      29065.70c   9.84096E-06
      14028.70c   1.26559E-04
      14029.70c   6.42638E-06
      14030.70c   4.23632E-06
      26054.70c   4.03358E-06
      26056.70c   6.33185E-05
      26057.70c   1.46230E-06
      25055.70c   7.38430E-06
      30000.70c   1.24080E-05   $ Tot   5.99935E-02
C    lift SS 304
m6   26054.70c   3.51905E-03
      26056.70c   5.52415E-02
      26057.70c   1.27577E-03
      26058.70c   1.69781E-04
      6000.70c   1.60142E-04
      25055.70c   8.75287E-04
      14028.70c   7.89554E-04
      14029.70c   4.00916E-05
      14030.70c   2.64287E-05
      24050.70c   7.63478E-04
      24052.70c   1.47229E-02
      24053.70c   1.66946E-03
      24054.70c   4.15564E-04
      28058.70c   5.29886E-03
      28060.70c   2.04111E-03
      28061.70c   8.87257E-05
      28062.70c   2.82896E-04
      28064.70c   7.20454E-05
      15031.70c   3.49310E-05
      16032.70c   2.13510E-05
      16033.70c   1.70934E-07
      16034.70c   9.64879E-07
      16034.70c   4.49827E-09   $ tot   8.75101E-02
C    Fe table
m7   26054.70c   4.66461E-03
      26056.70c   7.32245E-02
      26057.70c   1.69107E-03
      26058.70c   2.25051E-04
      6000.70c   9.43662E-04
```

```
      12024.70c   1.47344E-03
      12025.70c   1.86535E-04
      12026.70c   2.05375E-04
      15031.70c   2.92746E-05
      16032.70c   3.35506E-05
      16033.70c   2.68603E-07
      16034.70c   1.51619E-06
      16036.70c   7.06849E-09
      14028.70c   2.97765E-04
      14029.70c   1.51198E-05
      14030.70c   9.96708E-06
      29063.70c   9.86995E-05
      29065.70c   4.39917E-05   $ tot   8.31444E-02
mt1   o2/u.10t  u/o2.10t
mt2   al27.12t
mt4   al27.12t
mt5   al27.12t
mt10  grph.10t
kcode  1000000 1 150 2000
C  kcode  100 1 10 150
ksrc   0.0692  4.5245 0.77787  0  8.8072 0.7787
       0.0692 -4.3864 0.77787  0 -8.7382 0.7787
       3.8736 0 0.7787   7.6780 0 0.7787
      -3.7353 0 0.7787  -7.8510 0 0.7787
```

KENO Input Deck for Benchmark Models:

<u>*Case 1*</u>

```
'Input generated by GeeWiz SCALE 6.1 Compiled on Mon Jun  6 11:04:33 2011
=csas6
scca-001 case 1
ce_v7_endf
read composition
 u-234       1 0 0.0002214 296   end
 u-235       1 0 0.020332 296   end
 u-236       1 0 0.00010215 296   end
 u-238       1 0 0.0011573 296   end
 o           1 0 0.043627 296   end
 fe          2 0 0.0516934 296   end
 c           2 0 0.0001399 296   end
 mn          2 0 0.00076465 296   end
 si          2 0 0.00074787 296   end
 cr          2 0 0.014542 296   end
 ni          2 0 0.0078734 296   end
 p           2 0 3.0516e-05 296   end
 s           2 0 1.9648e-05 296   end
 nb          2 0 0.00029104 296   end
 ta-181      2 0 1.3076e-05 296   end
 al          3 0 0.06092 296   end
 cu          3 0 3.2553e-05 296   end
 si          3 0 0.00013994 296   end
 fe          3 0 7.0377e-05 296   end
 mn          3 0 7.5306e-06 296   end
 zn          3 0 1.2654e-06 296   end
 c-graphite  4 0 0.086953 296   end
 al          5 0 0.059902 296   end
 cu          5 0 3.1994e-05 296   end
 si          5 0 0.00013754 296   end
 fe          5 0 6.8974e-05 296   end
 mn          5 0 7.4015e-06 296   end
 zn          5 0 1.2437e-06 296   end
 al          6 0 0.059763 296   end
 cu          6 0 3.192e-05 296   end
```

```
 si          6 0 0.00013722 296   end
 fe          6 0 6.8814e-05 296   end
 mn          6 0 7.3843e-06 296   end
 zn          6 0 1.2408e-06 296   end
 fe          7 0 0.060206 296   end
 c           7 0 0.00016014 296   end
 mn          7 0 0.00087529 296   end
 si          7 0 0.00085607 296   end
 cr          7 0 0.017571 296   end
 ni          7 0 0.0077836 296   end
 p           7 0 3.4931e-05 296   end
 s           7 0 2.2491e-05 296   end
 fe          8 0 0.079805 296   end
 c           8 0 0.00094366 296   end
 mg          8 0 0.0018653 296   end
 si          8 0 0.00032285 296   end
 cu          8 0 0.00014269 296   end
 p           8 0 2.9275e-05 296   end
 s           8 0 3.5342e-05 296   end
end composition
read parameter
 gen=2150
 npg=100000
 nsk=150
 htm=yes
end parameter
read geometry
unit 1
com="fuel rod"
 cylinder 1   0.5705    46.05    16.17
 cylinder 2    0.584    46.05    16.17
 cylinder 3    0.635    46.35    15.87
 hexprism 4    0.635    46.63    15.87
 media 1 1 1
 media 0 1 -1 2
 media 2 1 -2 3
 media 0 1 -3 4
 boundary 4
unit 2
com="void position"
 hexprism 1    0.635    46.63    15.87
 media 0 1 1
 boundary 1
global unit 3
com="assembly 1"
 cylinder 1   11.145    46.63    15.87
 cylinder 2   11.435    46.63    15.52
 array 1 1  place 11 11 1 0 0 0
 cylinder 3   11.435    46.63     0.28
 cylinder 4   11.535    46.63        0
 cylinder 5   30.785    46.63        0
 cylinder 6     25.4    59.33    46.63
 cylinder 7     86.2    59.33    -4.67
 cylinder 8     10.8     0.28    -1.66
 cylinder 9    22.86    -1.66    -2.29
 cylinder 10    22.86    -2.29    -4.67
 cylinder 11    11.79        0    -1.66
 cuboid 12    60.95   -60.95    60.95   -60.95        0    -1.27
 media 3 1 -1 2
 media 4 1 -2 3
 media 0 1 -3 4 -8
 media 4 1 -4 5
 media 4 1 6
 media 0 1 -5 -6 7 -12 -11 -9 -10
 media 8 1 12 -11
 media 7 1 10
```

```
 media 6 1 9
 media 5 1 8
 media 0 1 11 -8
 boundary 7
end geometry
read array
ara=1 nux=21 nuy=21 nuz=1 typ=triangular
 com=''
 fill
    2    2    2    2    2    2    2    2    2    2    2    2    2    2    2    2    2
2    2    2    2
    2    2    2    2    2    2    2    2    2    2    2    2    1    1    1    1    1
1    2    2    2
    2    2    2    2    2    2    2    2    2    2    1    1    1    1    1    1    1
1    1    2    2
    2    2    2    2    2    2    2    2    1    1    1    1    1    1    1    1    1
1    1    1    2
    2    2    2    2    2    2    2    1    1    1    1    1    1    1    1    1    1
1    1    1    2
    2    2    2    2    2    2    1    1    1    1    1    1    1    1    1    1    1
1    1    1    2
    2    2    2    2    2    1    1    1    1    1    1    1    1    1    1    1    1
1    1    1    2
    2    2    2    2    1    1    1    1    1    1    1    1    1    1    1    1    1
1    1    1    2
    2    2    2    1    1    1    1    1    1    1    1    1    1    1    1    1    1
1    1    1    2
    2    2    2    1    1    1    1    1    1    1    1    1    1    1    1    1    1
1    1    2    2
    2    2    1    1    1    1    1    1    1    1    2    1    1    1    1    1    1
1    1    2    2
    2    2    1    1    1    1    1    1    1    1    1    1    1    1    1    1    1
1    2    2    2
    2    1    1    1    1    1    1    1    1    1    1    1    1    1    1    1    1
1    2    2    2
    2    1    1    1    1    1    1    1    1    1    1    1    1    1    1    1    1
2    2    2    2
    2    1    1    1    1    1    1    1    1    1    1    1    1    1    1    1    2
2    2    2    2
    2    1    1    1    1    1    1    1    1    1    1    1    1    1    1    2    2
2    2    2    2
    2    1    1    1    1    1    1    1    1    1    1    1    1    1    2    2    2
2    2    2    2
    2    1    1    1    1    1    1    1    1    1    1    1    1    2    2    2    2
2    2    2    2
    2    2    1    1    1    1    1    1    1    1    1    2    2    2    2    2    2
2    2    2    2
    2    2    2    1    1    1    1    1    1    2    2    2    2    2    2    2    2
2    2    2    2
    2    2    2    2    2    2    2    2    2    2    2    2    2    2    2    2    2
2    2    2    2  end fill
end array
end data
end
```

<u>Case 2</u>

```
'Input generated by GeeWiz SCALE 6.1 Compiled on Mon Jun  6 11:04:33 2011
=csas6
scca-001 case 2
ce_v7_endf
read composition
 u-234       1 0 0.0002214 296   end
 u-235       1 0 0.020332 296   end
 u-236       1 0 0.00010215 296   end
 u-238       1 0 0.0011573 296   end
 o           1 0 0.043627 296   end
```

```
 fe          2 0 0.0516934 296   end
 c           2 0 0.0001399 296   end
 mn          2 0 0.00076465 296   end
 si          2 0 0.00074787 296   end
 cr          2 0 0.014542 296   end
 ni          2 0 0.0078734 296   end
 p           2 0 3.0516e-05 296   end
 s           2 0 1.9648e-05 296   end
 nb          2 0 0.00029104 296   end
 ta-181      2 0 1.3076e-05 296   end
 al          3 0 0.06092 296   end
 cu          3 0 3.2553e-05 296   end
 si          3 0 0.00013994 296   end
 fe          3 0 7.0377e-05 296   end
 mn          3 0 7.5306e-06 296   end
 zn          3 0 1.2654e-06 296   end
 c-graphite  4 0 0.087581 296   end
 al          5 0 0.059902 296   end
 cu          5 0 3.1994e-05 296   end
 si          5 0 0.00013754 296   end
 fe          5 0 6.8974e-05 296   end
 mn          5 0 7.4015e-06 296   end
 zn          5 0 1.2437e-06 296   end
 al          6 0 0.059763 296   end
 cu          6 0 3.192e-05 296   end
 si          6 0 0.00013722 296   end
 fe          6 0 6.8814e-05 296   end
 mn          6 0 7.3843e-06 296   end
 zn          6 0 1.2408e-06 296   end
 fe          7 0 0.060206 296   end
 c           7 0 0.00016014 296   end
 mn          7 0 0.00087529 296   end
 si          7 0 0.00085607 296   end
 cr          7 0 0.017571 296   end
 ni          7 0 0.0077836 296   end
 p           7 0 3.4931e-05 296   end
 s           7 0 2.2491e-05 296   end
 fe          8 0 0.079805 296   end
 c           8 0 0.00094366 296   end
 mg          8 0 0.0018653 296   end
 si          8 0 0.00032285 296   end
 cu          8 0 0.00014269 296   end
 p           8 0 2.9275e-05 296   end
 s           8 0 3.5342e-05 296   end
end composition
read parameter
 gen=2150
 npg=100000
 nsk=150
 htm=yes
end parameter
read geometry
unit 1
com="fuel rod"
 cylinder 1   0.5705    46.05    16.17
 cylinder 2    0.584    46.05    16.17
 cylinder 3    0.635    46.35    15.87
 hexprism 4    0.635    46.63    15.87
 media 1 1 1
 media 0 1 -1 2
 media 2 1 -2 3
 media 0 1 -3 4
 boundary 4
unit 2
com="void position"
 hexprism 1    0.635    46.63    15.87
```

```
 media 0 1 1
 boundary 1
global unit 3
com="assembly 1"
 cylinder 1   11.145    46.63    15.87
 cylinder 2   11.435    46.63    15.52
 array 1 1  place 11 11 1 0 0 0
 cylinder 3   11.435    46.63     0.28
 cylinder 4   11.535    46.63        0
 cylinder 5   35.875    46.63        0
 cylinder 6     25.4    51.71    46.63
 cylinder 7     86.2    51.71    -4.67
 cylinder 8     10.8     0.28    -1.66
 cylinder 9    22.86    -1.66    -2.29
 cylinder 10    22.86    -2.29    -4.67
 cylinder 11    11.79        0    -1.66
 cuboid 12    60.95   -60.95    60.95   -60.95        0    -1.27
 media 3 1 -1 2
 media 4 1 -2 3
 media 0 1 -3 4 -8
 media 4 1 -4 5
 media 4 1 6
 media 0 1 -5 -6 7 -12 -11 -9 -10
 media 8 1 12 -11
 media 7 1 10
 media 6 1 9
 media 5 1 8
 media 0 1 11 -8
 boundary 7
end geometry
read array
ara=1 nux=21 nuy=21 nuz=1 typ=triangular
 com=''
 fill
    2    2    2    2    2    2    2    2    2    2    2    2    2    2    2    2    2
2    2    2    2
    2    2    2    2    2    2    2    2    2    2    2    2    1    1    1    1    1
1    2    2    2
    2    2    2    2    2    2    2    2    2    2    1    1    1    1    1    1    1
1    1    2    2
    2    2    2    2    2    2    2    2    1    1    1    1    1    1    1    1    1
1    1    1    2
    2    2    2    2    2    2    2    1    1    1    1    1    1    1    1    1    1
1    1    1    2
    2    2    2    2    2    2    1    1    1    1    1    1    1    1    1    1    1
1    1    1    2
    2    2    2    2    2    1    1    1    1    1    1    1    1    1    1    1    1
1    1    1    2
    2    2    2    2    1    1    1    1    1    1    1    1    1    1    1    1    1
1    1    1    2
    2    2    2    1    1    1    1    1    1    1    1    1    1    1    1    1    1
1    1    1    2
    2    2    2    1    1    1    1    1    1    1    1    1    1    1    1    1    1
1    1    2    2
    2    2    1    1    1    1    1    1    1    1    2    1    1    1    1    1    1
1    1    2    2
    2    2    1    1    1    1    1    1    1    1    1    1    1    1    1    1    1
1    2    2    2
    2    1    1    1    1    1    1    1    1    1    1    1    1    1    1    1    1
1    2    2    2
    2    1    1    1    1    1    1    1    1    1    1    1    1    1    1    1    1
2    2    2    2
    2    1    1    1    1    1    1    1    1    1    1    1    1    1    1    1    2
2    2    2    2
    2    1    1    1    1    1    1    1    1    1    1    1    1    1    1    2    2
2    2    2    2
```

```
    2    1    1    1    1    1    1    1    1    1    1    1    1    1    2    2    2
2    2    2    2
    2    1    1    1    1    1    1    1    1    1    1    1    1    2    2    2    2
2    2    2    2
    2    2    1    1    1    1    1    1    1    1    1    2    2    2    2    2    2
2    2    2    2
    2    2    2    1    1    1    1    1    1    2    2    2    2    2    2    2    2
2    2    2    2
    2    2    2    2    2    2    2    2    2    2    2    2    2    2    2    2    2
2    2    2    2  end fill
end array
end data
end
```

A.2 Buckling and Extrapolation Length Configurations

Buckling and extrapolation-length measurements were not performed.

A.3 Spectral-Characteristics Configurations

Spectral characteristic measurements were not evaluated.

A.4 Reactivity-Effects Configurations

MCNP5 Input Decks for Graphite Plug Worth:

The input decks for analysis of the graphite plug worth are those of the critical assembly described in Section 3.1.1 with the adjustments discussed in Section 3.4.1.

MCNP5 Input Decks for Center Fuel Element Worth:

The input decks for analysis of the center fuel element worth are that of the critical assembly described in Section 3.1.1 with the adjustments discussed in Section 3.4.1.

A.5 Reactivity Coefficient Configurations

Reactivity coefficient measurements were not performed

A.6 Kinetics Parameter Configurations

Kinetics measurements were not performed.

A.7 Reaction-Rate Configurations

MCNP5 Input Decks for Evaluating ^{235}U Fission Reaction-Rate Measurements:

The input decks for analysis of the radial and axial ^{235}U fission reaction-rate measurements is that of the critical assembly described in Section 3.1.1 with changes discussed in Section 3.7.1 with the following tally-card specifications appended to the end of the input deck:

<u>Axial Distribution of the Induced Fission in a Uranium Fission Counter Tally-Card</u>

```
m1000 92235.70 -.932
   92238.70 -.068
fmesh4:n geom cyl origin 0 0 0.005
     imesh 0.32 iints 1
     jmesh 41.915 jints 4191
     kmesh 1 kints 1
fm4 1 1000 -6
```

<u>Radial Activation of ^{235}U Fission Foils Tally-Card</u>

```
m1000 92235.70 -.932
   92238.70 -.068
fmesh4:n geom cyl origin 11.435 0 15.555
     axs 1 0 0 vec 0 0 1
     imesh 0.375 iints 1
     jmesh 19.31 jints 1931
     kmesh 1 kints 1
fm4 1 1000 -6
```

A.8 Power Distribution Configurations

The axial relative power distribution is the same as the relative fission rate as was measured in the core region of Assembly 1 (see Section A.7).

A.9 Isotopic Configurations

Isotopic measurements were not performed.

A.10 Configurations of Other Miscellaneous Types of Measurements

Other miscellaneous types of measurements were not performed.

APPENDIX B: DERIVATION OF FUEL AND FUEL-TUBE MASSES AND UNCERTAINTIES

The mass of one fuel tube was found using the measured mass of 314 fuel tubes plus the box the tubes were in and the mass of the box. The uncertainty in each of these values was ±1 g. Equations B.1through B.4 were used to find the mass of one fuel tube and the associated uncertainty.

$$m_{314\,Fuel\,Tubes} = m_{314\,Fuel\,Tubes+Box} - m_{\mathrm{Box}}$$

$$m_{314\,Fuel\,Tubes} = 14{,}045g = 14{,}442g - 937g \qquad \text{Equation B.1}$$

$$\sigma_{m_{314\,Fuel\,Tubes}} = \sqrt{\left(\sigma_{m_{314\,Fuel\,Tubes+Box}}\right)^2 + \left(\sigma_{m_{Box}}\right)^2}$$

$$\sigma_{m_{314\,Fuel\,Tubes}} = \sqrt{(1)^2 + (1)^2} = 1 \cdot \sqrt{2} \qquad \text{Equation B.2}$$

$$m_{1\,Fuel\,Tube} = \frac{m_{314\,Fuel\,Tubes}}{314}$$

$$m_{1\,Fuel\,Tube} = \frac{14{,}045g}{314} = 44.729g \qquad \text{Equation B.3}$$

$$\sigma_{m_{1\,Fuel\,Tube}} = \frac{\sigma_{m_{314\,Fuel\,Tubes}}}{314}$$

$$\sigma_{m_{1\,Fuel\,Tube1}} = \frac{\sigma_{m_{314\,Fuel\,Tubes}}}{314} = \frac{1 \cdot \sqrt{2}}{314} = 0.0045g \qquad \text{Equation B.4}$$

Next, the mass of one end cap was found. This was done using Equations B.5 and B.6.

$$m_{1\,End\,Cap} = \frac{m_{324\,\mathrm{End\,Caps}}}{324}$$

$$m_{1\,Fuel\,Tube} = \frac{207.706g}{324} = 0.64107g \qquad \text{Equation B.5}$$

$$\sigma_{m_{1\,End\,Cap}} = \frac{\sigma_{m_{324\,\mathrm{End\,Caps}}}}{324}$$

$$\sigma_{m_{1\,End\,Cap}} = \frac{\sigma_{m_{324\,\mathrm{End\,Caps}}}}{324} = \frac{0.001}{324} = 3.1x10^{-6}g \qquad \text{Equation B.6}$$

Finally the mass of the fuel tube plus two end caps was found. The uncertainty in the mass of an end cap is negligible in comparison to the mass of one fuel tube; thus, the uncertainty in the fuel tube plus two end caps' mass was ±0.0045 g. Equation B.7 was used to find the mass.

$$m_{\mathrm{Fuel\,Tube}+2\,End\,Caps} = m_{1\,Fuel\,Tube} + 2 * m_{1\,\mathrm{End\,Cap}}$$

$$m_{\mathrm{Fuel\,Tube}+2\,End\,Caps} = 44.729 + 2 * 0.64107 = 46.01114\ g \qquad \text{Equation B.7}$$

The mass of fuel per tube was also calculated. A total fuel mass of 82,533.26 g for 279 fuel tubes was reported. This value was obtained by measuring bundles of 26 pellets for 279 fuel tubes and then summing the masses. The uncertainty in the mass of each bundle of 26 pellets was ±0.01g. Equations B.8 and B.9 were used to calculate the mass and the associated uncertainty.

$$m_{\text{fuel per tube,average}} = \frac{m_{\text{fuel in 279 tubes}}}{279}$$

$$m_{\text{fuel per tube,average}} = \frac{82{,}533.26}{279} = 295.818\ g \qquad \text{Equation B.8}$$

$$\sigma_{m_{\text{fuel in 279 tubes}}} = \sqrt{\sum_{i=1}^{279} \sigma_{mass\ of\ i^{th} bundle\ of\ pellets}}$$

$$= \sigma_{mass\ of\ 1\ bundle\ of\ pellets}\sqrt{279}$$

$$\sigma_{m_{\text{fuel in 279 tubes}}} = 0.01 \cdot \sqrt{279} \qquad \text{Equation B.9}$$

$$\sigma_{m_{\text{fuel per tube,average}}} = \frac{\sigma_{m_{\text{fuel in 279 tubes}}}}{279}$$

$$\sigma_{m_{\text{fuel per tube,average}}} = \frac{0.01 \cdot \sqrt{279}}{279} = 0.0006$$

APPENDIX C: SAMPLE K_{EFF} RESULTS AND INPUT DECKS FOR DETAILED MODELS

C.1 Sample Calculation Results for Critical Assemblies, Detailed Model

Sample results for the detailed model have been included. As can be seen from Table C.1, the results of comparing the detailed model to the expected value agree with the results of comparing the sample results for the benchmark model to the benchmark k_{eff}.

Table C.1. Sample Results for the Detailed Model.

	Expected			Calculated MCNP5 ENDF/B-VII.0(c)			
	k_{eff}(a)	±	σ(b)	k_{eff}	±	σ	$\frac{C-E}{E}$
Case 1	1.00052	±	0.0005	1.00551	±	0.00006	0.50%
Case 2	1.00025	±	0.0005	1.00484	±	0.00006	0.46%

(a) Include bias of measured reactivity of critical configuration given in Table 2.1.
(b) Uncertainty includes measurement uncertainty determined in Section 2.1.
(c) Run using 100,000 histories for 2000 cycles, skipping the first 150 cycles.

C.2 Sample Input Decks, Detailed Model for MCNP5

MCNP5 Detailed Input Decks:
Case 1

```
SCCA-FUND-EXP-001-001
C
C
C   Cell Cards
C   Fuel Pellets
1   1   6.57374E-02  (-25 22 -26) u=10 imp:n=1  $ fuel pellet
2   100 4.97210E-05  -22:(22 -26 25):26 u=10 imp:n=1  $void around pellet
3   100 4.97210E-05  -28   lat=1 imp:n=1 u=11 fill= 0:0 0:0 -1:26
         11 10 10 10 10 10 10 10 10 10 10 10 10 10
           10 10 10 10 10 10 10 10 10 10 10 10 10 11
C     Fuel Rod
4   100 4.97210E-05  -21 22 -23  fill=11 u=1  imp:n=1 $ fuel rod
5   15  8.19858E-02  (1 -24 -20 21) u=1 imp:n=1 $ clad
6   16  2.17619E-02  (-21 1 -22):(23 -24 -21) u=1 imp:n=1
9   100 4.97210E-05  -1:(1 -24 20):24 u=1 imp:n=1
10   100 4.97210E-05  -999 u=9 imp:n=1
C   Core Assembly
12   100 4.97210E-05  -11  lat=2 imp:n=1 u=2 fill= -10:10  -10:10  0:0
     2 2 2 2 2 2 2 2 2 2  2  2 2 2 2 2 2 2 2 2 2
     2 2 2 2 2 2 2 2 2 2  2  2 1 1 1 1 1 1 2 2 2
     2 2 2 2 2 2 2 2 2 2  1  1 1 1 1 1 1 1 1 2 2
     2 2 2 2 2 2 2 2 1 1  1  1 1 1 1 1 1 1 1 1 2
     2 2 2 2 2 2 2 1 1 1  1  1 1 1 1 1 1 1 1 1 2
     2 2 2 2 2 2 1 1 1 1  1  1 1 1 1 1 1 1 1 1 2
     2 2 2 2 2 1 1 1 1 1  1  1 1 1 1 1 1 1 1 1 2
     2 2 2 2 1 1 1 1 1 1  1  1 1 1 1 1 1 1 1 1 2
     2 2 2 1 1 1 1 1 1 1  1  1 1 1 1 1 1 1 1 1 2
     2 2 2 1 1 1 1 1 1 1  1  1 1 1 1 1 1 1 1 2 2
```

```
C
     2 2 1 1 1 1 1 1 1 1  9  1 1 1 1 1 1 1 1 2 2
C
     2 2 1 1 1 1 1 1 1 1  1  1 1 1 1 1 1 1 2 2 2
     2 1 1 1 1 1 1 1 1 1  1  1 1 1 1 1 1 1 2 2 2
     2 1 1 1 1 1 1 1 1 1  1  1 1 1 1 1 1 2 2 2 2
     2 1 1 1 1 1 1 1 1 1  1  1 1 1 1 1 2 2 2 2 2
     2 1 1 1 1 1 1 1 1 1  1  1 1 1 1 2 2 2 2 2 2
     2 1 1 1 1 1 1 1 1 1  1  1 1 1 2 2 2 2 2 2 2
     2 1 1 1 1 1 1 1 1 1  1  1 1 2 2 2 2 2 2 2 2
     2 2 1 1 1 1 1 1 1 1  1  2 2 2 2 2 2 2 2 2 2
     2 2 2 1 1 1 1 1 1 2  2  2 2 2 2 2 2 2 2 2 2
     2 2 2 2 2 2 2 2 2 2  2  2 2 2 2 2 2 2 2 2 2
13  0    -151 1 -153 -101 -102 -103 -104 -105 -106 -107
             -108 -109 -110 -111 -112  fill=2 imp:n=1
C    Core Tank
20  2  6.11826E-02  (-153 1 151 -150):(-1 152 -150)  imp:n=1  $Core Tank
21  3  6.24138E-02  -151 -153 156 #13  imp:n=1  $Top shims
22  3  6.24138E-02  -151 1 -155 #13  imp:n=1  $Bottom shims
23  100 4.97210E-05        -151 155 -156 #13 imp:n=1 $space between shims
C   Reflectors
40   100 4.97210E-05    -310 -200 201 -311 imp:n=1
41  100 4.97210E-05  -310 314 -200 201 311 imp:n=1
42  100 4.97210E-05  -312 315 -200 201 imp:n=1
43  100 4.97210E-05  -313 316 -200 201 imp:n=1
44  10  8.81092E-02  -314 -200 201 311 imp:n=1
45  10  8.81092E-02  -315 -200 201 imp:n=1
46  10  8.81092E-02  -316 -200 201 imp:n=1
50  10  8.81092E-02  (-200 201 202 -203) 310 312 313 imp:n=1  $Side Reflector
C
51  12  8.81297E-02  -210 211 -212 imp:n=1  $Bottom
C
52  11  8.21800E-02  -220 317 221 -222 imp:n=1  $Top
53  11  8.21800E-02  -318 -222 221 imp:n=1
54  100 4.97210E-05   -317 318 -222 221 imp:n=1
C
55  100 4.97210E-05  (211 -152 -201 210):(152 -153 -201 150):
        (-211 202 -201 300) imp:n=1
C
60  4  6.01329E-02  -300  imp:n=1  $Al 1100 reflector 1
61  5  5.99935E-02  -301  imp:n=1  $Al 1100 reflector 2
62  6  8.75101E-02  -302  imp:n=1  $SS304 lift
63  7  8.31444E-02  -303 304 imp:n=1
C
C
990  100 4.97210E-05  300 301 302 #63 (-202 -500):(202 -203 200 -500):
          (203 -222 220 -500):(222 -500)  imp:n=1
991  111 8.0028E-02  500 -501  imp:n=1
992  100 4.97210E-05 501 -999 imp:n=1
999  0  999 imp:n=0

C   Surface Cards
1    pz  0
10   rcc  0 0 0  0 0 30.48  0.635
11   rhp  0 0 -10  0 0 50  0.635001 0 0
12   rcc  0 0 0  0 0 30.76  11.145
C
20   cz  0.635  $ OR Clad
21   cz  0.584  $IR Clad
22   pz  0.3    $ Top of bottom cap
23   pz  30.18  $ Bottom of Top cap
24   pz  30.48  $ Top of Tube
25   cz  0.5705 $ OR of pellet
26   pz  1.445  $ Top of bottom fuel pellet
27   pz  1.4494 $ Bottom of second fuel pellet
28   rpp -.9 .9  -.9 .9  0.2978 1.4472
```

```
C
101  p  -3.2585 10.6580 30  0 10.6580 15  3.2585 10.6580 30
102  p  3.2585 10.6580 30  5.50023 9.3375 15  7.7420 8.0170 30
103  p  7.7420 8.0170 30  9.3217 5.1671 15  10.9015 2.3172 30
104  p  10.9015 2.3172 30  10.9015 0 15  10.9015 -2.3172 30
105  p  10.9015 -2.3172 30  9.3217 -5.1671 15  7.7420 -8.0170 30
106  p  7.7420 -8.0170 30  5.50023 -9.3375 15  3.2585 -10.6580 30
107  p  3.2585 -10.6580 30  0 -10.6580 15  -3.2585 -10.6580 30
108  p  -3.2585 -10.6580 30  -5.50023 -9.3375 15  -7.7420 -8.0170 30
109  p  -7.7420 -8.0170 30  -9.3217 -5.1671 15  -10.9015 -2.3172 30
110  p  -10.9015 -2.3172 30  -10.9015 0 15  -10.9015 2.3172 30
111  p  -10.9015 2.3172 30  -9.3217 5.1671 15  -7.7420 8.0170 30
112  p  -7.7420 8.0170 30  -5.50023 9.3375 15  -3.2585 10.6580 30
C
150   cz  11.435 $ OR Core Tank
151   cz  11.145  $ IR Core Tank
152   pz    -0.35  $ Bottom Core Tank
153   pz    30.76  $ Top of Core Tank
C
155   pz    1.91  $top of bottom shims
156   pz    28.82 $bottom of top shims
C
200   cz  30.785  $OR Side Reflector
201   cz  11.535  $IR side reflector
202   pz  -15.87  $Bottom side reflector
203   pz  30.76   $Top of side reflector
C
210   cz  11.435  $OR Bottom Reflector
211   pz  -15.59  $Bottom of Bottom Reflector
212   pz  -0.35   $Top of Bottom Reflector
C
220   cz  25.40  $OR Top Reflector
221   pz  30.76  $Bottom of Top Reflector
222   pz  43.46  $Top of Top Reflector
C
300   rcc  0 0 -17.53  0 0 1.94  10.8
301   rcc  0 0 -18.16  0 0 0.63  22.86
302   rcc  0 0 -20.54  0 0 2.38  22.86
303   rpp  -60.95 60.95  -60.95 60.95  -17.14 -15.87
304   cz  11.79
C
310   rcc -40 0 15.555 80 0 0  0.635
311   px  0
312   rcc -40 -70 15.555 80 140 0  0.635
313   rcc -40 70 15.555 80 -140 0  0.635
314   rcc -40 0 15.555 80 0 0  .555
315   rcc -40 -70 15.555 80 140 0  .555
316   rcc -40 70 15.555 80 -140 0  .555
317   cz 0.635
318   cz 0.555
C
500   rpp  -367 703   -680 390  -280 630 $ inside surfaces
501   rpp  -517 763.96  -740.96 450  -340.96 690.96 $ outside Surface
C
999   rpp  -900 900  -900 900  -900 900

C   Data Cards
C     UO2
m1   92234.70c   2.22221E-04
      92235.70c   2.04075E-02
      92236.70c   1.02532E-04
      92238.70c   1.16161E-03
      8016.70c   4.36813E-02
      8017.70c   1.06404E-04
      47107.70c   5.62272E-07
      47109.70c   5.22379E-07
```

```
      4009.70c   9.73675E-08
      24050.70c   1.12435E-07
      24052.70c   2.16820E-06
      24053.70c   2.45856E-07
      24054.70c   6.11987E-08
      3006.70c   5.47058E-08
      3007.70c   6.74705E-07
      28058.70c   8.33992E-07
      28060.70c   3.21252E-07
      28061.70c   1.39646E-08
      28062.70c   4.45253E-08
      28064.70c   1.13393E-08
      50112.70c   7.17017E-09
      50114.70c   4.87867E-09
      50115.70c   2.51325E-09
      50116.70c   1.07479E-07
      50117.70c   5.67700E-08
      50118.70c   1.79032E-07
      50119.70c   6.34966E-08
      50120.70c   2.40829E-07
      50122.70c   3.42246E-08
      50124.70c   4.27992E-08
      13027.70c   3.57743E-06
      20040.70c   7.07498E-06
      20042.70c   4.72195E-08
      20043.70c   9.85261E-09
      20044.70c   1.52241E-07
      20046.70c   2.91929E-10
      20048.70c   1.36477E-08
      29063.70c   1.20986E-06
      29065.70c   5.39253E-07
      12024.70c   1.14073E-06
      12025.70c   1.44414E-07
      12026.70c   1.59000E-07
      15031.70c   9.44341E-06
      5010.70c   6.45871E-08
      5011.70c   2.59971E-07
      26054.70c   7.94519E-07
      26056.70c   1.24723E-05
      26057.70c   2.88039E-07
      26058.70c   3.83327E-08
      25055.70c   4.25932E-07
      56130.70c   2.25774E-10
      56132.70c   2.15124E-10
      56134.70c   5.14807E-09
      56135.70c   1.40406E-08
      56136.70c   1.67286E-08
      56137.70c   2.39235E-08
      56138.70c   1.52713E-07
      19039.70c   3.48837E-06
      19040.70c   4.37645E-10
      19041.70c   2.51747E-07
      11023.70c   1.27230E-06
      14028.70c   5.76320E-06
      14029.70c   2.92641E-07
      14030.70c   1.92911E-07   $ TOT   6.57374E-02
C
C    Core Tank - Al 1100
m2   13027.70c   6.09196E-02
      29063.70c   2.25167E-05
      29065.70c   1.00360E-05
      14028.70c   1.29067E-04
      14029.70c   6.55373E-06
      14030.70c   4.32027E-06
      26054.70c   4.11351E-06
      26056.70c   6.45733E-05
```

```
      26057.70c   1.49128E-06
      26058.70c   1.98462E-07
      25055.70c   7.53064E-06
      30000.70c   1.26539E-05   $ Tot   6.11826E-02
C    Shims - Al 1100
m3   13027.70c   6.21456E-02
      29063.70c   2.29698E-05
      29065.70c   1.02380E-05
      14028.70c   1.31665E-04
      14029.70c   6.68563E-06
      14030.70c   4.40722E-06
      26054.70c   4.19630E-06
      26056.70c   6.58729E-05
      26057.70c   1.52129E-06
      25055.70c   7.68220E-06
      30000.70c   1.29085E-05   $ Tot   6.24138E-02
C    bot. reflt. 1 - Al 1100
m4   13027.70c   5.98746E-02
      29063.70c   2.21304E-05
      29065.70c   9.86383E-06
      14028.70c   1.26853E-04
      14029.70c   6.44131E-06
      14030.70c   4.24616E-06
      26054.70c   4.04295E-06
      26056.70c   6.34657E-05
      26057.70c   1.46570E-06
      25055.70c   7.40146E-06
      30000.70c   1.24368E-05   $ Tot   6.01329E-02
C    bot. reflt. 2 - Al 1100
m5   13027.70c   5.97358E-02
      29063.70c   2.20791E-05
      29065.70c   9.84096E-06
      14028.70c   1.26559E-04
      14029.70c   6.42638E-06
      14030.70c   4.23632E-06
      26054.70c   4.03358E-06
      26056.70c   6.33185E-05
      26057.70c   1.46230E-06
      25055.70c   7.38430E-06
      30000.70c   1.24080E-05   $ Tot   5.99935E-02
C    lift SS 304
m6   26054.70c   3.51905E-03
      26056.70c   5.52415E-02
      26057.70c   1.27577E-03
      26058.70c   1.69781E-04
      6000.70c   1.60142E-04
      25055.70c   8.75287E-04
      14028.70c   7.89554E-04
      14029.70c   4.00916E-05
      14030.70c   2.64287E-05
      24050.70c   7.63478E-04
      24052.70c   1.47229E-02
      24053.70c   1.66946E-03
      24054.70c   4.15564E-04
      28058.70c   5.29886E-03
      28060.70c   2.04111E-03
      28061.70c   8.87257E-05
      28062.70c   2.82896E-04
      28064.70c   7.20454E-05
      15031.70c   3.49310E-05
      16032.70c   2.13510E-05
      16033.70c   1.70934E-07
      16034.70c   9.64879E-07
      16034.70c   4.49827E-09   $ tot   8.75101E-02
C    Fe table
m7   26054.70c   4.66461E-03
```

```
       26056.70c   7.32245E-02
       26057.70c   1.69107E-03
       26058.70c   2.25051E-04
       6000.70c   9.43662E-04
       12024.70c   1.47344E-03
       12025.70c   1.86535E-04
       12026.70c   2.05375E-04
       15031.70c   2.92746E-05
       16032.70c   3.35506E-05
       16033.70c   2.68603E-07
       16034.70c   1.51619E-06
       16036.70c   7.06849E-09
       14028.70c   2.97765E-04
       14029.70c   1.51198E-05
       14030.70c   9.96708E-06
       29063.70c   9.86995E-05
       29065.70c   4.39917E-05   $ tot   8.31444E-02
C
C    ATL Side Reflector
m10   13027.70c   1.06341E-05
       56130.70c   1.80457E-10
       56132.70c   1.71945E-10
       56134.70c   4.11477E-09
       56135.70c   1.12224E-08
       56136.70c   1.33709E-08
       56137.70c   1.91217E-08
       56138.70c   1.22061E-07
       5010.70c   9.78046E-09
       5011.70c   3.93676E-08
       20040.70c   2.10774E-05
       20042.70c   1.40674E-07
       20043.70c   2.93524E-08
       20044.70c   4.53549E-07
       20046.70c   8.69701E-10
       20048.70c   4.06585E-08
       27059.70c   5.40958E-08
       24050.70c   1.42083E-08
       24052.70c   2.73993E-07
       24053.70c   3.10686E-08
       24054.70c   7.73363E-09
       29063.70c   1.15673E-08
       29065.70c   5.15570E-09
       26054.70c   4.38211E-06
       26056.70c   6.87897E-05
       26057.70c   1.58865E-06
       26058.70c   2.11421E-07
       19039.70c   1.26736E-07
       19040.70c   1.59001E-11
       19041.70c   9.14623E-09
       3006.70c   2.29653E-08
       3007.70c   2.83238E-07
       71175.70c   5.91629E-09
       71176.70c   1.57306E-10
       12024.70c   3.45365E-08
       12025.70c   4.37226E-09
       12026.70c   4.81386E-09
       25055.70c   1.93432E-08
       42092.70c   8.21876E-09
       42094.70c   5.12288E-09
       42095.70c   8.81689E-09
       42096.70c   9.23780E-09
       42097.70c   5.28903E-09
       42098.70c   1.33638E-08
       42100.70c   5.33333E-09
       11023.70c   1.38672E-07
       28058.70c   3.32814E-07
```

```
      28060.70c   1.28199E-07
      28061.70c   5.57274E-09
      28062.70c   1.77683E-08
      28064.70c   4.52507E-09
      14028.70c   1.88445E-06
      14029.70c   9.56877E-08
      14030.70c   6.30781E-08
      38084.70c   3.39591E-10
      38086.70c   5.97924E-09
      38087.70c   4.24489E-09
      38088.70c   5.00776E-08
      22046.70c   9.88771E-08
      22047.70c   8.91691E-08
      22048.70c   8.83542E-07
      22049.70c   6.48394E-08
      22050.70c   6.20828E-08
      23000.70c   4.58937E-06
      39089.70c   1.31481E-07
      6000.70c   8.79920E-02   $ tot   8.81092E-02
C    ATL Top Reflector
m11   13027.70c   9.91847E-06
      56130.70c   1.68314E-10
      56132.70c   1.60374E-10
      56134.70c   3.83787E-09
      56135.70c   1.04672E-08
      56136.70c   1.24711E-08
      56137.70c   1.78349E-08
      56138.70c   1.13847E-07
      5010.70c   9.12230E-09
      5011.70c   3.67184E-08
      20040.70c   1.96590E-05
      20042.70c   1.31208E-07
      20043.70c   2.73772E-08
      20044.70c   4.23028E-07
      20046.70c   8.11175E-10
      20048.70c   3.79225E-08
      27059.70c   5.04555E-08
      24050.70c   1.32522E-08
      24052.70c   2.55555E-07
      24053.70c   2.89779E-08
      24054.70c   7.21320E-09
      29063.70c   1.07889E-08
      29065.70c   4.80875E-09
      26054.70c   4.08722E-06
      26056.70c   6.41606E-05
      26057.70c   1.48175E-06
      26058.70c   1.97193E-07
      19039.70c   1.18208E-07
      19040.70c   1.48301E-11
      19041.70c   8.53075E-09
      3006.70c   2.14198E-08
      3007.70c   2.64178E-07
      71175.70c   5.51816E-09
      71176.70c   1.46720E-10
      12024.70c   3.22124E-08
      12025.70c   4.07804E-09
      12026.70c   4.48992E-09
      25055.70c   1.80416E-08
      42092.70c   7.66569E-09
      42094.70c   4.77814E-09
      42095.70c   8.22357E-09
      42096.70c   8.61615E-09
      42097.70c   4.93311E-09
      42098.70c   1.24645E-08
      42100.70c   4.97443E-09
      11023.70c   1.29340E-07
```

```
      28058.70c   3.10418E-07
      28060.70c   1.19572E-07
      28061.70c   5.19773E-09
      28062.70c   1.65726E-08
      28064.70c   4.22056E-09
      14028.70c   1.75764E-06
      14029.70c   8.92486E-08
      14030.70c   5.88333E-08
      38084.70c   3.16739E-10
      38086.70c   5.57687E-09
      38087.70c   3.95924E-09
      38088.70c   4.67077E-08
      22046.70c   9.22233E-08
      22047.70c   8.31686E-08
      22048.70c   8.24085E-07
      22049.70c   6.04761E-08
      22050.70c   5.79050E-08
      23000.70c   4.28053E-06
      39089.70c   1.22633E-07
      6000.70c   8.20707E-02   $ tot   8.21800E-02
C    ATL Bottom Reflector
m12   13027.70c   1.06365E-05
      56130.70c   1.80499E-10
      56132.70c   1.71985E-10
      56134.70c   4.11573E-09
      56135.70c   1.12250E-08
      56136.70c   1.33740E-08
      56137.70c   1.91261E-08
      56138.70c   1.22089E-07
      5010.70c   9.78273E-09
      5011.70c   3.93767E-08
      20040.70c   2.10823E-05
      20042.70c   1.40707E-07
      20043.70c   2.93592E-08
      20044.70c   4.53654E-07
      20046.70c   8.69903E-10
      20048.70c   4.06680E-08
      27059.70c   5.41084E-08
      24050.70c   1.42116E-08
      24052.70c   2.74057E-07
      24053.70c   3.10758E-08
      24054.70c   7.73543E-09
      29063.70c   1.15700E-08
      29065.70c   5.15690E-09
      26054.70c   4.38313E-06
      26056.70c   6.88057E-05
      26057.70c   1.58902E-06
      26058.70c   2.11470E-07
      19039.70c   1.26766E-07
      19040.70c   1.59038E-11
      19041.70c   9.14836E-09
      3006.70c   2.29706E-08
      3007.70c   2.83304E-07
      71175.70c   5.91767E-09
      71176.70c   1.57343E-10
      12024.70c   3.45446E-08
      12025.70c   4.37328E-09
      12026.70c   4.81498E-09
      25055.70c   1.93477E-08
      42092.70c   8.22067E-09
      42094.70c   5.12407E-09
      42095.70c   8.81894E-09
      42096.70c   9.23995E-09
      42097.70c   5.29026E-09
      42098.70c   1.33669E-08
      42100.70c   5.33457E-09
```

```
      11023.70c   1.38704E-07
      28058.70c   3.32891E-07
      28060.70c   1.28229E-07
      28061.70c   5.57403E-09
      28062.70c   1.77725E-08
      28064.70c   4.52612E-09
      14028.70c   1.88489E-06
      14029.70c   9.57100E-08
      14030.70c   6.30927E-08
      38084.70c   3.39671E-10
      38086.70c   5.98063E-09
      38087.70c   4.24588E-09
      38088.70c   5.00893E-08
      22046.70c   9.89001E-08
      22047.70c   8.91899E-08
      22048.70c   8.83747E-07
      22049.70c   6.48545E-08
      22050.70c   6.20973E-08
      23000.70c   4.59044E-06
      39089.70c   1.31512E-07
      6000.70c   8.80125E-02   $ tot   8.81297E-02
C   Fuel Clad- SS347
m15   26054.70c   3.25448E-03
      26056.70c   5.10884E-02
      26057.70c   1.17985E-03
      26058.70c   1.57017E-04
      6000.70c   1.50688E-04
      25055.70c   8.23618E-04
      14028.70c   7.42946E-04
      14029.70c   3.77250E-05
      14030.70c   2.48686E-05
      24050.70c   6.80598E-04
      24052.70c   1.31247E-02
      24053.70c   1.48823E-03
      24054.70c   3.70452E-04
      28058.70c   5.77334E-03
      28060.70c   2.22388E-03
      28061.70c   9.66705E-05
      28062.70c   3.08228E-04
      28064.70c   7.84965E-05
      15031.70c   3.28690E-05
      16032.70c   2.00907E-05
      16033.70c   1.60844E-07
      16034.70c   9.07921E-07
      16036.70c   4.23273E-09
      41093.70c   3.13488E-04
      73181.70c   1.40839E-05   $ tot   8.19858E-02
m16   26054.70c   8.63854E-04
      26056.70c   1.35607E-02
      26057.70c   3.13175E-04
      26058.70c   4.16778E-05
      6000.70c   3.99979E-05
      25055.70c   2.18617E-04
      14028.70c   1.97204E-04
      14029.70c   1.00135E-05
      14030.70c   6.60099E-06
      24050.70c   1.80655E-04
      24052.70c   3.48374E-03
      24053.70c   3.95029E-04
      24054.70c   9.83310E-05
      28058.70c   1.53245E-03
      28060.70c   5.90295E-04
      28061.70c   2.56597E-05
      28062.70c   8.18144E-05
      28064.70c   2.08357E-05
      15031.70c   8.72458E-06
```

```
      16032.70c   5.33276E-06
      16033.70c   4.26936E-08
      16034.70c   2.40994E-07
      16034.70c   1.12352E-09
      41093.70c   8.32108E-05
      73181.70c   3.73835E-06   $ tot   2.17619E-02
mt1   o2/u.10t  u/o2.10t
mt2   al27.12t
mt3   al27.12t
mt4   al27.12t
mt5   al27.12t
mt10  grph.10t
mt11  grph.10t
mt12  grph.10t
m100   8016.70c   1.04160E-05
      8017.70c   2.53730E-08
      7014.70c   3.91350E-05
      7015.70c   1.44550E-07   $tot   4.97210E-05
c ------ Oak Ridge Concrete (rho=2.3 g/cc) ------
m111  1001.70c 8.4990E-03
      1002.70c 9.7750E-07
      6000.70c 2.0200E-02
      8016.70c 3.5487E-02
      8017.70c 1.3490E-05
      12024.70c 1.4692E-03
      12025.70c 1.8600E-04
      12026.70c 2.0479E-04
      14028.70c 1.5679E-03
      14029.70c 7.9614E-05
      14030.70c 5.2482E-05
      13027.70c 5.5600E-04
      19039.70c 3.7583E-04
      19040.70c 4.7151E-08
      19041.70c 2.7123E-05
      11023.70c 1.6300E-05
      20040.70c 1.0760E-02
      20042.70c 7.1817E-05
      20043.70c 1.4985E-05
      20044.70c 2.3155E-04
      20046.70c 4.4400E-07
      20048.70c 2.0757E-05
      26054.70c 1.1281E-05
      26056.70c 1.7709E-04
      26057.70c 4.0897E-06
      26058.70c 5.4426E-07
c total 8.0028E-02
kcode  100000 1 150 2000
C  kcode  100 1 10 150
ksrc   0.0692  4.5245 0.77787  0  8.8072 0.7787
       0.0692 -4.3864 0.77787  0 -8.7382 0.7787
       3.8736 0 0.7787   7.6780 0 0.7787
      -3.7353 0 0.7787  -7.8510 0 0.7787
```

Case 2

```
SCCA-FUND-EXP-001-002
C
C
C   Cell Cards
C   Fuel Pellets
1   1   6.57374E-02  (-25 22 -26) u=10 imp:n=1  $ fuel pellet
2   100 4.97210E-05  -22:(22 -26 25):26 u=10 imp:n=1  $void around pellet
3   100 4.97210E-05  -28   lat=1 imp:n=1 u=11 fill= 0:0 0:0 -1:26
         11 10 10 10 10 10 10 10 10 10 10 10 10 10
```

```
           10 10 10 10 10 10 10 10 10 10 10 10 10 11
C      Fuel Rod
4    100 4.97210E-05  -21 22 -23  fill=11 u=1  imp:n=1 $ fuel rod
5    15  8.19858E-02  (1 -24 -20 21) u=1 imp:n=1 $ clad
6    16  2.17619E-02  (-21 1 -22):(23 -24 -21) u=1 imp:n=1
9    100 4.97210E-05  -1:(1 -24 20):24 u=1 imp:n=1
10    100 4.97210E-05  -999 u=9 imp:n=1
C    Core Assembly
12    100 4.97210E-05  -11  lat=2 imp:n=1 u=2 fill= -10:10  -10:10  0:0
      2 2 2 2 2 2 2 2 2 2 2  2  2 2 2 2 2 2 2 2 2 2 2
      2 2 2 2 2 2 2 2 2 2 2  2  2 1 1 1 1 1 1 1 2 2 2
      2 2 2 2 2 2 2 2 2 2 2  1  1 1 1 1 1 1 1 1 1 2 2
      2 2 2 2 2 2 2 2 2 1 1  1  1 1 1 1 1 1 1 1 1 1 2
      2 2 2 2 2 2 2 2 1 1 1  1  1 1 1 1 1 1 1 1 1 1 2
      2 2 2 2 2 2 2 1 1 1 1  1  1 1 1 1 1 1 1 1 1 1 2
      2 2 2 2 2 2 1 1 1 1 1  1  1 1 1 1 1 1 1 1 1 1 2
      2 2 2 2 1 1 1 1 1 1 1  1  1 1 1 1 1 1 1 1 1 1 2
      2 2 2 1 1 1 1 1 1 1 1  1  1 1 1 1 1 1 1 1 1 1 2
      2 2 2 1 1 1 1 1 1 1 1  1  1 1 1 1 1 1 1 1 1 2 2
C
      2 2 1 1 1 1 1 1 1 1 1  9  1 1 1 1 1 1 1 1 1 2 2
C
      2 2 1 1 1 1 1 1 1 1 1  1  1 1 1 1 1 1 1 1 2 2 2
      2 1 1 1 1 1 1 1 1 1 1  1  1 1 1 1 1 1 1 1 2 2 2
      2 1 1 1 1 1 1 1 1 1 1  1  1 1 1 1 1 1 1 2 2 2 2
      2 1 1 1 1 1 1 1 1 1 1  1  1 1 1 1 1 1 2 2 2 2 2
      2 1 1 1 1 1 1 1 1 1 1  1  1 1 1 1 1 2 2 2 2 2 2
      2 1 1 1 1 1 1 1 1 1 1  1  1 1 1 2 2 2 2 2 2 2 2
      2 1 1 1 1 1 1 1 1 1 1  1  1 1 2 2 2 2 2 2 2 2 2
      2 2 1 1 1 1 1 1 1 1 1  1  2 2 2 2 2 2 2 2 2 2 2
      2 2 2 1 1 1 1 1 1 1 2  2  2 2 2 2 2 2 2 2 2 2 2
      2 2 2 2 2 2 2 2 2 2 2  2  2 2 2 2 2 2 2 2 2 2 2
13   100 4.97210E-05    -151 1 -153 -101 -102 -103 -104 -105 -106 -107
              -108 -109 -110 -111 -112  fill=2 imp:n=1
C     Core Tank
20   2  6.11826E-02  (-153 1 151 -150):(-1 152 -150)  imp:n=1  $Core Tank
21   3  6.24138E-02  -151 -153 156 #13  imp:n=1  $Top shims
22   3  6.24138E-02  -151 1 -155 #13  imp:n=1  $Bottom shims
23   100 4.97210E-05    -151 155 -156 #13 imp:n=1 $space between shims
C    Reflectors
40    100 4.97210E-05    -310 -200 201 -311 imp:n=1
41   100 4.97210E-05  -310 314 -200 201 311 imp:n=1
42   100 4.97210E-05  -312 315 -200 201 imp:n=1
43   100 4.97210E-05  -313 316 -200 201 imp:n=1
44   10  8.80543E-02  -314 -200 201 311 imp:n=1
45   10  8.80543E-02  -315 -200 201 imp:n=1
46   10  8.80543E-02  -316 -200 201 imp:n=1
50   10   8.80543E-02  (-200 201 202 -203) 310 312 313 imp:n=1  $Side Reflector
C
51   12  8.81297E-02  -210 211 -212 imp:n=1  $Bottom
C
52   11  8.21606E-02  -220 317 221 -222 imp:n=1  $Top
53   11  8.21606E-02  -318 -222 221 imp:n=1
54   100 4.97210E-05   -317 318 -222 221 imp:n=1
C
55   100 4.97210E-05  (211 -152 -201 210):(152 -153 -201 150):
         (-211 202 -201 300) imp:n=1
C
60   4  6.01329E-02  -300  imp:n=1  $Al 1100 reflector 1
61   5  5.99935E-02  -301  imp:n=1  $Al 1100 reflector 2
62   6  8.75101E-02  -302  imp:n=1  $SS304 lift
63   7  8.31444E-02  -303 304 imp:n=1
C
C
990  100 4.97210E-05  300 301 302 #63 (-202 -500):(202 -203 200 -500):
           (203 -222 220 -500):(222 -500)  imp:n=1
```

```
991  111 8.0028E-02  500 -501 imp:n=1
992  100 4.97210E-05 501 -999 imp:n=1
999  0  999 imp:n=0

C   Surface Cards
1    pz  0
10   rcc  0 0 0  0 0 30.48  0.635
11   rhp  0 0 -10  0 0 50  0.635001 0 0
12   rcc  0 0 0  0 0 30.76  11.145
C
20   cz  0.635  $ OR Clad
21   cz  0.584  $IR Clad
22   pz  0.3    $ Top of bottom cap
23   pz  30.18  $ Bottom of Top cap
24   pz  30.48  $ Top of Tube
25   cz  0.5705 $ OR of pellet
26   pz  1.445  $ Top of bottom fuel pellet
27   pz  1.4494 $ Bottom of second fuel pellet
28   rpp -.9 .9  -.9 .9  0.2978 1.4472
C
101  p  -3.2585 10.6580 30  0 10.6580 15  3.2585 10.6580 30
102  p  3.2585 10.6580 30  5.50023 9.3375 15  7.7420 8.0170 30
103  p  7.7420 8.0170 30  9.3217 5.1671 15  10.9015 2.3172 30
104  p  10.9015 2.3172 30  10.9015 0 15  10.9015 -2.3172 30
105  p  10.9015 -2.3172 30  9.3217 -5.1671 15  7.7420 -8.0170 30
106  p  7.7420 -8.0170 30  5.50023 -9.3375 15  3.2585 -10.6580 30
107  p  3.2585 -10.6580 30  0 -10.6580 15  -3.2585 -10.6580 30
108  p  -3.2585 -10.6580 30  -5.50023 -9.3375 15  -7.7420 -8.0170 30
109  p  -7.7420 -8.0170 30  -9.3217 -5.1671 15  -10.9015 -2.3172 30
110  p  -10.9015 -2.3172 30  -10.9015 0 15  -10.9015 2.3172 30
111  p  -10.9015 2.3172 30  -9.3217 5.1671 15  -7.7420 8.0170 30
112  p  -7.7420 8.0170 30  -5.50023 9.3375 15  -3.2585 10.6580 30
C
150   cz  11.435 $ OR Core Tank
151   cz  11.145  $ IR Core Tank
152   pz    -0.35  $ Bottom Core Tank
153   pz    30.76  $ Top of Core Tank
C
155   pz    1.91  $top of bottom shims
156   pz    28.82 $bottom of top shims
C
200   cz  35.875  $OR Side Reflector
201   cz  11.535  $IR side reflector
202   pz  -15.87  $Bottom side reflector
203   pz  30.76   $Top of side reflector
C
210   cz  11.435  $OR Bottom Reflector
211   pz  -15.59  $Bottom of Bottom Reflector
212   pz  -0.35   $Top of Bottom Reflector
C
220   cz  25.40  $OR Top Reflector
221   pz  30.76  $Bottom of Top Reflector
222   pz  35.84  $Top of Top Reflector
C
300   rcc  0 0 -17.53  0 0 1.94  10.8
301   rcc  0 0 -18.16  0 0 0.63  22.86
302   rcc  0 0 -20.54  0 0 2.38  22.86
303   rpp  -60.95 60.95  -60.95 60.95  -17.14 -15.87
304   cz  11.79
C
310   rcc -40 0 15.555 80 0 0  0.635
311   px  0
312   rcc -40 -70 15.555 80 140 0  0.635
313   rcc -40 70 15.555 80 -140 0  0.635
314   rcc -40 0 15.555 80 0 0  .555
315   rcc -40 -70 15.555 80 140 0  .555
```

```
316   rcc -40 70 15.555 80 -140 0  .555
317   cz 0.635
318   cz 0.555
C
500   rpp  -367 703   -680 390  -280 630 $ inside surfaces
501   rpp  -517 763.96  -740.96 450  -340.96 690.96 $ outside Surface
C
999   rpp  -900 900  -900 900  -900 900

C   Data Cards
C     UO2
m1   92234.70c   2.22221E-04
      92235.70c   2.04075E-02
      92236.70c   1.02532E-04
      92238.70c   1.16161E-03
      8016.70c   4.36813E-02
      8017.70c   1.06404E-04
      47107.70c   5.62272E-07
      47109.70c   5.22379E-07
      4009.70c   9.73675E-08
      24050.70c   1.12435E-07
      24052.70c   2.16820E-06
      24053.70c   2.45856E-07
      24054.70c   6.11987E-08
      3006.70c   5.47058E-08
      3007.70c   6.74705E-07
      28058.70c   8.33992E-07
      28060.70c   3.21252E-07
      28061.70c   1.39646E-08
      28062.70c   4.45253E-08
      28064.70c   1.13393E-08
      50112.70c   7.17017E-09
      50114.70c   4.87867E-09
      50115.70c   2.51325E-09
      50116.70c   1.07479E-07
      50117.70c   5.67700E-08
      50118.70c   1.79032E-07
      50119.70c   6.34966E-08
      50120.70c   2.40829E-07
      50122.70c   3.42246E-08
      50124.70c   4.27992E-08
      13027.70c   3.57743E-06
      20040.70c   7.07498E-06
      20042.70c   4.72195E-08
      20043.70c   9.85261E-09
      20044.70c   1.52241E-07
      20046.70c   2.91929E-10
      20048.70c   1.36477E-08
      29063.70c   1.20986E-06
      29065.70c   5.39253E-07
      12024.70c   1.14073E-06
      12025.70c   1.44414E-07
      12026.70c   1.59000E-07
      15031.70c   9.44341E-06
      5010.70c   6.45871E-08
      5011.70c   2.59971E-07
      26054.70c   7.94519E-07
      26056.70c   1.24723E-05
      26057.70c   2.88039E-07
      26058.70c   3.83327E-08
      25055.70c   4.25932E-07
      56130.70c   2.25774E-10
      56132.70c   2.15124E-10
      56134.70c   5.14807E-09
      56135.70c   1.40406E-08
      56136.70c   1.67286E-08
```

```
      56137.70c   2.39235E-08
      56138.70c   1.52713E-07
      19039.70c   3.48837E-06
      19040.70c   4.37645E-10
      19041.70c   2.51747E-07
      11023.70c   1.27230E-06
      14028.70c   5.76320E-06
      14029.70c   2.92641E-07
      14030.70c   1.92911E-07   $ TOT   6.57374E-02
C
C    Core Tank - Al 1100
C
C    Core Tank - Al 1100
m2   13027.70c   6.09196E-02
      29063.70c   2.25167E-05
      29065.70c   1.00360E-05
      14028.70c   1.29067E-04
      14029.70c   6.55373E-06
      14030.70c   4.32027E-06
      26054.70c   4.11351E-06
      26056.70c   6.45733E-05
      26057.70c   1.49128E-06
      26058.70c   1.98462E-07
      25055.70c   7.53064E-06
      30000.70c   1.26539E-05   $ Tot   6.11826E-02
C    Shims - Al 1100
m3   13027.70c   6.21456E-02
      29063.70c   2.29698E-05
      29065.70c   1.02380E-05
      14028.70c   1.31665E-04
      14029.70c   6.68563E-06
      14030.70c   4.40722E-06
      26054.70c   4.19630E-06
      26056.70c   6.58729E-05
      26057.70c   1.52129E-06
      25055.70c   7.68220E-06
      30000.70c   1.29085E-05   $ Tot   6.24138E-02
C    bot. reflt. 1 - Al 1100
m4   13027.70c   5.98746E-02
      29063.70c   2.21304E-05
      29065.70c   9.86383E-06
      14028.70c   1.26853E-04
      14029.70c   6.44131E-06
      14030.70c   4.24616E-06
      26054.70c   4.04295E-06
      26056.70c   6.34657E-05
      26057.70c   1.46570E-06
      25055.70c   7.40146E-06
      30000.70c   1.24368E-05   $ Tot   6.01329E-02
C    bot. reflt. 2 - Al 1100
m5   13027.70c   5.97358E-02
      29063.70c   2.20791E-05
      29065.70c   9.84096E-06
      14028.70c   1.26559E-04
      14029.70c   6.42638E-06
      14030.70c   4.23632E-06
      26054.70c   4.03358E-06
      26056.70c   6.33185E-05
      26057.70c   1.46230E-06
      25055.70c   7.38430E-06
      30000.70c   1.24080E-05   $ Tot   5.99935E-02
C    lift SS 304
m6   26054.70c   3.51905E-03
      26056.70c   5.52415E-02
      26057.70c   1.27577E-03
      26058.70c   1.69781E-04
```

```
      6000.70c   1.60142E-04
      25055.70c   8.75287E-04
      14028.70c   7.89554E-04
      14029.70c   4.00916E-05
      14030.70c   2.64287E-05
      24050.70c   7.63478E-04
      24052.70c   1.47229E-02
      24053.70c   1.66946E-03
      24054.70c   4.15564E-04
      28058.70c   5.29886E-03
      28060.70c   2.04111E-03
      28061.70c   8.87257E-05
      28062.70c   2.82896E-04
      28064.70c   7.20454E-05
      15031.70c   3.49310E-05
      16032.70c   2.13510E-05
      16033.70c   1.70934E-07
      16034.70c   9.64879E-07
      16034.70c   4.49827E-09   $ tot   8.75101E-02
C    Fe table
m7   26054.70c   4.66461E-03
      26056.70c   7.32245E-02
      26057.70c   1.69107E-03
      26058.70c   2.25051E-04
      6000.70c   9.43662E-04
      12024.70c   1.47344E-03
      12025.70c   1.86535E-04
      12026.70c   2.05375E-04
      15031.70c   2.92746E-05
      16032.70c   3.35506E-05
      16033.70c   2.68603E-07
      16034.70c   1.51619E-06
      16036.70c   7.06849E-09
      14028.70c   2.97765E-04
      14029.70c   1.51198E-05
      14030.70c   9.96708E-06
      29063.70c   9.86995E-05
      29065.70c   4.39917E-05   $ tot   8.31444E-02
C
C    ATL Side Reflector
m10   13027.70c   1.06275E-05
      56130.70c   1.80345E-10
      56132.70c   1.71838E-10
      56134.70c   4.11221E-09
      56135.70c   1.12154E-08
      56136.70c   1.33625E-08
      56137.70c   1.91098E-08
      56138.70c   1.21985E-07
      5010.70c   9.77437E-09
      5011.70c   3.93431E-08
      20040.70c   2.10643E-05
      20042.70c   1.40586E-07
      20043.70c   2.93341E-08
      20044.70c   4.53266E-07
      20046.70c   8.69159E-10
      20048.70c   4.06332E-08
      27059.70c   5.40621E-08
      24050.70c   1.41994E-08
      24052.70c   2.73822E-07
      24053.70c   3.10492E-08
      24054.70c   7.72881E-09
      29063.70c   1.15601E-08
      29065.70c   5.15249E-09
      26054.70c   4.37938E-06
      26056.70c   6.87469E-05
      26057.70c   1.58766E-06
```

```
      26058.70c   2.11289E-07
      19039.70c   1.26657E-07
      19040.70c   1.58902E-11
      19041.70c   9.14053E-09
      3006.70c   2.29510E-08
      3007.70c   2.83062E-07
      71175.70c   5.91261E-09
      71176.70c   1.57208E-10
      12024.70c   3.45150E-08
      12025.70c   4.36954E-09
      12026.70c   4.81087E-09
      25055.70c   1.93312E-08
      42092.70c   8.21364E-09
      42094.70c   5.11969E-09
      42095.70c   8.81140E-09
      42096.70c   9.23204E-09
      42097.70c   5.28573E-09
      42098.70c   1.33555E-08
      42100.70c   5.33001E-09
      11023.70c   1.38585E-07
      28058.70c   3.32607E-07
      28060.70c   1.28119E-07
      28061.70c   5.56927E-09
      28062.70c   1.77573E-08
      28064.70c   4.52225E-09
      14028.70c   1.88328E-06
      14029.70c   9.56282E-08
      14030.70c   6.30388E-08
      38084.70c   3.39380E-10
      38086.70c   5.97551E-09
      38087.70c   4.24225E-09
      38088.70c   5.00464E-08
      22046.70c   9.88155E-08
      22047.70c   8.91136E-08
      22048.70c   8.82991E-07
      22049.70c   6.47990E-08
      22050.70c   6.20442E-08
      23000.70c   4.58651E-06
      39089.70c   1.31399E-07
      6000.70c   8.79372E-02   $ tot   8.80543E-02
C    ATL Top Reflector
m11   13027.70c   9.91613E-06
      56130.70c   1.68274E-10
      56132.70c   1.60337E-10
      56134.70c   3.83697E-09
      56135.70c   1.04647E-08
      56136.70c   1.24682E-08
      56137.70c   1.78307E-08
      56138.70c   1.13820E-07
      5010.70c   9.12014E-09
      5011.70c   3.67097E-08
      20040.70c   1.96544E-05
      20042.70c   1.31177E-07
      20043.70c   2.73707E-08
      20044.70c   4.22928E-07
      20046.70c   8.10984E-10
      20048.70c   3.79135E-08
      27059.70c   5.04436E-08
      24050.70c   1.32490E-08
      24052.70c   2.55494E-07
      24053.70c   2.89710E-08
      24054.70c   7.21150E-09
      29063.70c   1.07863E-08
      29065.70c   4.80762E-09
      26054.70c   4.08625E-06
      26056.70c   6.41454E-05
```

```
          26057.70c   1.48140E-06
          26058.70c   1.97147E-07
          19039.70c   1.18180E-07
          19040.70c   1.48266E-11
          19041.70c   8.52873E-09
          3006.70c   2.14148E-08
          3007.70c   2.64116E-07
          71175.70c   5.51686E-09
          71176.70c   1.46686E-10
          12024.70c   3.22048E-08
          12025.70c   4.07708E-09
          12026.70c   4.48886E-09
          25055.70c   1.80373E-08
          42092.70c   7.66388E-09
          42094.70c   4.77701E-09
          42095.70c   8.22163E-09
          42096.70c   8.61412E-09
          42097.70c   4.93194E-09
          42098.70c   1.24615E-08
          42100.70c   4.97326E-09
          11023.70c   1.29310E-07
          28058.70c   3.10344E-07
          28060.70c   1.19544E-07
          28061.70c   5.19650E-09
          28062.70c   1.65687E-08
          28064.70c   4.21956E-09
          14028.70c   1.75722E-06
          14029.70c   8.92275E-08
          14030.70c   5.88194E-08
          38084.70c   3.16664E-10
          38086.70c   5.57556E-09
          38087.70c   3.95830E-09
          38088.70c   4.66967E-08
          22046.70c   9.22015E-08
          22047.70c   8.31490E-08
          22048.70c   8.23890E-07
          22049.70c   6.04618E-08
          22050.70c   5.78914E-08
          23000.70c   4.27952E-06
          39089.70c   1.22605E-07
          6000.70c   8.20513E-02   $ tot   8.21606E-02
C     ATL Bottom Reflector
m12   13027.70c   1.06365E-05
          56130.70c   1.80499E-10
          56132.70c   1.71985E-10
          56134.70c   4.11573E-09
          56135.70c   1.12250E-08
          56136.70c   1.33740E-08
          56137.70c   1.91261E-08
          56138.70c   1.22089E-07
          5010.70c   9.78273E-09
          5011.70c   3.93767E-08
          20040.70c   2.10823E-05
          20042.70c   1.40707E-07
          20043.70c   2.93592E-08
          20044.70c   4.53654E-07
          20046.70c   8.69903E-10
          20048.70c   4.06680E-08
          27059.70c   5.41084E-08
          24050.70c   1.42116E-08
          24052.70c   2.74057E-07
          24053.70c   3.10758E-08
          24054.70c   7.73543E-09
          29063.70c   1.15700E-08
          29065.70c   5.15690E-09
          26054.70c   4.38313E-06
```

```
      26056.70c   6.88057E-05
      26057.70c   1.58902E-06
      26058.70c   2.11470E-07
      19039.70c   1.26766E-07
      19040.70c   1.59038E-11
      19041.70c   9.14836E-09
      3006.70c   2.29706E-08
      3007.70c   2.83304E-07
      71175.70c   5.91767E-09
      71176.70c   1.57343E-10
      12024.70c   3.45446E-08
      12025.70c   4.37328E-09
      12026.70c   4.81498E-09
      25055.70c   1.93477E-08
      42092.70c   8.22067E-09
      42094.70c   5.12407E-09
      42095.70c   8.81894E-09
      42096.70c   9.23995E-09
      42097.70c   5.29026E-09
      42098.70c   1.33669E-08
      42100.70c   5.33457E-09
      11023.70c   1.38704E-07
      28058.70c   3.32891E-07
      28060.70c   1.28229E-07
      28061.70c   5.57403E-09
      28062.70c   1.77725E-08
      28064.70c   4.52612E-09
      14028.70c   1.88489E-06
      14029.70c   9.57100E-08
      14030.70c   6.30927E-08
      38084.70c   3.39671E-10
      38086.70c   5.98063E-09
      38087.70c   4.24588E-09
      38088.70c   5.00893E-08
      22046.70c   9.89001E-08
      22047.70c   8.91899E-08
      22048.70c   8.83747E-07
      22049.70c   6.48545E-08
      22050.70c   6.20973E-08
      23000.70c   4.59044E-06
      39089.70c   1.31512E-07
      6000.70c   8.80125E-02   $ tot   8.81297E-02
C   Fuel Clad- SS347
m15   26054.70c   3.25448E-03
      26056.70c   5.10884E-02
      26057.70c   1.17985E-03
      26058.70c   1.57017E-04
      6000.70c   1.50688E-04
      25055.70c   8.23618E-04
      14028.70c   7.42946E-04
      14029.70c   3.77250E-05
      14030.70c   2.48686E-05
      24050.70c   6.80598E-04
      24052.70c   1.31247E-02
      24053.70c   1.48823E-03
      24054.70c   3.70452E-04
      28058.70c   5.77334E-03
      28060.70c   2.22388E-03
      28061.70c   9.66705E-05
      28062.70c   3.08228E-04
      28064.70c   7.84965E-05
      15031.70c   3.28690E-05
      16032.70c   2.00907E-05
      16033.70c   1.60844E-07
      16034.70c   9.07921E-07
      16036.70c   4.23273E-09
```

```
      41093.70c   3.13488E-04
      73181.70c   1.40839E-05   $ tot   8.19858E-02
m16   26054.70c   8.63854E-04
      26056.70c   1.35607E-02
      26057.70c   3.13175E-04
      26058.70c   4.16778E-05
      6000.70c   3.99979E-05
      25055.70c   2.18617E-04
      14028.70c   1.97204E-04
      14029.70c   1.00135E-05
      14030.70c   6.60099E-06
      24050.70c   1.80655E-04
      24052.70c   3.48374E-03
      24053.70c   3.95029E-04
      24054.70c   9.83310E-05
      28058.70c   1.53245E-03
      28060.70c   5.90295E-04
      28061.70c   2.56597E-05
      28062.70c   8.18144E-05
      28064.70c   2.08357E-05
      15031.70c   8.72458E-06
      16032.70c   5.33276E-06
      16033.70c   4.26936E-08
      16034.70c   2.40994E-07
      16034.70c   1.12352E-09
      41093.70c   8.32108E-05
      73181.70c   3.73835E-06   $ tot   2.17619E-02
C
mt1   o2/u.10t  u/o2.10t
mt2   al27.12t
mt3   al27.12t
mt4   al27.12t
mt5   al27.12t
mt10  grph.10t
mt11  grph.10t
mt12  grph.10t
m100   8016.70c   1.04160E-05
      8017.70c   2.53730E-08
      7014.70c   3.91350E-05
      7015.70c   1.44550E-07   $tot   4.97210E-05
c ------ Oak Ridge Concrete (rho=2.3 g/cc) ------
m111  1001.70c 8.4990E-03
      1002.70c 9.7750E-07
      6000.70c 2.0200E-02
      8016.70c 3.5487E-02
      8017.70c 1.3490E-05
      12024.70c 1.4692E-03
      12025.70c 1.8600E-04
      12026.70c 2.0479E-04
      14028.70c 1.5679E-03
      14029.70c 7.9614E-05
      14030.70c 5.2482E-05
      13027.70c 5.5600E-04
      19039.70c 3.7583E-04
      19040.70c 4.7151E-08
      19041.70c 2.7123E-05
      11023.70c 1.6300E-05
      20040.70c 1.0760E-02
      20042.70c 7.1817E-05
      20043.70c 1.4985E-05
      20044.70c 2.3155E-04
      20046.70c 4.4400E-07
      20048.70c 2.0757E-05
      26054.70c 1.1281E-05
      26056.70c 1.7709E-04
      26057.70c 4.0897E-06
```

```
      26058.70c 5.4426E-07
c total 8.0028E-02
kcode  100000 1 150 2000
C  kcode  100 1 10 150
ksrc   0.0692  4.5245 0.77787  0  8.8072 0.7787
       0.0692 -4.3864 0.77787  0 -8.7382 0.7787
       3.8736 0 0.7787   7.6780 0 0.7787
      -3.7353 0 0.7787  -7.8510 0 0.7787
print 40 60
```